TEXTILE RESEARCH JOURNAL

VOLUME XXIV October, 1954 NUMBER 10

PUBLICATION OF
TEXTILE RESEARCH INSTITUTE

Editorial Office: 10 East 40th Street, New York 16, N. Y.

SCOTT TESTERS
Trademark

From fibre to rope

(well, a small one anyway)

From a bonded fabric to a tarpaulin

Scott Testers* produces a universal line of physical testing equipment with a full range of capacities from 4 grams maximum to 2000 lbs. tensile.

In use in 49 countries, Scott Testers conform to ASTM, U.S. Government, ISO and other internationally recognized standards . . . they "speak a universal language."

SCOTT TESTERS, INC. 145 Blackstone St. Providence, R. I.

Southern Service and Repair Facilities:
SCOTT TESTERS (Southern) INC., 216 Reidville Road, Spartanburg, S. C.

Southern Sales Rep.: JOHN KLINCK
304 West Forest Ave., North Augusta, S. C.

Scott Testers — Standard of the World

TEXTILE RESEARCH JOURNAL

VOL. XXIV, No. 10 October, 1954

In This Issue

The Interaction of Hair Fibers with Alkali Bromide Solutions
W. S. Barnard, A. Palm, P. B. Stam, D. L. Underwood, and H. J. White, Jr. 863

Physical Chemical Studies Related to the Role of Whiteness-Retention Additives in Detergent Action
W. Fong and W. H. Ward 881

The Influence of Chemical Treatment on the Properties of Wool
J. H. Dusenbury, E. H. Mercer, and J. H. Wakelin 890
I. Alkali Solubility as a Measure of Sulfuric Acid Degradation

A Multiple-Unit Stress Relaxometer
Walter J. Thorsen 899

Properties of Apparel Wools
Harris M. Burte 903
VIII. The Aging of Worsted Yarns

Mechanics of Elastic Performance of Textile Materials
M. M. Platt, W. G. Klein, and W. J. Hamburger 907
Part XI: Factors Affecting the Translation of Certain Mechanical Properties of Cordage Fibers and Yarns into Cordage Strands and Ropes

Fundamental Fiber-Fabric Relationships; A Symposium 939

BOOK REVIEW 940

Editor: **Julian S. Jacobs** ***Production Editor:*** **Hilda Taft**

Associate Editors

H. J. Ball **W. J. Hamburger** **H. Mark**
Earl E. Berkley **Milton Harris** **E. R. Schwarz**
Henry Eyring **K. L. Hertel** **Kyle Ward, Jr.**

TEXTILE RESEARCH JOURNAL, published monthly at Prince and Lemon Streets, Lancaster, Pa., is devoted to the interest of research in textile and allied industries. It is published by Textile Research Institute.

Entered as second-class matter, April 27, 1945, at the post office at Lancaster, Pa., under the Act of August 24, 1912. Accepted for mailing at special rate of postage provided for in paragraph (d-2), Section 34.40, P. L. & R. of 1948, authorized May 9, 1950.

Manuscripts and communications should be sent to the editorial office, 10 East 40th Street, New York 16, N. Y.

Subscription rates: $15.00 per year; additional for postage, 50 cents to Canada, $1.00 to all other countries. Single copies, $1.50 each.

Contents copyrighted 1954 by Textile Research Institute. Advertising rates supplied on request.

NEW *DIFFERENT*

C & R TESTER

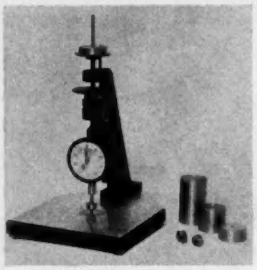

- Combines a number of ASTM spec. for thickness in one instrument.
- Will test compression and recovery.
- Applies dead load to sample without impact.

The C & R Tester was designed to give the technician a versatile instrument. By a selection of pressure feet this instrument will meet ASTM specifications for thickness for asbestos, knit goods, woven glass fibers, pile floor coverings, backing, solid electrical insulation, paper, rubber, etc. This instrument has a 1/2 oz. preload and 5 lb. maximum dead weight load. The indenting load is transferred from a ball-bearing support to the indenting plunger, by means of a screw and handwheel.

Custom Scientific Instruments, Inc.

Post Office Box 170 Arlington, New Jersey

Manufacturers of Custom-Built Laboratory Equipment

T.R.I. ANNUAL MEETING

March 10-11, 1955

Textile Research Institute will hold its Twenty-Fifth Annual Meeting at Hotel Commodore, New York City, March 10 and 11, 1955.

Sr. Research Engineer

Advanced degree in physics, mechanical or textile engineering, with yarn utilization experience, preferably in mechanical goods industry. Will study new and unique ways of using fibers, both old and new, in apparel and industrial fabrics. Provides broad responsibility in developing the technology of yarn utilization.

Sr. Research Chemist or ChE

BS degree, experience in industrial research (textile preferred). For research and development work in the field of synthetic fiber spinning, including processes for producing new fibers as well as improvement of existing fibers.

These are permanent positions in Celanese's modern research laboratories in Summit, New Jersey, a pleasant residential community within 30 miles of metropolitan New York. Interviews will be arranged for qualified applicants. Please submit resumes, including initial salary requirements, to Mr. J. A. Berg, Head—Personnel Administration.

Celanese CORP. OF AMERICA

Summit, New Jersey

FOR SALE

Complete Set of Back Issues

TEXTILE RESEARCH JOURNAL

A subscriber offers for sale a complete set of TEXTILE RESEARCH JOURNAL, 1945–1953. In addition, the two preceding volumes of Textile Research, the JOURNAL's predecessor (Nov. 1942–Dec. 1944). This set is in excellent condition and must be purchased complete up to December 1953. It is offered at approximately one-third savings.

For information write to

TEXTILE RESEARCH JOURNAL

TEXTILE RESEARCH JOURNAL

VOL. XXIV, No. 10 OCTOBER, 1954

The Interaction of Hair Fibers with Alkali Bromide Solutions*

W. S. Barnard,† A. Palm,‡ P. B. Stam,§ D. L. Underwood,‖ and H. J. White, Jr.¶

Frick Chemical Laboratory, Princeton University, and Textile Research Institute, Princeton, New Jersey

Abstract

The interaction of hair with alkali bromide solutions has been studied by measuring the amount of salt taken up from a given solution, using a radioactive-tracer technique, and the amount of water taken up from the solution, using a gravimetric technique.

It has been found that: (*1*) alkali bromides are taken up in a manner primarily dependent on the activity of the salt in the solution; (*2*) the amount of water absorbed is increased over the normal regain by the presence of the salt in the hair; (*3*) the ratio of salt to water is greater in the hair than in the external solution; (*4*) the rate of absorption of the salt is slower than the rate of diffusion of the same salt in water; (*5*) both rates and equilibrium are temperature-sensitive.

The interpretation of these results in terms of various simple models of the absorption process is discussed.

Introduction

Dyeing and other forms of wet processing involve the immersion of fibers in an aqueous bath and subsequent partitioning of the various components of the bath between the bath and the fibers. It is obvious that a complete understanding of these processes depends on a complete knowledge of the extent of the partitioning of each component and the rate at which partitioning is achieved. As part of a program on dyeing research we have attempted to provide more complete and comprehensive information than has previously been available on a few simple systems. The systems most completely studied were human hair in NaBr solutions and human hair in LiBr solutions.

Results have been given in previous papers on the swelling of hair in various solutions, including NaBr and LiBr solutions [1], and the uptake of NaBr from solution [15]. In the present paper further results are given on the uptake of alkali halides, including NaBr, NaCl, LiBr, and KBr, from aqueous solutions. In addition, an experimental method has been devised to measure indirectly the amount of water taken up from the aqueous solution, and has been applied to the case of hair in NaBr, NaCl, and LiBr solutions.

* This article is based in part on a thesis to be submitted by D. L. Underwood in partial fulfillment of the requirements for the degree of Doctor of Philosophy at Princeton University.

† Present address: Chicopee Manufacturing Corp., Chicopee Falls, Mass.

‡ Present address: Mystic Tape Co., Chicago, Ill.

§ Present address: Dan River Mills, Danville, Va.

‖ Research Fellow, Textile Research Institute.

¶ Associate Director of Research, Textile Research Institute.

The measurement of salt uptake was made by a technique using radioactive tracers, which has previously been described in part [15]. Further details are discussed in this paper. In certain cases the radioactive measurements were confirmed gravimetrically.

The measurement of the water uptake depends on the following reasoning: If a fiber is brought to equilibrium with a salt solution, removed, washed in such a way as to remove externally adhering solution but not to remove absorbed salt from the interior, and dried, it will increase in weight to the extent that it has absorbed salt. This method can be used as a gravimetric check on the radioactive technique, although it is inferior in sensitivity, at least by our techniques, because of weighing difficulties. If the fiber containing the salt is then exposed to the vapor of the solution from which it absorbed the salt, it will absorb water vapor. The amount of water absorbed will depend on the partial molal free energy of the water in the solution and on the composition of the nonvolatile solid phase—namely, the fiber. Since the partial molal free energy of the water is the same in the solution and in the vapor, and since the amount of salt in the fiber is the same as when the fiber was immersed in the solution, the amount of water absorbed from the vapor should be the same as the amount taken up from the solution. Thus, the increase in weight of the salt-containing fiber gives the amount of water present in the fiber when it is brought to equilibrium with the aqueous solution.

Experimental

As in previous work [15] the radioactive-tracer method for measuring salt uptake consisted of treating fibers in radioactive solutions, removing them, washing them free of entrained solution, mounting, and counting them. The counts were then referred to the counts from standards made by evaporating small volumes of radioactive solutions of known chemical composition. The experimental details were the same as previously reported except for certain changes and amplifications, and are given in *Appendix I*.

Hair Samples

It was not possible to do all of the work on hairs from the same tress used in previous work. Thus, unmedullated, solvent-extracted hairs from two different heads, denoted hair *I* and hair *II*, were used. Hair *I* was used in the previous work [1, 15]. Identification of the hairs was necessary because they did not have identical absorptive properties.

Since larger samples of hair were used for the gravimetric work, it was not feasible to examine each hair to avoid medullation. Thus, medullated and unmedullated hairs were used in the gravimetric work. Hair *III*, a brunette tress of hair,* was used with NaBr solutions. Randomly medullated samples of hair *I*, called for convenience hair *Ia*, were used with LiBr solutions.

Conversion Factors and Experimental Error

Partly because of necessity and partly because of the gradual evolution of the experimental techniques, several different types of hair and of wash liquids were used. In an effort to minimize the differences resulting from these variations, tracer experiments were run to compare the various alternatives, with one hair type and one wash method chosen as standard. The standards chosen were hair *I* and a 95% alcohol rinse. Hair *I* was chosen because all swelling measurements were made using it, and the alcohol rinse was chosen as the most satisfactory rinse, allowing both tracer and gravimetric experiments to be compared. A series of conversion factors was then determined to allow all results to be converted to equivalent results for hair *I* given an alcohol rinse. These factors were:

Hair *II*, alcohol rinse, 0.92
Hair *I*, inactive rinse, 1.08
Hair *Ia*, benzene-acetone rinse, 0.81
Hair *III*, alcohol rinse, 0.88

* Obtained through the courtesy of the Artistic Hairdressers, Princeton, N. J.

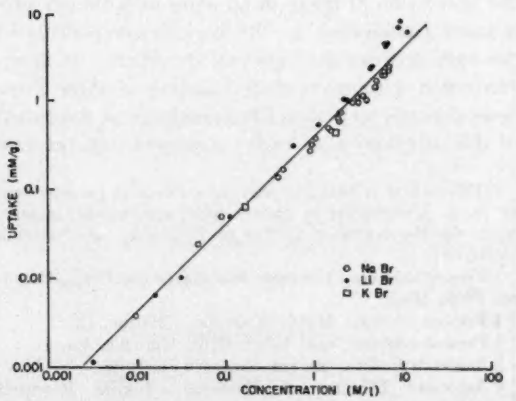

FIG. 1. *Equilibrium uptake of alkali bromides by hair as a function of concentration.*

The last two factors were used on the salt uptake results which were measured gravimetrically. The essential correctness of the third factor, which represents a rather large correction, is shown by the close agreement of the results of the one experiment done using an alcohol wash (see Table VII). The water uptake results, and the salt-water ratios derived from them, were not changed since no reasonable basis for correction could be established.

The coefficient of variation for a single fiber measurement was 13%. Equilibrium points in the tables and on the graphs were taken using a minimum of three fibers and usually four or more. The standard error for these points was about 7%. The standard error for the measurement of water absorption by hairs containing NaBr was about 2.5%, and for hairs containing LiBr about 4%. The standard error for the salt uptake results was determined using results pooled from several sources, and for this reason is larger than the standard errors for the water-absorption measurements. For an individual measurement the results taken using tracers show, in general, a smaller error than similar results measured gravimetrically. The errors shown in the tables were calculated using 90% confidence limits.

Results

Salt-Absorption Measurements

Equilibrium absorption.—Results on the equilibrium uptake of NaBr by hair from solutions of different concentrations are given in Table I and Figure 1. The results, some of which have been published previously [15], were obtained using the tracer method, with either Br^{82} or Na^{22} as tracer, and the gravimetric method. As explained above, the uptake data have been converted, where necessary, to equivalent data on unmedullated hair *I* washed with ethyl alcohol. The conversion factors are given above. Three measures of the concentration are given in Table I—the molarity, *M*, the molality, *m*, and the activity, *a*. The molarity results directly from the experimental measurements. The molality is determined from the molarity and the density.

TABLE I. EQUILIBRIUM UPTAKE OF NaBr BY HAIR FROM AQUEOUS SOLUTION AT ~25°C AS A FUNCTION OF CONCENTRATION

Hair sample	Method or isotope	Wash	Concentration (M/l.)	Concentration (M/1000 g. water)	Activity (*a*)	Uptake (mM/g.)
I	Br^{82}	alcohol	0.0096	0.0096	0.0088	0.0038
			0.048	0.048	0.041	0.024
			0.091	0.091	0.074	0.050
			0.460	0.460	0.328	0.173
			0.910	0.930	0.639	0.276
			0.955	0.990	0.655	0.328
			1.90	2.04	1.50	0.61
			1.91	2.05	1.51	0.64
I	Br^{82}	inactive	1.60	1.68	1.19	0.492
			3.20	3.53	3.08	0.98
			6.40	7.9	14.6	1.99
I	Na^{22}	inactive	0.400	0.400	0.282	0.140
			1.05	1.08	0.743	0.380
			2.02	2.15	1.60	0.75
			3.13	3.42	2.93	1.13
			3.63	4.05	3.79	1.18
			5.01	5.82	7.27	1.49
			6.20	7.56	13.1	2.18
			6.36	7.82	14.2	2.20
			7.25	9.20	21.0	2.21
II	Na^{22}	alcohol	2.05	2.17	1.61	0.76
III	gravimetric	alcohol	1.49	1.55	1.09	0.49
			2.81	3.02	2.46	0.99
			3.97	4.46	4.34	1.09
			5.18	6.06	7.86	1.73
			6.16	7.50	12.6	2.01
			7.25	9.20	21.0	2.46

TABLE II. EQUILIBRIUM UPTAKE OF LiBr BY HAIR FROM AQUEOUS SOLUTION AT ~25°C AS A FUNCTION OF CONCENTRATION

Hair sample	Method or isotope	Wash	Concentration (M/l.)	Concentration (M/1000 g. water)	Activity (*a*)	Uptake (mM/g.)
I	direct, Br^{82}	alcohol	0.0032	0.0032	0.0030	0.0011
			0.016	0.016	0.014	0.0063
			0.032	0.032	0.028	0.011
			0.116	0.116	0.090	0.050
			0.600	0.604	0.506	0.318
			1.16	1.20	1.02	0.55
I	replacement, Br^{82}	alcohol	2.30	2.50	2.88	1.06
			4.50	5.16	14.5	2.42
			6.71	8.23	78.3	4.57
			9.9	13.5	1010	~8*
Ia	replacement, gravimetric	75% benzene, 25% acetone	2.4	2.60	3.12	1.04
			4.7	5.40	16.75	2.55
			7.0	8.70	100	4.61
			9.3	12.3	605	6.8†
			11.6	16.75	4200	6.0†
Ia	replacement, gravimetric	alcohol	7.1	8.70	100	4.71
I	direct, Br^{82}	inactive	2.38	2.58	2.97	1.03‡
			4.80	5.51	18.2	1.87‡
			6.90	8.57	91.7	1.73‡
			9.07	12.04	605	0.05‡
			11.3	17.02	4500	0.39‡
I	direct, Br^{82}	alcohol	6.71	8.23	78.1	4.38§
			4.50	5.16	15.0	2.37§

* As can be seen from an inspection of Figure 6, the rate of attainment of equilibrium in concentrated LiBr solutions is very slow, even when the replacement technique is used. The value of 8 has been chosen as a likely equilibrium value from consideration of the rate data.

† This is probably not an equilibrium value.

‡ Hairs left in the solution about 12 hrs.

§ Hairs left in the solution 118 hrs.

The densities have been obtained from the *International Critical Tables*. The determination of the activities is described in *Appendix II*.

Steinhardt and Harris [17] have shown that the absorption of acid at a given pH is increased by the presence of a salt containing a common ion. Considerable amounts of acid are absorbed at pH values quite near the isoionic point from solutions of high ionic strength. However, as has been pointed out, the treating solutions probably remain near the isoionic point so that, although acid uptake may contribute to the scatter of the results, it is unlikely that appreciable amounts of absorbed acid are included as salt. The essential agreement between results taken using Na^{22} and Br^{82} offer confirmation of this.

In Table II results are given on the equilibrium uptake of LiBr from aqueous solutions by hair as a function of concentration. As in the case of the swelling experiments [1], a metastable equilibrium was reached if hairs were immersed directly in very concentrated LiBr solutions. Most of the results for concentrated solutions were taken using the replacement technique, in which the fibers are brought to equilibrium with each of a series of successively more concentrated solutions until the desired concen-

TABLE III. ADDITIONAL DATA ON THE EQUILIBRIUM UPTAKE OF ALKALI HALIDES FROM AQUEOUS SOLUTION BY HAIR AT ~25°C

Salt	Method or tracer	Wash	Concentration (M/l.)	Concentration (M/1000 g. water)	Activity (*a*)	Uptake (mM/g.)
KBr	Br^{82}	inactive	0.171	0.20	0.145	0.069
KBr	Br^{82}	inactive	1.71	1.85	1.10	0.459
NaCl	Na^{22}	inactive	0.987	0.990	0.648	0.234

TABLE IV. EQUILIBRIUM ABSORPTION OF NaBr FROM SOLUTION BY HAIR AT HIGHER TEMPERATURES

Hair	Method or tracer	Wash	Temp. (°C)	Concentration (M/1000 g. water)	Activity (a)	Uptake (mM/g.)	Uptake at ~25°C (mM/g.)
I	Br^{82}	alcohol	50°C	0.0096		0.0024	0.0038
				0.048		0.012	0.024
				0.091		0.052	0.050
				0.46		0.134	0.173
				0.93		0.276	0.276
I	Br^{82}	inactive	51°C	1.68	1.19	0.409	0.49
				3.5	3.02	0.93	0.98
				7.9		1.97	1.99
I	Br^{82}	inactive	77°C	1.68	1.17	0.307	0.49
				3.5	3.03	0.81	0.98
				7.9		1.85	1.99
III	gravimetric	alcohol	50°C	6.06		1.61	1.73

TABLE V. EQUILIBRIUM ABSORPTION OF LiBr FROM SOLUTION BY HAIR AT HIGHER TEMPERATURES

Hair	Tracer	Wash	Temp. (°C)	Concentration (M/1000 g. water)	Uptake (mM/g.)	Uptake at ~25°C (mM/g.)
I	Br^{82}	alcohol	50	0.0032	0.00098	0.0011
				0.016	0.0065	0.0063
				0.032	0.0093	0.011
				0.116	0.036	0.050
				1.20	0.54	0.55

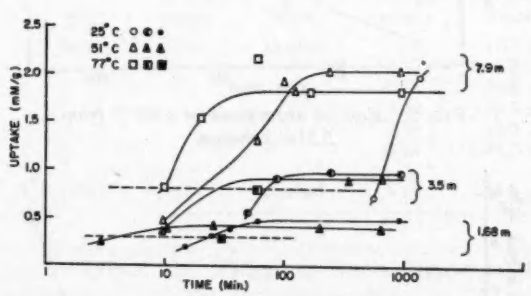

FIG. 2. *Rate of absorption of $NaBr^{82}$ by hair at three concentrations and three temperatures.*

tration is obtained. Results, using the direct technique, are given at the bottom of the table. The uptake values found with the replacement technique are plotted in Figure 1. As is noted, the rate of attainment of equilibrium is very slow at the highest concentrations, and the values of the uptake found at these concentrations may be low.

In Table III some equilibrium uptake values for KBr and NaCl are given. All results in Table III were taken using hair *I*.

Effect of temperature on equilibrium absorption.—Results for equilibrium absorption at higher temperatures are given in Table IV for NaBr, and in Table V for LiBr.

Although there is some scattering of individual points, comparison of the data at higher temperatures with the data for the same solutions at ~25°C, given in the last column, shows that the amount of salt absorbed at a given concentration decreases as the temperature increases.

Rates of absorption.—In Figure 2 rate of absorption results, taken using $NaBr^{82}$ solutions, are shown for three temperatures, 25°, 51°, and 77°C, and three molalities, 1.68, 3.5, and 7.9*m*. The solid lines represent visual estimates of the time path of each process, and are included for convenience in examining the figure. The dotted lines were drawn in cases where the rate was too fast to be followed by our methods. Since the points on these dotted lines are equilibrium points, presumably the experimental curve, if filled in, would be parallel to the abscissa in the time range shown.

The usual marked increase in rate with increase in temperature is evident, as is a decrease in equilibrium absorption with increase in temperature. A marked decrease in rate with increasing salt concentration is also apparent.

The rate of absorption of $Na^{22}Br$ by hair from a 7.82*m* $Na^{22}Br$ solution at room temperature is shown

in Figure 3, and the rate of absorption of KBr^{82} from a 1.85*m* solution is shown in Figure 4.

In Figure 5 the rate of absorption at $LiBr^{82}$ by a hair placed in a 5.51*m* solution at ~25°C is shown. In each of Figures 3–5 the solid curve was derived using Fick's Law. In Figure 6 is shown the rate of absorption of $LiBr^{82}$ by hair on transfer from a solution of concentration 8.2*m* to a solution of concentration 13.5*m*. The remarkably slow attainment of equilibrium which has been mentioned as the cause of the uncertainty of the values for equilibrium absorption from solutions of high concentrations is plainly evident.

In some cases the equilibrium values read from the rate curves differ slightly from those listed in the tables for solutions of the same concentration. In such cases the values in the tables include other samples in addition to those from the rate curves.

The rate of desorption of LiBr and NaBr from hair into various solvents will be considered in the discussion of washing of hair in preparation for counting. See Appendix I.

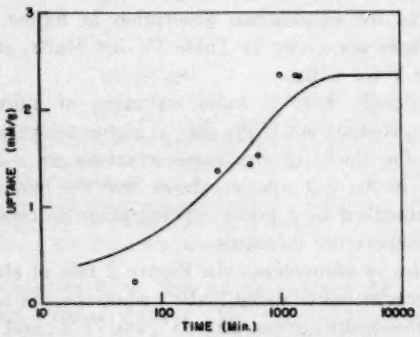

FIG. 3. *Rate of absorption of $Na^{22}Br$ by hair from 7.82*m *solution.*

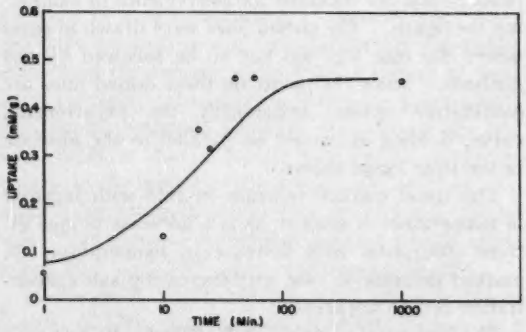

FIG. 4. *Rate of absorption of KBr^{82} by hair from a 1.85*m *solution.*

As discussed previously [15], the results of the rate experiments are subject to an undetermined error caused by the application to nonequilibrium results of a self-absorption correction factor determined from equilibrium measurements. This error must necessarily be less than the self-absorption correction and is probably negligible. Also, each point on a rate curve usually represents an average value for fewer hairs than is the case with the equilibrium points. Finally, continuous agitation was lacking and probably not necessary in single fiber experiments.

Water-Absorption Measurements

Measurements made using NaBr solutions and one experiment with an NaCl solution are tabulated in Table VI. Measurements made using LiBr solutions are shown in Table VII. The results for NaBr and LiBr solutions are shown in Figure 7 along with the absorption isotherm for salt-free hairs taken by Chamberlain and Speakman [4]. Since the experiment was designed to measure the amount of water present in a sample when it is at equilibrium in a solution, the amount of water taken up is

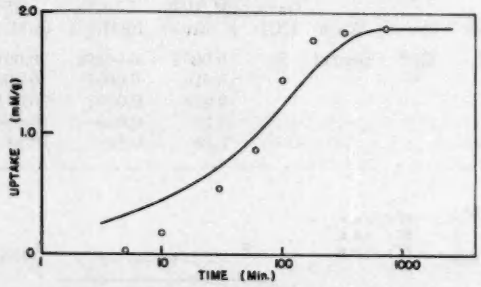

FIG. 5. *Rate of absorption of $LiBr^{82}$ from 5.51*m *solution.*

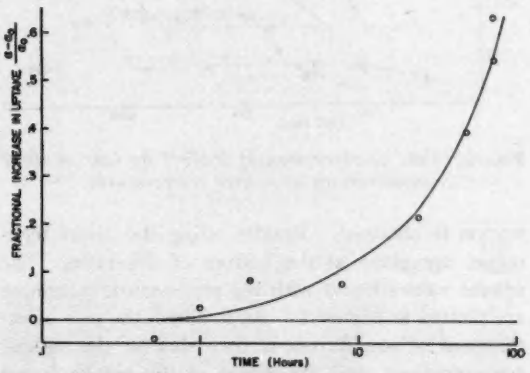

FIG. 6. *Rate of absorption of $LiBr^{82}$ by hair on transfer from an 8.2*m *solution to a 13.5*m *solution.*

designated "equilibrium water" in Tables VI and VII. The standard regain of salt-free hairs at the relative humidity of the treating solution is given for comparison. The amounts of salt taken up from the solution are also shown. These differ from the values shown in Tables I and II because they have not been corrected by the factor discussed previously to equivalent values for hair *I* using an alcohol rinse. These uncorrected salt uptakes were used with the equilibrium water measurements to determine the number of moles of salt within the fiber per 1000 g. of water, which can be called the "internal molality," shown in the last column of each table. Uncorrected salt uptakes were used rather than the values in Tables I or II because there was no apparent way to determine a correction factor for the water absorbed. It seemed preferable to be consistent and use uncorrected results throughout in the determination of internal molality. The use of salt absorption values from Tables I and II and water absorption values from Tables VI and VII will give internal molalities roughly 15% lower than those shown. Such a change will not alter the basic conclusions drawn from these results.

In Figure 8 the internal molality is plotted against the external molality. Finally, in Table VIII some results are given on the water uptake as a function of the relative humidity for hairs containing 2.94 mM/g. LiBr.

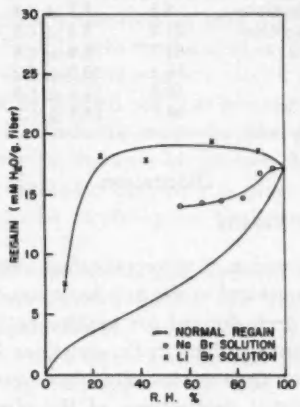

FIG. 7. *Water uptake of salt-free and salt-containing hairs (normal regain from Chamberlain and Speakman [4]).*

TABLE VI. AMOUNT OF WATER PRESENT IN HAIR AT EQUILIBRIUM IN NaBr AND NaCl SOLUTIONS AT ~25°C

Salt	Hair sample	Wash	Concentration (M salt/1000 g. water)	Equil. water (mM/g.)	Equil. salt (mM/g.)	Standard regain (mM/g.)	Internal molality (M salt/1000 g. water)
NaBr	*III*	alcohol	1.55	17.2 ± 0.8	0.56 ± 0.03	15.1	1.81 ± 0.12
			3.02	16.8 ± 0.4	1.13 ± —	13.4	3.74 ± —
			4.44	14.8 ± 0.5	1.24 ± 0.11	11.7	4.64 ± 0.43
			6.06	14.6 ± 0.7	1.98 ± 0.28	10.0	7.5 ± 1.1
			7.46	14.4 ± 1.4	2.30 ± 0.26	8.7	8.9 ± 1.3
			9.13	14.1 ± 1.2	2.81 ± 0.21	7.4	11.0 ± 1.2
NaCl	*III*	alcohol	6.15	14.1 ± 1.4	1.86 ± 0.22	10.3	7.3 ± 1.1

TABLE VII. AMOUNT OF WATER PRESENT IN HAIR AT EQUILIBRIUM IN LiBr SOLUTIONS AT ~25°C

Hair sample	Wash	Concentration (M salt/1000 g. water)	Equil. water (mM/g.)	Equil. salt (mM/g.)	Standard regain (mM/g.)	Internal molality (M salt/1000 g. water)
Ia	benzene-acetone	2.60	18.6 ± 1.5	1.29 ± 0.20	13.2	3.8 ± 0.7
		5.40	19.4 ± 0.6	3.15 ± 0.28	9.3	9.0 ± 0.8
		8.70	17.9 ± 2.1	5.7 ± 0.3	6.1	17.6 ± 2.3
		12.03	18.2 ± 1.6	8.5 ± 0.2	3.9	25.8 ± 2.3
		16.75	7.5 ± 1.1	7.5 ± 0.5	2.2	55 ± 4
	alcohol	8.70	18.9 ± 4.1	52. ± 0.9	6.1	15.3 ± 4.3

TABLE VIII. UPTAKE OF WATER BY HAIR CONTAINING 2.94 MM/G. LiBr AS A FUNCTION OF RELATIVE HUMIDITY AT 25°C

Hair sample	Wash	R.H. (%)	Water uptake (mM/g.)	Standard regain (mM/g.)
Ia	benzene-acetone	8.5	5.7 ± 1.8	2.2
		21.8	6.4 ± 0.8	3.8
		44.7	8.9 ± 1.4	6.1
		56.3	13.0 ± 0.2	7.4
		60.5	14.4 ± 1.3	8.0
		69.7	18.4 ± 1.2	9.3

Discussion

Equilibrium Results

In the discussion of the equilibrium absorption results it is convenient to use as a basis some equations which have been derived for application to dye absorption. Since nothing in the equations limits their application to dyes exclusively, they serve equally well as potential descriptions of the absorption of alkali bromides.

The equations, which refer to the absorption of a uni-univalent electrolyte from a binary solution, can be written in the present case:

$$\frac{-\Delta\mu^\circ}{RT} = \ln\frac{X^f}{V^f} + \ln\frac{\mathrm{Br}^f}{V^f} - \ln[X]^s - \ln[\mathrm{Br}]^s, \quad (1)$$

$$\frac{-\Delta\mu^\circ}{RT} = \ln\frac{\mathrm{Br}^f}{B_{\mathrm{Br}^f} - \mathrm{Br}^f} + \ln\frac{X^f}{V^f} - \ln[X]^s - \ln[\mathrm{Br}]^s, \quad (2)$$

$$\frac{-\Delta\mu^\circ}{RT} = \ln\frac{\mathrm{Br}^f}{B^f - \mathrm{Br}^f} + \ln\frac{X^f}{B^f - X^f} - \ln[X]^s - \ln[\mathrm{Br}]^s, \quad (3)$$

where $\Delta\mu^\circ/RT$ is a constant containing a free energy term and the temperature, X^f and Br^f are the number of moles of cation and bromide ion absorbed per gram of fiber, V^f is the amount of the fiber volume occupied by an internal solution per gram of fiber, and $[X]^s$ and $[\mathrm{Br}]^s$ are the concentrations of cation and bromide ions in the external solution. B_{Br^f} in equation (2) represents the number of sites for the absorption of bromide ion per gram of fiber, and B^f in equation (3) represents the number of sites for bromide ion absorption as well as the number of sites for cation absorption since these have been assumed to be equal in the derivation of equation (3).

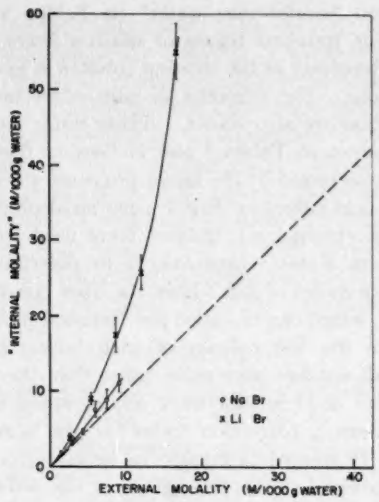

FIG. 8. *"Internal molality" as a function of the molality of the external solution.*

It is not the purpose of this paper to discuss the derivation of these equations. A detailed discussion of the equations and their application to experimental results on dyeing has been given by Vickerstaff [19]. Certain features about the physical meaning and limitations of these equations, however, should be mentioned.

The first two terms on the right-hand side of equation (1) represent the concentration of each ion within the fiber in terms of the amount of the ion and the volume of solution. Equation (1) can also be expressed in terms of molal instead of molar concentrations. The molal scale is certainly as acceptable as the molar, and probably even more because of the difficulty in determining V^f experimentally. Thus equation (1) can alternatively be written

$$m^f = km^s, \quad (4)$$

where $k = e^{-\Delta\mu^\circ/2RT}$, and m^f and m^s are the molalities of the fiber phase and the solution phase, respectively.

The advantage of using the molality (or molarity) as a measure of the partial molal free energy of the solute in a solution lies in the fact that in dilute solution it is a measure of the mole fraction. The use of the mole fraction as a meaure of partial molal free energy can be justified theoretically for a simple model in which complete random mixing occurs be-

tween the solvent and solute. Correction terms for cases in which the random mixing is slightly modified by specific solvent-solute interaction or electrostatic interaction between ions can also be developed theoretically and introduced as activity coefficients. For more concentrated solutions in which the corrections are no longer slight, it is convenient to retain the product of the molality and the activity coefficient as a measure of the partial molal free energy since it is a logical extrapolation of the procedure for dilute solutions, although such a procedure becomes empirical.

The remarks in the preceding paragraph apply equally well to the use of the molality within the fiber. If a dilute external solution is considered, equation (1) or (4) can be derived on the assumption that the water and salt within the fiber exist as an ideal solution which is identical with the external solution except for the influence of an absorptive potential provided by the surfaces of the pores of the fiber. When more concentrated solutions are considered, equation (4) will retain its validity if the activity coefficients are identical in the fiber and out. This again implies that, except for the action of a weak absorptive potential, the solution within the fiber is the same as the solution outside of the fiber. Large differences between activity coefficients in the fiber and in the solution would indicate strong specific forces within the fiber. In such a case, some other mechanism of interaction is to be sought [for example, that which leads to equation (3)], and there is little or nothing to be gained in retaining the form of equation (1) or equation (4) with activity coefficients added.

Equation (3) can be derived on the assumption that each ion can be absorbed onto a site within the fiber. All sites of each type (for cation or anion) are assumed to be identical, and the absorption of one ion is assumed not to influence the absorption of a neighboring ion. Equation (3) can be written

$$a = \frac{B'ka}{1 + ka}, \qquad (5)$$

where a is the amount of salt absorbed, k is a constant, and the activity of the salt in the solution has been used in place of its concentration, thus enabling the equation to be used with solutions of higher salt concentration.

Equation (2) is obviously intermediate between equation (1) and (3). All of the assumptions of both equations (1) and (3) are inherent in equation (2), except that only one ion (the anion has been chosen) is assumed to be absorbed onto sites. It has also been assumed that, for practical purposes, all of the anions within the fiber are absorbed on sites. Since there seems to be very little reason to choose either the bromide ion or the alkali cation as being specifically absorbed on sites when the other is not, equation (2) will not be used in the discussion of the experimental results.

It might be pointed out that in none of equations (1)–(3) is allowance made for the possibility of mixing between segments of polymer chains and absorbed molecules or ions, such as plays a prominent part in theories of absorption by rubber-like materials [6].

Some consequences of equations (4) and (5) can now be examined. Consider first the case where $k = 1$ in equation (4). In this case the internal and external solutions are identical, and the solution is merely filling void space in the fiber. No swelling beyond the swelling produced by water would occur. Also, there would be no change (for practical purposes) in the amount absorbed from a solution of a given molarity with a small temperature change. The internal and external molalities would be the same, and the amount of salt within the fiber would be independent of chemical type and linear with molar concentration.

Figure 1 shows a plot of the salt absorption data against the molar concentration. The solid line is a 45° line such as would be expected from the above model [see equation (1)]. The line is a good representation of all of the points; however, lines for NaBr and LiBr would be different, the latter having a slightly greater slope than the 45° line and the former a slightly smaller slope. The swelling produced by alkali bromide solutions (especially LiBr solutions), which has been discussed previously [1], the effects of temperature shown in Tables IV and V and Figure 2, and the differences in internal and external molality shown in Tables VI and VIII and Figure 8 all combine to eliminate the simple filling of void space in the fiber as a possible mechanism for the absorption of these salts.

The elimination of forms of equation (4) in which $k \neq 1$ is more difficult. In this case, the value of k can be expected to be different for different salts, and the temperature effects can occur. Also, differences in internal and external molality can be expected. However, it is well known [10] from heat of absorp-

tion and other measurements that a portion of the water absorbed by a hair is strongly absorbed and cannot be considered to be liquid water available to act as a solvent. The presence of this portion of the absorbed water within the fiber makes it likely that, for any internal solution theory to apply, the internal molality must be less than the external molality. In the present case the reverse is true. It seems probable that the existence of an absorption potential strong enough to cause the internal molality to be greater than the external molality implies the existence of localized absorption forces of such strength that mixing of ions and water molecules identical with that in the external solution is impossible. The existence of extensive swelling beyond the water-swollen state has similar implications. The work done against cohesive forces in the hair during swelling is difficult to estimate quantitatively. However, it probably is large enough to require correspondingly large heats of absorption, since the entropy increase resulting from polymer-monomer mixing can be assumed to be small.

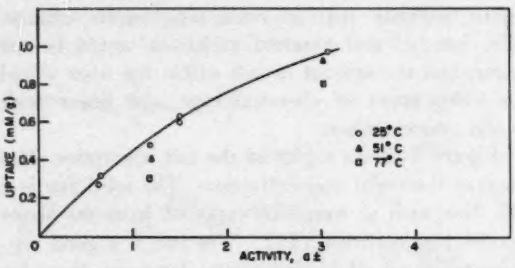

FIG. 9. *Absorption isotherms for NaBr on hair.*

Equation (5) can now be considered. When ka is small, α is linear with respect to a with a slope $B'k$; when ka is large, α approaches B' asymptotically. Thus, a plot of α against a should have a constantly decreasing slope and approach some limiting value B'. In Figure 9 some of the results on the uptake of NaBr are plotted against the mean ionic activity of the salt in the external solution. Results for three different temperatures were used. It is evident that curves through the points would have the required shape. In Figure 10 all of the results for the absorption at 25°C of LiBr, NaBr, and KBr are plotted against the activity of the salt. A log-log plot is used because of the range of the results. Two features of Figure 10 may be pointed out—the results for the three bromides fall along the same curve, and the apparent existence of a maximum absorption value is in the vicinity of 8–10 mM/g. fiber. The close correspondence in the dependence of the uptake on the activity for the three salts suggests that the dominant factor in determining the free energy of the salt in the fiber is the same in each case. The absorption of the bromide ion on sites within the fiber is a possible common process.

An absorption maximum in the region 8–10 mM/g. would correspond closely with the number of amino acid residues since the average residue weight in wool is about 110–120 g./M [18], although this is probably a fortuitous occurrence. It seems likely that the salt penetrates throughout the fiber in view of the fact that above concentrations of about 5*M* LiBr (activities of > 20) the characteristic x-ray pattern of the keratin is replaced by a diffuse amorphous halo [7]. The original x-ray pattern of the

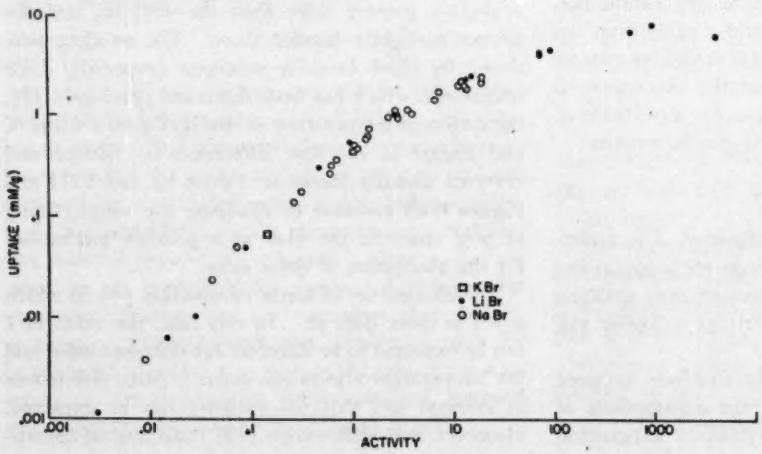

FIG. 10. *Uptake of alkali bromides as a function of activity.*

hair is recovered when the salt is washed out, so that this part of the change is reversible. However, the swelling recovery is slow [1]. The mechanical properties of the hair are also markedly altered when they are in equilibrium with LiBr solutions of similar concentrations [16].

The water content of the fibers can now be considered. It is evident from Figure 7 that considerably more water is present within a fiber containing salt than is absorbed by salt-free fibers at the same relative humidity. At the same time it is evident from Figure 8 that the salt is selectively absorbed from the solution since the internal molality, which is a ratio of the amount of salt to the amount of water within the fiber, is greater than the external molality. Although the internal molality, being a derived value involving two experimentally measured quantities, may be in error up to 10% or 15%, it is clear that the difference between external molality and internal molality is real except possibly in dilute NaBr solutions. From Table VIII it is also evident that the presence of a fixed amount of LiBr within the fiber increases the amount of water absorbed at all relative humidities.

The explanation of this behavior would seem to lie in the properties of the alkali ions. The alkali ions are known to be heavily hydrated in aqueous solution, and it seems reasonable that at least part of the hydrate water bound to a lithium or sodium ion in solution would accompany it into the fiber. Thus, the water within a fiber containing salt serves two purposes—it satisfies the natural absorptive forces within the fiber, and it fills the hydration spheres of the small, highly charged, alkali cations. A rough measure of the amount of water involved in hydrating ions can be obtained by comparing the excess water absorbed beyond the standard regain with the amount of salt in the fiber. This is done in Figure 11. The number of moles of excess water per mole of salt runs from 1 to 4, depending on conditions. These are reasonable values for the water of hydration of lithium or sodium ions [3]. It seems possible that hydrated cations and water molecules compete for absorption sites within the fiber, and that actually less free water is absorbed in the presence of salt, although more total water is absorbed.

The results on salt uptake from a given solution as a function of temperature give an indication of the heat evolved during a transfer of salt from the external solution to the fiber. It can be shown that, unless the salt is absorbed independently of any other component of the external solution, the use of the Clausius-Clapeyron equation to obtain the heat of absorption is not justified. If all interactions between salt and water within the fiber are ignored, the heats of absorption given in Table IX can be obtained. Until more is known about the state of the salt and the water within the fiber, the value of these heats is dubious.

Since the physical nature of the absorption of alkali halides by hair seems to point to absorption onto sites as the most plausible model of the absorption process, it is logical to attempt to apply equation (5) to the experimental results. If equation (5) holds, it can be seen that a plot of $1/\alpha$ against $1/a$ should be a straight line. A plot of the results in Figure 10 in this form does not give a straight line, and hence equation (5) does not hold. Actually there is ample reason from the experiments done to expect that equation (5) would be an oversimplification. Four factors have been ignored which can be expected to alter the equation substantially.

From the chemical constitution [18] of keratin it can be seen that there are approximately 0.8 meq./g.

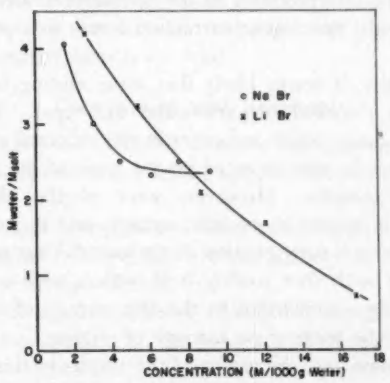

FIG. 11. *Moles of water absorbed, in excess of normal regain, per mole of salt absorbed as a function of the concentration of the external solution.*

TABLE IX. HEAT OF ABSORPTION OF NaBr FROM AN INFINITELY DILUTE SOLUTION AT ~35°C ASSUMING NO SALT–WATER INTERACTION WITHIN THE FIBER

Uptake of salt (mM/g.)	ΔH (cal.)
0.33	−4000
0.46	−2500
1.0	−1600

of free acidic and also of free basic groups on side-chains in the fiber. These are known to be ionized in the presence of water. These ions along with absorbed ions will create a concentration of charged particles such that a large electric-interaction free energy will necessarily be present.

The complex chemical nature of keratin makes it unlikely that all sites within a fiber would be equivalent even as isolated sites. However, even if such equivalence exists, physical factors are present which would prevent equivalence within the fibers. It has been shown that an increase in swelling accompanies salt absorption, and that in certain concentrated solutions the physical structure is so disrupted that the x-ray pattern of the fiber is destroyed. These two effects are external evidence of work done against internal cohesive forces, and this work is done at the expense of the free energy of absorption. Since this work is undoubtedly not the same for sites in crystalline and amorphous regions, a spectrum of absorption energies can be expected.

It is also possible that there is competition between the solvent, water, and the salt for absorption sites. This alone would not necessarily alter the form of equation (5) in the simplest case, but would alter the interpretation of the constants in any event, and might necessitate correction terms in a practical case.

Finally, it seems likely that some mixing between weakly absorbed ions and water will occur. Mixing to the same extent as occurs in the external solution has already been rejected on the basis of the experimental results. However, some of the absorbed water is known to be held weakly, and it would be surprising if some portion of the ions did not undergo mixing with this weakly held water, with a corresponding contribution to the free energy of absorption in the form of an entropy of mixing.

In summary, discussion of the results in this paper in terms of equations (1)–(3) shows that neither equation (1) nor equation (3) provides an adequate description of the results. Equation (2) has not been considered as extensively, but also is not satisfactory. The fact that none of these three equations is satisfactory is not unexpected. Each has been derived using a model known to be an oversimplification which omits certain factors of fiber behavior.

It is probable that an accurate description of fiber behavior would combine features from all three models and also factors such as ionic interaction and the physical heterogeneity of the fiber, which are not considered in any of the models. To this extent the models are not mutually exclusive, and each could form the basis for a satisfactory description. However, the experimental results make it seem likely that a suitable elaboration of the model which forms the basis for equation (3) would be the most satisfactory. In other words, a model of absorption of ions onto sites duly modified to account for ionic interaction, a variety of absorption sites, competition between water and ions for these sites, and swelling would seem most appropriate. Further experiments are necessary to determine the magnitude and form of these various corrections and to decide whether or not an entropy of mixing should be included.

Some mention should be made of the apparent parallelism between the uptake of simple acids and alkali halides on the one hand, and acid and milling dyes on the other. Vickerstaff [19] differentiated between acid and milling dyes in the following ways. Acid dyes are absorbed at an optimum pH of between 2 and 4. There is a well-defined break in the curve of absorption against external concentration corresponding closely with the maximum found for simple acids and the maximum predicted from the chemical analysis of keratin. Acid dyes can be taken up beyond this maximum, but changes in fiber properties indicate that the dye absorbed beyond the maximum is held in a different manner than the rest of the dye. The optimum pH range for the absorption of milling dyes runs from 5 to 7. The maximum absorption for milling dyes is much greater than that for acid dyes.

From this brief description it seems possible that alkali halides and milling dyes attach themselves to the same series of sites. If this is true, the alkali halides can provide information on the absorption of milling dyes in the same way that the absorption of simple acids provides information on acid dyeing.

Rate Experiments

The rate experiments shown in Figures 2–6 were done primarily to provide evidence on the time of immersion necessary to ensure the attainment of equilibrium. Because of the possible errors mentioned previously, only qualitative conclusions can be drawn from them.

It can be seen from Figure 2 that there is an appreciable increase in rate of penetration with in-

crease in temperature, which means that there is an appreciable activation energy for the absorption process. A marked decrease in rate of absorption with increase in concentration of salt in the external solution is also noticeable. This effect of concentration on the rate of absorption when LiBr solutions were used and the metastable states which result have already been discussed both in this paper and in previous work on swelling [1]. Further evidence can be obtained by comparing Figures 5 and 6.

In Figures 3, 4, and 5 the solid lines have been drawn in attempts to apply Fick's Law to the diffusion process. Fick's Law was used in a form suitable for absorption by a uniform cylinder of constant diameter which is initially empty of diffusant, in a bath providing a constant surface concentration of diffusant [2]. The diffusion constant was assumed independent of concentration within the fiber. Similar applications of Fick's Law to the diffusion of Na^{22} from an NaCl solution and of Br^{82} from an NaBr-HBr solution have already been discussed [15]. For the results shown in Figures 3–5 the theory does not provide an adequate fit of the experimental values, as was also the case with the rate of absorption of NaCl. The experimental points rise too abruptly to be fitted by Fick's Law; the effect is similar to what would be found if the diffusion constant increased as salt was absorbed.

Although the hairs were preswollen in water vapor before treatment, it seems likely that the state of swelling varied in a complex way during treatment. In previous work [1] it was shown that the swelling of a hair transferred from water to a 5.7*m* LiBr solution passed through a minimum with time, showing that diffusion of water from the fiber and salt into the fiber occurred at different rates. In very concentrated solutions this resulted in the need for a replacement technique and metastable equilibria, as shown in Table II. Since the diffusion constant can be expected to be roughly proportional to the degree of swelling, a possible reason for the existence of an induction period is established.

In addition to swelling, the morphology of keratin fibers can be expected to complicate rate of absorption phenomena. It is known that keratin fibers have a thin membranous layer, the epicuticle on the surface, and a layer of scales under this [11]. These outer layers are resistant to diffusion, and hence can be expected to change the diffusion properties from those of an ideal cylinder.

TABLE X. DIFFUSION CONSTANTS FOR DIFFUSION IN HAIR

Solution	Concentration (M/l.)	D (cm.²/sec.)
$Na^{22}Cl$	0.99	3.2×10^{-9}
KBr^{82}	1.71	7.2×10^{-10}
$LiBr^{82}$	4.80	1.9×10^{-10}
$Na^{22}Br$	6.36	3.8×10^{-11}

Other causes for deviations from Fick's Law for polymer systems have been proposed and discussed. In particular, Crank studied absorption processes in which swelling and other complications occur, and may be consulted for further information [5].

If, in spite of the inapplicability of Fick's Law, the diffusion constants are used as an index of the type of diffusion process occurring, it is evident that the process is not a simple aqueous diffusion. Aqueous diffusion processes involving simple salts have diffusion constants of the order of 10^{-5} to 10^{-6} cm.²/sec. [8]. The diffusion constants for penetration of the fiber, given in Table X, are several orders of magnitude smaller than aqueous diffusion constants. This is confirming evidence for the strong influence of the fiber material on absorbed molecules or ions and the essential disparity between the external solution and the water and salt within the hair. The marked reduction of the diffusion constant with increasing salt concentration is evident.

Conclusions and Summary

In brief, the following features are apparent from the absorption and swelling experiments carried out so far.

1. Alkali bromides are taken up by hair in a manner primarily dependent on the activity of the salt in the treating solution.

2. The amount of water absorbed is increased over the normal regain by the presence of the salt in the hair.

3. The internal molality is greater than the molality of the external solution.

4. The uptake of salt and water by the hair causes swelling. The swelling, in general, is greater than that produced by water alone.

5. The rates of absorption of salt are slow, much slower than the rates of diffusion of the same salts in water.

6. Both the rates and equilibrium uptakes are temperature-dependent, the amount of salt absorbed decreasing with an increase of temperature.

The experimental results seem to be the most compatible with a theory of absorption of ions onto sites within the fiber. The alkali cations must be assumed to be hydrated when absorbed. It is possible that the absorption of the solute ions competes with the absorption of water.

The results, for the most part, apply to more concentrated solutions than are usually present in technical processes such as dyeing. However, there is no reason why the mechanism of interaction most probable for the more concentrated solutions should not apply in the case of more dilute ones. Perhaps, with appropriate refinements, rate of absorption and equilibrium absorption measurements can be made with more dilute solutions to give evidence on this point.

Appendix I

Experimental Techniques

Radioactive-Tracer Techniques

The washing technique used previously in absorption experiments [15] consisted of immersion of fibers which had been treated with a radioactive solution in a solution of identical chemical composition and concentration as the treating solution but containing no radioactive component. The washing was thus an exchange process and it is obvious that such a method would not be acceptable for use with a gravimetric technique. Accordingly, attempts were made to find satisfactory volatile wash liquids.

Two criteria were used to determine the suitability of a given volatile wash liquid. In the first place, washed fibers were examined microscopically. If small crystals of salt were observed on the surface of the fibers, the wash liquid was considered to have dehydrated adhering droplets, leaving the salt as a contamination. The second criterion was that used in the exchange experiments—namely, the existence of a plateau in the short-time region of a plot of activity on the fibers against the logarithm of immersion time in the wash liquid.

In Figure 12 the activity of hairs brought to equilibrium in 7.82*m* $Na^{22}Br$ solution is plotted against the logarithm of the washing time for three wash liquids—water, ethyl alcohol, and an inactive solution. The points were determined by removing fibers from the wash liquid and measuring their activity. Each point represents an average for two or more fibers. Different fibers were used for each point, the fibers being chosen to minimize effects resulting from variations in diameter. It is evident that the criterion of a plateau in the short-time region of the plot is met for the alcohol wash and for the inactive wash. However, the curve for a water wash has quite a steep slope over all the practical time range for washing and hence water is not a satisfactory wash liquid. There is a difference of roughly 8% between the activity of hairs washed for 1 sec. with an alcohol wash and those washed with an inactive wash. The reason for the lower activity of the hairs washed with inactive solution is not known. Possibly the state of adsorption on the outer surface of the fiber is different in the two cases.

Figure 13 shows results of washing experiments made on fibers containing $LiBr^{82}$. In this figure the activity relative to fibers washed for 1 sec. is plotted. Four curves are shown. The curves for water and the inactive solution were obtained using hairs in equilibrium with a saturated LiBr solution. The inactive wash solution was also saturated. The curves for the alcohol wash were obtained using

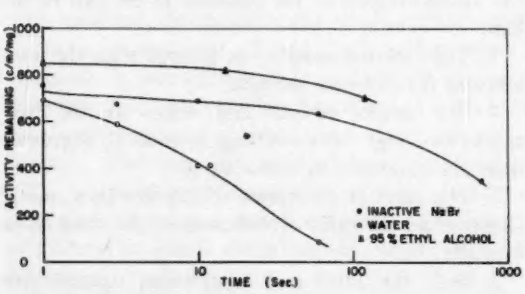

FIG. 12. *Rate of removal of $Na^{22}Br$ from hair by various wash liquids.*

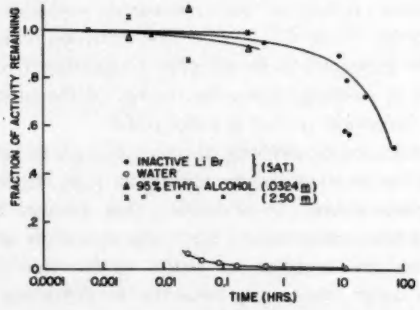

FIG. 13. *Rate of removal of $LiBr^{82}$ from hair by various wash liquids.*

hairs at equilibrium with a 2.50*m* solution and hairs at equilibrium with a 0.0324*m* solution. A relative scale was used for the ordinate so that all of the curves could be included in a single plot. Again, water would be an unsatisfactory wash liquid, but an alcohol wash or an inactive wash is satisfactory. As was the case with the sodium salt, the total activity of hairs washed with alcohol was slightly higher than for those washed with inactive solution.

Self-Absorption Correction Factors

As in previous work [15], hair was coiled in a loose spiral on a metal disc coated with albumen fixative and counted. The counts were then compared with those from a standard, formed by evaporating a few milliliters of a solution of known chemical composition on a similar disc, and a self-absorption correction was applied.

In comparing the activity of a fiber sample with that of a standard, three effects—absorption, scattering, and geometry—combine to make up the practical self-absorption coefficient. The thickness of the standard is such that self-absorption removes a negligible fraction of the total radiation. The fiber, on the other hand, may be thick enough to remove an appreciable fraction of the total radiation. The fraction removed depends on the diameter and density of the fiber and on the average energy of the radiation used, which in turn depends on the isotope being used. The primary scattering effect is an increase in the measured activity because of back-scattering from the backing material. For the standard, the backing surface is stainless steel. For the fiber, the backing surface is stainless steel covered with a thin layer of albumen from the fixative. This change with backing material may sometimes be quite appreciable. Finally, it is obvious that differences in geometry exist between sample and standard.

Although some approximate theories of self-absorption exist, it is impossible to apply them rigorously to the case at hand, and, in any event, the theories are not good enough to give more than an order-of-magnitude correction factor. For this reason it is advisable to measure standards and samples under conditions as similar as possible and to determine self-absorption factors experimentally.

Since the self-absorption correction factor depends on the nature of the radioactive isotope used, each isotope must be considered separately. Two direct methods of determining the self-absorption correction have been used. In the first, the fibers mounted on discs for counting are dissolved using an appropriate volatile solvent and the solvent is then evaporated off. This forms a thin film in place of the fiber, thus minimizing self-absorption. In the second method, the fiber is leached with water rather than mounted on a disc. An aliquot of the water solution is then evaporated onto a disc and compared with the standard. The fiber then can be re-treated with solution and mounted in the conventional way to give a mounted activity for determination of a self-absorption coefficient. Each method has certain advantages and drawbacks.

When the salt is leached out of a fiber and the fiber re-treated with solution so that it can be mounted on a disc and counted, there is a chance that the fiber will not contain the same amount of salt on re-treatment as it held initially because of differences resulting from the treatment and rinsing. If different sets of fibers are used for leaching and mounting, error arising from fiber-to-fiber variation is introduced which lowers the precision of the self-absorption determination. If the mounted fiber is dissolved on the disc, there is no possibility of a difference in amount of salt present in the fiber initially. However, there is a possibility that activity can be lost as a volatile component during evaporation of the solvent.

If the mounted fiber is dissolved, the final sample for counting consists of a thin radioactive protein film. This is still different from the standard, where no protein film is present, and differences in back-scattering, or possibly a slight amount of self-absorption, are possible. Furthermore, the volatile solvents which can be used to dissolve hair, such as nitric acid or tetramethyl ammonium hydroxide, are chemically very active. It seems likely from the results of these investigations that they can be expected to alter the surface of such metals as stainless steel, which, for practical purposes, are resistant to them, in such a way as to change their properties as backing materials. The data in Table XI were taken in the following way. A standard was prepared and counted. Another standard was then prepared on a disc which had been coated with albumen, and an untreated hair was dissolved on the disc using the solvent listed. The ratio of the activity of the treated standard to the untreated standard is listed as I/I_o. If the standard is treated with a drop of

water and redried, the effect is negligible. Thus, results such as those in the first line of Table XI can be attributed to changes in scattering and self-absorption rather than to changes in geometry of the standard.

If the salt taken up by a hair is leached out of the hair and an aliquot of the resulting solution is evaporated on a disc and counted, the disc prepared in this way is almost identical with the standard. All problems arising from polymer films and etching of the surface of the backing disc are obviated. However, it is difficult to leach the last traces of salt out of the fiber. Experiments with $Na^{22}Br$ have shown that 2.7% of the Na^{22} remains on the fiber and another 1% is absorbed on the glass vessel during a leaching experiment. Finally, for some reason as yet unknown, probably resulting from the increased number of operations involving micro quantities of salt, the leaching method gave poor precision in all cases and in the case of Na^{22} gave spurious results, which are discussed later. Because of these difficulties, the dissolving technique was considered the primary method of obtaining self-absorption correction factors.

For Br^{82} the dissolving method, using tetramethyl ammonium hydroxide as a solvent and a stainless-steel disc as a backing, and the leaching method agreed with each other within the limits of experimental error. A plot of self-absorption against fiber weight for $NaBr^{82}$ with a stainless-steel backing is shown in Figure 14. The curve in Figure 14 was obtained from a least-squares line through a plot of log self-absorption factor against fiber weight. The true activity is obtained by dividing the apparent activity by the self-absorption factor.

This figure is shown primarily for illustrative purposes. The sensitivity of the curve to experimental conditions makes it advisable that others running similar experiments use their own experimentally determined curve, unless the technique is nearly identical with the one reported here.

This self-absorption curve has been applied to hairs containing LiBr and KBr, as well as NaBr. The efficiency with which matter absorbs β-rays is primarily dependent on the path length and density and is relatively insensitive to atomic number. Thus, no appreciable differences are to be expected in the self-absorption coefficient resulting from the use of different cations. The amount of salt present in the fiber when large amounts are taken up is of more importance. An estimate of the approximate amount of salt taken up can be used to determine an effective fiber weight (untreated fiber plus approximate weight of absorbed salt), which can be used to obtain a better estimate of the amount of salt taken up. More than one approximation is not necessary.

An independent experimental check of the self-absorption curve is provided by the results on the amount of salt absorbed as a function of concentration, determined gravimetrically. The details of the gravimetric method are given below. In Table I and Figure 1 the results of the two techniques are compared, and it is evident that, with allowances for differences in technique, the agreement is satisfactory.

An attempt was made to determine self-absorption factors for Na^{22}, using both dissolving and leaching techniques. However, the results of the leaching method were discarded. The apparent true activity of the fiber, as determined from the leachings, was less than the activity of the mounted fibers—*i.e.*, the self-absorption coefficient was greater than 1. The precision of the determination was very bad. While it is possible for what is defined here as the self-absorption coefficient to be greater than 1 because

TABLE XI. EFFECT OF BACKING AND DISSOLVING AGENTS FOR HAIR ON THE ACTIVITY OF RADIOACTIVE STANDARDS

Isotope and compound	Backing	Reagent	I/I_o
$Na^{22}Br$	stainless steel	HNO_3 + hair	0.80 ± 0.05
$Na^{22}Br$	tantalum	HNO_3 + hair	1.01 ± 0.01
$Na^{22}Br$	stainless steel	$(CH_3)_4NOH$ + hair	0.96 ± 0.01
$Na^{22}Br$	tantalum	$(CH_3)_4NOH$ + hair	0.97 ± 0.01
$NaBr^{82}$	stainless steel	$(CH_3)_4NOH$ + hair	0.99 ± 0.02

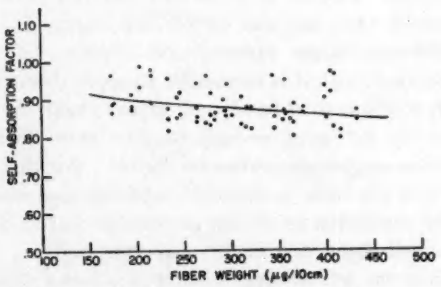

FIG. 14. *Self-absorption factor for Br^{82} in hair on a stainless-steel backing as a function of fiber weight.*

of scattering effects [12], the lack of agreement between the two methods of determining the self-absorption coefficient would still need to be explained. Furthermore, the self-absorption coefficient determined by dissolving gives salt uptakes in agreement with those determined gravimetrically and using Br^{82}.

It is not necessary that results obtained with Br^{82} agree with those obtained using Na^{22} if the fiber acts as an ion-exchange medium. However, although the pH of a treating solution was not measured systematically throughout its useful life, it was originally made up to a pH between 6 and 7, and spot checks showed that in most cases a pH close to 6 was maintained. At such a pH little or no acid or base absorption is to be expected, since the isoionic point of keratin lies at pH 6.2 [9]. Again the difference between the methods of measuring self-absorption could not be explained by selective absorption. For these reasons, the self-absorption factor was determined by dissolving the hairs in tetramethyl ammonium hydroxide on a stainless-steel backing. The average self-absorption factor, using Na^{22}, was essentially independent of fiber weight over the range of weights used, and was 0.86.

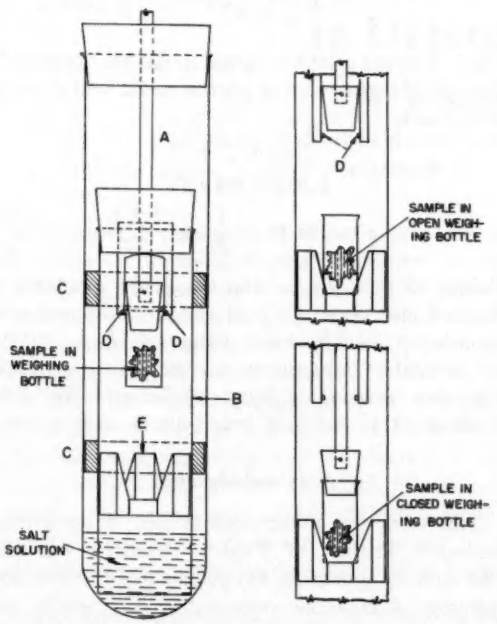

FIG. 15. *Remote-handling device for weighing bottles at constant temperature and relative humidity.*

Gravimetric Techniques

The principle of the gravimetric technique has already been explained. Measurements were made using NaBr and LiBr solutions.

Apparatus.—It was necessary, for this experiment, to have some method of exposing samples to atmospheres of different relative humidities and resealing them without exposing them to the room atmosphere. The simple remote-handling device shown in Figure 15 was devised for this purpose.

A small weighing bottle was equipped with a rubber stopper, which was fastened by a small piece of wire to the brass rod *A*, which fitted into a hole in the top of the stopper. The stoppered weighing bottle was put into an open-ended glass tube, *B*, which fitted into a large test tube containing a salt solution of the appropriate concentration. Both tubes were fitted with stoppers through which the brass rod passed. The arrangement of concentric tubes enabled the whole of the working part of the system to be well below the surface of the water in a thermostat which was set for 25.0° ± 0.1°C. The rings of electrician's tape, *C*, provided mechanical stability and helped isolate the lower end of the tube from the upper end, where temperature gradients were possible.

The weighing bottle was opened by pulling the brass rod up. This brought the lip of the weighing bottle against the fingers *D*, and the stopper was pulled from the bottle. The bottle dropped into a holder, *E*, made of pieces of rubber stopper cemented to the inner tube. To close the tube, the brass rod was pushed down, forcing the stopper into the bottle. The diagrams to the right in Figure 15 show the inner tube with the bottle open (top) and just as the bottle is closed (bottom).

Procedure.—Two separate runs were made. In the first, the amount of water taken up from a series of NaBr solutions was measured, and in the second, the amount of water taken up from a series of LiBr solutions. As a preliminary experiment, the amount of water absorbed by salt-free hair was measured as a function of the relative humidity at 30°C and compared with the data of Chamberlain and Speakman [4] taken at 25°C. As can be seen from Table XII, the agreement is good.

The procedure used with the NaBr solutions was as follows. Ten or fifteen hairs were used in each sample. The total weight of the sample was about 3000 μg. The dry weights were determined, and

TABLE XII. WATER ABSORPTION OF SALT-FREE HAIR AT 30°C COMPARED WITH DATA OF CHAMBERLAIN AND SPEAKMAN [4]

R.H. (%)	Regain at 30°C (%)	Chamberlain and Speakman's regain at 25°C (%)
5.95	4.2	3.2
50.9	12.7	12.2
55.8	13.2	13.3
83.5	21.4	21.7
93.3	25.1	25.2

the hairs were treated and washed after treatment as in the tracer experiments. A 2-sec. wash in 95% ethyl alcohol was used.

Several changes were made in working with LiBr solutions. Since tracer experiments had shown appreciable differences between different types of hair, the brunette hair (hair *III*) was not used, and in its place hair *Ia* was used. A 75% benzene 25% acetone wash liquid was used. This was later found to leave the surface of the fiber slightly contaminated; however, the error introduced in this way should be slight. A check using a 8.70*m* LiBr solution and an alcohol wash showed this to be true, as can be seen from the results. Finally, the fibers were dried in their weighing bottles, and the dry weight was determined directly. This method was selected because its use seemed more consistent with the rest of the experiment.

The fibers were left in the tubes for 48 hrs. or, in some cases, longer. This was found to be adequate for equilibrium by preliminary rate experiments.

Appendix II

Determination of Activities

In the tables reporting the experimental results, the activity of the salt solution in which the fiber was immersed is usually given. These activities were useful in the discussion. Except for two cases, the activities were determined using the molality of the solution and practical activity coefficients taken from Robinson and Stokes [14] or Harned and Owen [8]. The two cases mentioned are the activity of NaBr solutions above 4*m* at 25°C and of NaBr solutions at temperatures of 51°C and 77°C.

For NaBr solutions above 4*m* the vapor pressure data of Pearce, Taylor, and Bartlett [13] were used. One form of the Gibbs-Duhem equation can be written

$$\ln \gamma_{\pm 2} = \ln \gamma_{\pm 1} + (\phi_2 - \phi_1) - \int_{m_1}^{m_2} \frac{1 - \phi}{m}\, dm, \quad (6)$$

where $\gamma_{\pm 2}$ is the practical mean ionic activity coefficient at m_2 and $\gamma_{\pm 1}$ that at m_1, and

$$\phi = \frac{-55.51}{\nu m} \ln \frac{P}{P_o},$$

where P/P_o is the relative humidity, and ν is the number of ions formed on dissociation of the salt.

Pearce *et al.* calculated activity coefficients from their results using a long extrapolation in the low concentration range. Their activities do not agree well with those of Stokes and Robinson over the range in which they overlap. For the purposes of this paper, the value of $\gamma_{\pm}$ at $m = 2.5$ given by Stokes and Robinson was used as $\gamma_{\pm 1}$, and the necessary integration was done graphically. In this way, a maximum difference of 1% was found in the region of overlapping. In the higher concentration range the activities are probably reliable to 2%–3%.

For NaBr at temperatures of 51°C and 77°C, the activity data at 25°C were extended by using the equation

$$\log \gamma_{\pm}(T) = \log \gamma_{\pm}(25°C) + \frac{y}{\nu} \bar{L}\ (25°C) - \frac{z}{\nu} \bar{J}\ (25°C), \quad (7)$$

where $\bar{L}$ is the relative partial molal heat content of the salt, $\bar{J}$ is the relative partial molal heat capacity of the salt,

$$y = \frac{298.1 - T}{2.303R(298.1T)},$$

$$z = 298.1y - \frac{1}{R} \log \frac{298.1}{T}.$$

Values of y, z, $\bar{L}_{NaBr}$, and $\bar{J}_{NaBr}$ are available in Harned and Owen [8], as is also a discussion of equation (7). However, values of $\bar{L}_{NaBr}$ (25°C) are available only up to a concentration of 6*m*. For this reason, activity coefficients for 7.9*m* NaBr at 51°C and 77°C could not be determined.

Acknowledgment

This work was undertaken as part of the Dyeing Research Project of Textile Research Institute. The authors appreciate the guidance of the Project's Advisory Committee representing the textile and chemical manufacturing firms who sponsored this work. Two of us (W. S. B. and D. L. U.) wish

to thank Textile Research Institute for the grant of a fellowship held during the course of this work.

Literature Cited

1. Barnard, W. S., and White, H. J., Jr., TEXTILE RESEARCH JOURNAL **24**, 695–704 (1954).
2. Barrer, R. M., "Diffusion In and Through Solids," Cambridge University Press, 1941.
3. Bernal, J. D., and Fowler, R. H., *J. Chem. Phys.* **1**, 515 (1933).
4. Chamberlain, N. H., and Speakman, J. B., *Z. Elektrochem.* **27**, 374 (1931).
5. Crank, J., and Park, G. S., *Research* **4**, 515 (1951).
6. Flory, P. J., and Rehner, J., Jr., *J. Chem. Phys.* **11**, 512 (1943).
7. Hambraeus, E., and Steele, R. O., "International Congress of Sciences Applied to the Textile Industry" (collected papers), Ghent, 1951, p. 119.
8. Harned, H. S., and Owen, B. B., "The Physical Chemistry of Electrolytic Solutions," 2nd ed., New York, Reinhold, 1950.
9. Lemin, D. R., and Vickerstaff, T., in "Fibrous Proteins," Leeds, The Society of Dyers and Colourists, 1946, p. 129.
10. McLaren, A. D., and Rowen, J. W., *J. Polymer Sci.* **7**, 289 (1951).
11. Mercer, E. H., TEXTILE RESEARCH JOURNAL **23**, 388 (1953).
12. Nervik, W. E., and Stevenson, P. C., *Nucleonics* **10**, 18 (1952).
13. Pearce, J. N., Taylor, M. D., and Bartlett, R. M., *J. Am. Chem. Soc.* **50**, 2951 (1928).
14. Robinson, R. A., and Stokes, R. H., *Trans. Faraday Soc.* **45**, 612 (1949).
15. Stam, P. B., and White, H. J., Jr., TEXTILE RESEARCH JOURNAL **24**, 785–91 (1954).
16. Steele, R. O., *J. Soc. Cosmetic Chem.* **3**, 99 (1952).
17. Steinhardt, J., and Harris, M., *J. Research Natl. Bur. Standards* **24**, 335 (1940).
18. Traill, D., *J. Soc. Dyers Colourists* **67**, 257 (1951).
19. Vickerstaff, T., "The Physical Chemistry of Dyeing," New York, Interscience, 1950.

(Manuscript received May 27, 1954.)

Physical Chemical Studies Related to the Role of Whiteness-Retention Additives in Detergent Action*

W. Fong and W. H. Ward

Western Utilization Research Branch, Agricultural Research Service, U. S. Department of Agriculture, Albany, California

SEVERAL explanations have been proposed for the action of whiteness-retention additives in preventing the redeposition of soil during laundering. The ability of an additive to maintain soil in suspension has been said to play an important role. It has been recognized by many workers [13, 14, 23, 24] that whiteness-retention action is closely related to the sorption of ions or molecules from solution by fabric and soil, suggesting that a reduction in coulombic or van der Waals' attractive forces is involved. The importance of an additional factor—namely, mechanical-occlusion or entrapment in the irregularities of the fiber surfaces or between fibers—has been demonstrated by the recent work of Compton and Hart [3].

Previous studies at this laboratory [5] have shown that several proteins and certain nonionic water-soluble synthetic polymers exhibit whiteness-retention properties similar to those of sodium carboxymethyl cellulose, an additive widely used in detergent formulations to inhibit soil redeposition during laundering.

This work has been extended to survey a number of physical chemical properties of the system consisting of detergent, additive, soil, and fabric, in an attempt to improve the experimental basis for interpretation of the role of whiteness-retention additives in detergent action. Electrophoretic measurements have been carried out with suspensions of carbon black and of powdered cotton in the presence of vari-

* This work was supported in part by a Working Fund provided by the Quartermaster Corps, Department of the Army.

ous effective additives to show their effect on surface electrostatic charge. Sedimentation measurements of carbon black suspensions have been made by means of the ultracentrifuge to examine the influence of these additives on the state of aggregation of the dispersed carbon. Since any observed changes in the surface physical conditions of soil or fabric are related undoubtedly to selective adsorption of ions or molecules from solution, additional data have been obtained on the extent of adsorption of these additives by carbon black and by cotton. Finally, evidence is presented for complex formation between detergent and whiteness-retention additive.

Experimental

The materials * used were those employed previously in our soil redeposition studies referred to above. The whiteness-retention additives included were (*1*) polyvinyl alcohol (PVA), Elvanol 51-05, low viscosity, 86%–89% hydrolysis (du Pont); (*2*) polyvinylpyrrolidone (PVP), K-29, approximate average molecular weight, 40,000 (Schenley); (*3*) sodium carboxymethyl cellulose (CMC), low viscosity, CT grade (Hercules); (*4*) gliadin, a laboratory-prepared fraction soluble in 20% ethyl alcohol. All of these additives have been shown to be highly effective at concentration levels between 0.005%–0.01% in reducing deposition of a carbon black test soil on cotton fabric under representative aqueous cleaning conditions.

The standard aqueous test medium, made up to approximate typical laundering conditions, contained 0.08% sodium tripolyphosphate (Westvaco), 0.04% sodium carbonate (reagent grade), and 0.12% Nacconol NRSF, a sodium alkylarylsulfonate (National Aniline).

As a test soil, Aquablak B (Binney & Smith) was employed. This material is a channel black supplied as an aqueous paste containing a small percentage of an anionic type dispersing agent. The reported average diameter of the carbon particles is 25 to 28 mμ [2]. The cotton cloth used was bleached, unsized Indianhead muslin.

Results and Discussion

Electrophoresis

In recent years several investigations have been made in an attempt to establish the role of electrokinetic effects in suspensibility and detergency. For example, correlation between the stability of carbon suspended in soap solutions and the electrophoretic mobility of carbon particles has been reported by Urbain and Jensen [21] and later confirmed by Ray and Hutchison [15]. In the cases of cationic and nonionic detergents, however, Doscher [4] indicated that a change in zeta potential is not necessarily an important factor in suspensibility.

Goette [7] attributed soil removal from fibers to the action of the detergent in raising the zeta potential of both soil and fiber. This hypothesis is in agreement with experimental measurements of Stubblebine [20] showing correlation between soil removal and the electrophoretic mobilities of cotton and carbon in alkaline soap solutions. From a recent comprehensive study Kling and Lange [10] concluded that the increased negative charge contributed by anionic detergents to carbon black has a favoring influence that is, however, not essential to the washing process.

The importance of electrostatic repulsion between fabric and soil in whiteness-retention action has been suggested by several workers [13, 14, 23]. However, no experimental study of the relation between electrophoretic mobility and soil redeposition has been reported.

In the references cited above, the microscope method was used in measuring the mobilities of individual particles. In this investigation the moving-boundary electrophoresis method was employed so that the mobilities of the detergent and whiteness-retention additive could be correlated, if possible, with the mobilities of cotton and carbon measured under similar conditions.

A Tiselius-Klett electrophoresis apparatus was used, equipped with a cylindrical-lens optical system. All experiments were carried out in a constant-temperature bath at 0.7°C. In measuring the mobilities of cotton and carbon, since the suspensions were opaque, the limit of the opaque zone was used instead of the usual schlieren pattern to determine the position of the moving boundary. The results are expressed directly in mobility units ($\times 10^{-5}$ cm.^{2} v.$^{-1}$ sec.$^{-1}$) referred to 0°C. In all measurements the current was adjusted to 5 ma. This corresponds to a potential gradient close to 10 v./cm.

In the case of cotton, the cloth was cut into small pieces, Wiley-milled to pass 20-mesh screen, and then reduced to a fine powder in a vibratory ball mill similar to that described by Forziati *et al.* [6]. This finely powdered cotton was suspended in the

* Mention of products by commercial names does not imply endorsement by the Department of Agriculture over others of a similar nature not mentioned.

TABLE I. ELECTROPHORETIC MOBILITY OF WHITENESS-RETENTION ADDITIVES WITH AND WITHOUT DETERGENT

Solute*	Mobility ($\times 10^{-5}$ cm.^{2} v.$^{-1}$ sec.$^{-1}$)† Falling boundary	Rising boundary	Remarks
1.0% Nacconol NRSF	22	27	
0.2% Gliadin	5	5	Solution opaque
0.2% Gliadin + 0.48% Nacconol NRSF	18 (leading edge)	20	Clear solution. Falling, spreading M-shaped boundary. Rising, single sharp boundary
1.0% PVA-Elvanol 51-05	nil	nil	
0.1% PVA + 0.9% Nacconol NRSF	18 (leading edge)	22	Falling, spreading M-shaped boundary. Rising, single sharp boundary
1.0% PVP-Schenley K-29	nil	nil	
0.1% PVP + 0.9% Nacconol NRSF	20	27	Falling, spreading M-shaped boundary. Rising, single sharp boundary
0.1% CMC	18	21	
0.1% CMC + 0.25% Nacconol NRSF	18 (probably CMC) 21 (probably Nacconol)	22	Falling, two distinct boundaries. Rising, only one boundary

* The experiments with indicated solutes were carried out in a solvent solution containing 0.08% sodium tripolyphosphate and 0.04% sodium carbonate.

† Referred to 0°C. All mobilities are negative.

solution under test (in approximately the same ratio as used in the previous soil redeposition studies), and then allowed to settle for ½ hr. The portion remaining suspended was used in the electrophoresis study.

The electrophoretic mobilities of PVA, PVP, gliadin, and CMC, with and without added Nacconol NRSF, are summarized in Table I. In each case, the indicated solute was added to the standard alkaline solvent containing 0.08% sodium tripolyphosphate and 0.04% sodium carbonate. Under the experimental conditions, PVA and PVP alone have no mobility, gliadin alone has a relatively low mobility, and CMC alone shows a relatively high mobility. Throughout this report all mobility values refer to movement toward the positive electrode—that is, the moving species are negatively charged. With added Nacconol NRSF, gliadin, PVA, and PVP all exhibit a fast-moving, spreading, M-shaped boundary on the falling side, and a single sharp boundary on the rising side. This boundary anomaly and the increase in mobility are evidence of interaction. Interaction of detergents with various proteins is well established, so that this behavior of gliadin is reasonable. Further investigations of complex formation of PVA and PVP with Nacconol NRSF are described in a following section.

In the case of CMC, there is no apparent interaction with the detergent, since electrophoresis of the mixture shows two separate and distinct boundaries on the falling side which correspond to the mobilities of CMC and Nacconol determined separately.

The effect of detergent and whiteness-retention additives on the electrophoretic mobilities of Aquablak B suspended in the standard alkaline buffer are shown in Table II. The mobility of the carbon without additives is between 22, as measured on the falling side, and 24, as measured on the rising side. The addition of Nacconol alone or with CMC, gliadin, PVA, or PVP results in a slight lowering of this value. Since the mobilities of Nacconol alone, CMC, and the Nacconol complexes with PVA, PVP, and gliadin are all near that of the original carbon, an inference as to the role of surface charge is not possible. However, these results show clearly that the mechanism by which these effective whiteness-retention additives act is, in our cases, not limited by the surface charge of the carbon. For this carbon test soil and under our conditions other factors are critical.

The electrophoretic results for cotton, shown in Table III, are of greater interest. In the presence of Nacconol alone in the standard alkaline solution, cotton shows a very low mobility of 3 as determined

TABLE II. ELECTROPHORETIC MOBILITY OF CARBON IN THE PRESENCE OF WHITENESS-RETENTION ADDITIVES

Solvent	Solute	Mobility of carbon ($\times 10^{-5}$ cm.^{2} v.$^{-1}$ sec.$^{-1}$)† Falling boundary	Rising boundary
Standard*	0.1% Aquablak B	22	24
Standard + 0.12% Nacconol	0.1% Aquablak B	21	22
Standard + 0.12% Nacconol	0.1% Aquablak B + 0.05% CMC	18	20
Standard + 0.12% Nacconol	0.1% Aquablak B + 0.05% gliadin	19	20
Standard + 0.12% Nacconol	0.1% Aquablak B + 0.01% PVA	16	19
Standard + 0.12% Nacconol	0.1% Aquablak B + 0.01% PVP	18	22

* 0.08% sodium tripolyphosphate and 0.04% sodium carbonate.

† Referred to 0°C. All mobilities are negative.

by the falling boundary; whereas, the addition of CMC increases the mobility of the cotton to 18. This value agrees with the mobility of CMC determined independently and is a result of the selective adsorption of CMC by cotton demonstrated by Bartholomé and Buschmann [1]. On the basis of electroosmotic measurements Stackelberg and coworkers [19] have recently reported that CMC causes a marked increase in the zeta potential of several types of fibers.

The observed increase in the negative surface charge of cotton with the addition of CMC is in agreement with the view of Nieuwenhuis [13] and others who attribute the soil-suspending action of CMC to increased electrostatic repulsion between fabric and soil, both of which in most instances carry a negative charge in an alkaline solution.

Addition of gliadin to the cotton suspension in the presence of Nacconol results in an increase in the mobility of cotton to 8. This mobility value is between those for gliadin alone and for the gliadin-detergent complex. As in the case of CMC, the increase in mobility of cotton with added gliadin may be interpreted as evidence for adsorption of gliadin and/or detergent on the cotton surface.

The addition of the nonionic additives PVA or PVP to the powdered cotton suspension has no observable effect on the mobility of the cotton.

TABLE III. ELECTROPHORETIC MOBILITY OF COTTON IN THE PRESENCE OF WHITENESS-RETENTION ADDITIVES

Solute*	Mobility of cotton ($\times 10^{-5}$ cm.^{2} v.$^{-1}$ sec.$^{-1}$)§ Falling boundary	Rising boundary
Powdered cotton†	3	not visible
Same, with 0.05% CMC	18	17
Same, with 0.05% gliadin	8	not visible
Powdered cotton‡	7	6
Same, with 0.02% PVP	8	6
Same, with 0.02% PVA	9	7

* The experiments with these solutes were carried out in a solvent solution containing 0.12% Nacconol NRSF, 0.08% sodium tripolyphosphate, and 0.04% sodium carbonate.

† Cotton fabric (bleached, unsized Indianhead muslin) obtained from Testfabrics, Inc.

‡ Cotton fabric (bleached, unsized Indianhead muslin) obtained from Textron, Inc.

§ Referred to 0°C. All mobilities are negative.

As shown in the Table III, there is a considerable difference in mobility between the two samples of cotton used. The higher value of 7, when corrected for temperature, is in fair agreement with that reported by other workers [4, 18, 20]. The other value, approximately 3, is lower than is usually observed.

In summary, electrophoretic measurements show that none of the additives has an appreciable influence on the surface electrical charge of the carbon black used as a test soil. Therefore, it is clear, in our case, that stabilization of dispersed soil as a result of electrokinetic effects is not the limiting factor in whiteness-retention action. CMC, and to a lesser extent gliadin, increase the negative surface charge of cotton, indicating that the whiteness-retention action of these materials may be related to an electrostatic repulsive force between fabric and soil. On the other hand, the nonionogenic additives cannot act through such a mechanism, since they do not show any effect on the surface charge of either fabric or soil.

Sedimentation

The stabilization of dispersed soil in solution by the suspending action of added materials may be shown, if it exists, by a decrease in the rate of sedimentation of the soil. Among recent investigations of suspending action reported in the published literature are those of Vold and coworkers [8, 22], Merrill and Getty [12] and Mankowich [11]. In a gen-

erally accepted mechanism, suspending action is attributed to an increase in the electrostatic charge of suspended particles through adsorption of ions.

Stabilization of dispersed soil has been suggested as a factor in the ability of a detergent solution to prevent redeposition. However, no systematic investigation of suspending action of whiteness-retention additives has been reported.

As another phase of this study of factors related to the mechanism of action of whiteness-retention additives, the effects of detergent and additives on the state of aggregation of the carbon black have been examined through measurement of the sedimentation rate of carbon in an ultracentrifuge. The application of the ultracentrifuge is a logical refinement of conventional gravity settling methods of studying colloid stability. The results are evaluated in terms of state of aggregation of the carbon black and adsorption affecting the solvation, particle radius, density, and surface charge.

The sedimentation velocity of the carbon black referred to the standard medium of water at 20°C, and unit centrifugal field, the sedimentation constant (expressed in Svedberg units: $\times 10^{-13}$ sec.) was measured near 25°C using a Spinco Model E ultracentrifuge to apply average fields of 15,000 or 11,000 times that of gravity (14,290 or 12,590 r.p.m.). This difference in centrifugal field was shown not to affect the sedimentation constant of carbon black in water alone. Photographic records of the sedimentation runs were made in the usual manner; the position of the sedimenting boundary in each record was determined from densitometer tracings. Computations were made by standard methods. For reference to standard conditions the densities and viscosities of the solutions without carbon black were measured with a specific gravity balance and Ostwald viscometer. The solution densities differed by not more than 3 parts per thousand. The partial specific volume of the carbon black was taken to be 0.57 $cm.^3$ $g.^{-1}$, in accordance with published data [2] and invariant with temperature. This assumption is not an important source of error in referring the results to standard conditions. However, the computed particle diameter is appreciably dependent on the assumed particle density.

Table IV shows the separate effects of the alkaline salts, detergent, and whiteness-retention additives on the sedimentation rate of carbon black and, for comparison, on the viscosity of the medium of dispersion. The carbon sediments less rapidly in the presence of the alkaline builders than in their absence. Further addition of sulfonate detergent without or with the nonionogenic polymers PVP or PVA has little or no effect. However, the sedimentation rate is lowered somewhat by gliadin and very markedly lowered by CMC. These effects parallel increases in the viscosity of the medium, but they are much greater. Furthermore, the effects of the viscosity of the medium have been allowed for in computing the standard sedimentation constants.

It is of interest to compare the sedimentation constants found with those that would be given by uncharged hard carbon spheres of the reported average diameter: 28 mμ. Such particles are computed to have a sedimentation constant of 320 S. The observed rates correspond to spheres of about 56 mμ in diameter, or to slightly more massive aggregates of irregular shape. Clusters of eight 28-mμ particles sedimenting together would have approximately the maximum observed sedimentation constant. It may be noted also that the decrease in sedimentation rate from 1,330 to 860 S corresponds closely to halving the mass of the sedimenting unit.

As a second important consideration, the possible effect of adsorption on the sedimentation rate is computed. Under the appropriate experimental condi-

TABLE IV. SEDIMENTATION OF CARBON BLACK IN THE PRESENCE OF WHITENESS-RETENTION ADDITIVES

Composition of medium	Relative viscosity*	Sedimentation constant†
Water, without detergent or electrolyte, pH 8.5	1	1,350
Same as above (except for lower centrifugal field)	1	1,310
Sodium tripolyphosphate: 0.08%; Na_2CO_3: 0.04%	1.002	1,130
Same, plus 0.12% Nacconol NRSF	1.006	1,140
Polyvinylpyrrolidone, K-29, Schenley: 0.01%‡	1.000	1,200
Polyvinyl alcohol, du Pont Elvanol 51-05: 0.01%‡	1.006	1,150
Gliadin, 0.05%‡	1.008	1,050
Carboxymethyl cellulose, Hercules, CT grade, low viscosity: 0.01%‡	1.030	860

* Viscosity of medium relative to water at the same temperature.

† Specific sedimentation rate, or sedimentation constant, referred to standard conditions: water at 20°C; in Svedberg units: 10^{-13} sec. The carbon black concentration was 0.1%.

‡ The experiments with additives were made at pH 10 in the presence of 0.12% Nacconol NRSF, 0.08% sodium tripolyphosphate, and 0.04% sodium carbonate.

tions, adsorption studies (reported in next section) have shown that 15 mg. of PVP is taken up per gram of carbon black. Adsorption of this amount on a 56-mμ sphere would be too small to give a coherent covering or to effect the sedimentation constant appreciably through the particle mass or density. It corresponds to about 40 polymer molecules adsorbed for each carbon particle.

The small decrease in rate produced by gliadin and the marked decrease produced by CMC may be due to the ionogenic properties of these additives, in contrast to the nonionogenic PVP and PVA. It is impossible, by any amount of adsorption of these substances, to reduce the calculated sedimentation constant of carbon spheres by the observed amounts through a direct effect on the average density and mass of a particle. Since the electrophoretic mobilities of carbon black in the given medium in the presence of the various additives are closely similar, it does not seem possible that the decreased sedimentation rate in the presence of CMC can be due to an increase in electrical charge resulting from adsorption.

A final possibility is that adsorption of gliadin or especially CMC results in a unique increase in hydration of the carbon particle. The amount of hydration required is about 0.6 g. of water per gram of carbon in the case of CMC or about 0.12 g. in the case of gliadin. The hydration would presumably be mediated by simultaneous adsorption of relatively small amounts of the charged additives and would be directly related to the amounts of these adsorbed. Such hydration does not necessarily indicate firmly bound water, but may express in part an increase in the frictional resistance of a particle as a result of portions of adsorbed polymer molecules extending into the medium.

Recapitulating: Ultracentrifugal measurements indicate an average particle diameter for our sample of carbon black approximately twice the reported diameter. Ours is a minimum estimate based on the assumption of a spherical particle. Adsorption of small amounts of the various components of experimental laundering media was computed to affect the sedimentation rate directly only by a barely measurable amount. Nevertheless, the electrolytic alkaline builders of a representative formula slightly decreased the sedimentation rate. Sulfonate detergent had no additional effect. Effective whiteness-retention additives are of two sorts. The nonionic polymers tested had little or no effect on sedimentation. This result is in agreement with the measured adsorption in one instance. The charged additives tested here produced a further decrease in order of their molecular charge. The decreases are interpreted most simply as partial disaggregation of clusters of particles. Alternatively, the decreases may be related to increased hydration. An electrokinetic effect is probably not involved because the carbon electrophoretic mobility is approximately the same with any of these additives.

From the foregoing, it appears that there is no direct relation between suspending power and whiteness-retention action. This is immediately evident for the nonionogenic materials. In the case of CMC there is an apparent correlation between deflocculation and whiteness-retention action; however, the facts that CMC is not generally effective on noncellulosic fabrics [13] and that the other additives do not show this effect suggest that preferential adsorption of CMC at the cotton-solution interface is probably a more important factor in its mode of action.

Adsorption

One of the fundamental factors underlying the action of additives for the prevention of soil redeposition is the adsorption of these agents at the fiber-solution and at the soil-solution interfaces. This selective adsorption at a given interface could contribute to the prevention of soil redeposition by an effect on interfacial tension, or through effects on the surface charge, solvation, and hydrophobicity of the soil and fiber surfaces. In this investigation, only data on the adsorption of PVP were obtained for comparison with the reported adsorption of CMC [1].

The adsorption of PVP (Schenley, K-29) on carbon black (Aquablak B, 0.1% concentration) from an alkaline solution (0.08% sodium tripolyphosphate and 0.04% sodium carbonate) was determined over a range of PVP concentration levels with or without an initial concentration of 0.12% Nacconol NRSF. The extent of adsorption was determined by shaking the carbon black dispersion containing varying concentrations of PVP in a mechanical shaker for approximately 16 hrs. at room temperature. After agitation, the carbon black was removed from the solution by sedimentation in the ultracentrifuge. The PVP concentrations in the initial and

equilibrium solutions were calculated from the nitrogen contents determined by micro-Kjeldahl analysis. The amount of PVP adsorbed by the carbon black was determined by difference.

The results (Table V) show that PVP is adsorbed to an appreciable extent by the carbon black. Further, the extent of adsorption is reduced by approximately one-half in the presence of added detergent. This reduction in the adsorption of PVP may be due to a competition between PVP and Nacconol for the adsorption sites on the carbon black surface, or it may be due to molecular interaction between PVP and Nacconol reducing the activity of the PVP.

In the case of the solutions with Nacconol present, an attempt was made to analyze for the initial and equilibrium concentrations of detergent. The presence of a dispersing agent in the Aquablak B carbon black interfered with the determination. However, it appears that the amount of Nacconol adsorbed by the carbon black is lowered somewhat by the presence of PVP.

A single adsorption experiment was carried out at a high PVP concentration using cotton cloth. No adsorption of PVP by the cotton was observed. This is in contrast to the reported behavior of CMC which is highly substantive to cotton [1].

On the basis of these adsorption results, PVP appears to act in preventing soil redeposition at the surface of the carbon test soil, rather than at the surface of the cotton. The electrophoretic measurements reported above indicate that the electrostatic charge of the carbon is not changed. Furthermore, sedimentation results show that PVP has no significant influence on the degree of dispersion of carbon. Therefore, it is proposed that the whiteness-retention activity of PVP as a consequence of its selective adsorption by the soil is related to its effect on nonelectrostatic forces of the van der Waals' type between soil and fabric. In such a picture, increased solvation associated with the lyophilic character of PVP would possibly play a contributing role.

Although no actual measurements of adsorption were carried out with PVA, it may be considered provisionally to act in a manner analogous to PVP insofar as these materials exhibit similar properties.

Further evidence that these nonionogenic additives function through an effect on the surface of the carbon test soil rather than that of the fiber is inferred from the finding that both PVP and PVA exhibit excellent whiteness retention action toward wool fabric (unpublished results) as well as toward cotton, in contrast to the behavior of CMC which is effective only toward cellulosic fabrics. The general effectiveness of PVA as a whiteness-retention additive for various types of textile fibers has recently been reported by Hart and Compton [9].

Molecular Interaction between Detergent and Whiteness-Retention Additives

Preliminary evidence for the interaction of Nacconol with PVA and with PVP has been reported above. To confirm these observations further studies based upon electrophoresis and sedimentation measurements were carried out.

A series of electrophoresis runs was carried out at varying weight ratios of PVA and PVP to Nacconol NRSF at a constant total concentration of 1% (wt.) in an alkaline buffer containing 0.08% sodium tripolyphosphate and 0.04% sodium carbonate. The experiments were carried out at 0.7°C. A current of 5 ma. was employed. Under the experimental conditions this current corresponds to a potential gradient of approximately 10 v./cm.

The mobility-concentration relationship is shown in Figure 1 for PVA and Figure 2 for PVP.

Several anomalies were observed in the electrophoresis patterns for both PVA and PVP. On the rising side a single very sharp spike-shaped boundary

TABLE V. ADSORPTION OF POLYVINYLPYRROLIDONE BY CARBON BLACK WITH AND WITHOUT ADDED DETERGENT

Initial concentration* (g. PVP/l.)	Equilibrium concentration (g. PVP/l.)	Adsorption† (g. PVP/g. carbon)
In absence of added detergent		
0.0092	0.0021	0.0071
0.046	0.0085	0.037
0.092	0.042	0.050
0.46	0.042	0.056
0.92	0.856	0.060
In presence of added detergent (0.12% *Nacconol NRSF*)		
0.0092	0.0043	0.0049
0.0046	0.029	0.016
0.092	0.077	0.015
0.46	0.433	0.025
0.92	0.888	0.028

* Indicated concentration of PVP (Schenley, K-29) added to a 0.1% Aquablak B solution in alkaline buffer containing 0.08% tripolyphosphate and 0.04% sodium carbonate.

† Calculated by difference between initial and equilibrium concentration of PVP in solution.

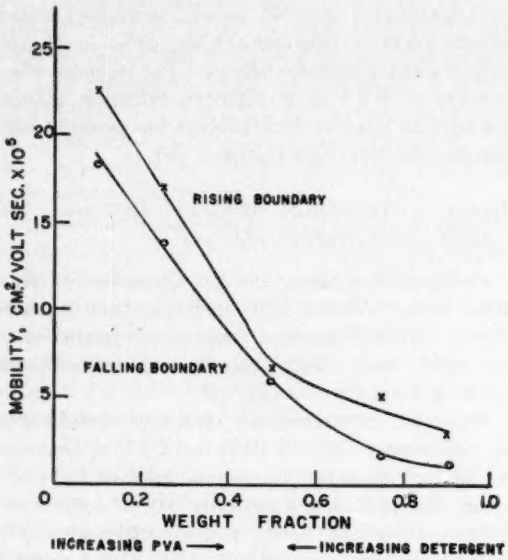

FIG. 1. *Electrophoretic mobilities of polyvinyl alcohol-detergent mixtures.*

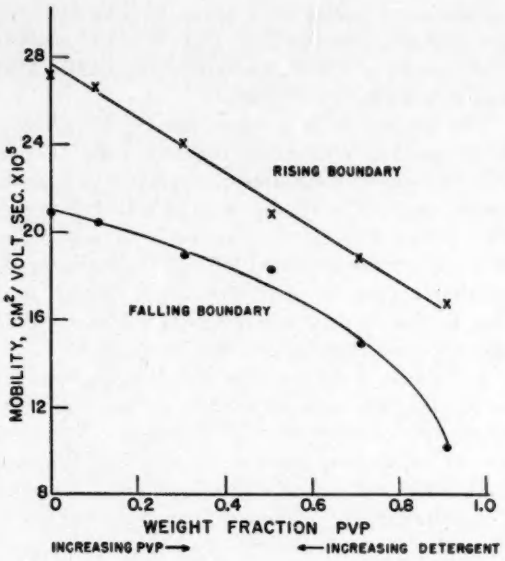

FIG. 2. *Electrophoretic mobilities of polyvinyl-pyrrolidone-detergent mixtures.*

moved out, whereas on the falling side a spreading boundary was observed. At high Nacconol concentrations this major boundary was preceded by a fast moving minor boundary. The extent of spread of the major boundary became very large as the weight fraction of PVP or PVA in the solution increased. The electrolyte boundary on the rising side was larger than that on the falling side in all cases.

When the results obtained with PVA are compared with PVP, for equivalent weight concentrations the decrease in mobility of the moving component in the presence of PVA is observed to be greater than that with PVP. Even on a base-molar basis the decrease in mobility of the complex (compared to pure detergent) is greater for PVA than for PVP.

Further evidence of molecular interaction between polyvinyl alcohol and detergent is based upon sedimentation measurements with a Spinco Model E ultracentrifuge. In the analysis, PVA was analyzed at a concentration of 0.25% in an alkaline buffer containing 0.08% sodium tripolyphosphate and 0.04% sodium carbonate. It showed a single sedimenting boundary with the average sedimentation constant 1.0 S (Svedberg units) as measured in the buffer at 27.0°C.

At the same time, the PVA at 0.25% plus 0.25% Nacconol NRSF was analyzed in the same medium. This mixture showed one boundary with the average sedimentation constant of 1.5 S as measured in the buffer at 27.0°C. The area under the sedimentation boundary in the presence of detergent was larger than that in the case of PVA alone. Nacconol alone in the same medium would give a very slowly sedimenting boundary. The foregoing analysis is compatible with the complete interaction of PVA with detergent to form a sedimenting unit.

The observations above are in agreement with the recent work of Saito [16] who has reported evidence of interaction between polyvinyl alcohol and detergent. A comprehensive study of the interaction between polyvinylpyrrolidone and dyes has recently been published [17]. Our observation of the interaction between PVP and detergent is probably analogous.

The role of the interaction of detergent and whiteness-retention additive in the over-all picture of whiteness retention is not immediately apparent. Significantly, the formation of a charged complex as a result of interaction has been shown to be without appreciable effect on the surface electrostatic charge of carbon or cotton. The observed interaction

agrees with the adsorption data, which show that the presence of detergent in solution reduces the adsorption of PVP by carbon black. However, this decrease in the adsorption of PVP is not reflected in a decrease in whiteness-retention activity as was shown in our previous soil redeposition studies.

Summary

Physical chemical studies have been carried out related to the mode of action of whiteness-retention additives in decreasing the extent of soil redeposition during laundering. For this purpose the methods of electrophoresis, sedimentation, and adsorption analysis have been used.

Electrophoretic measurements indicate that the ionogenic additives CMC and to a lesser extent gliadin increase the negative surface charge of cotton, whereas the nonionogenic additives PVP and PVA have no observable effect. None of the additives alters the surface charge of the carbon black test soil. Ultracentrifugal measurements show that the nonionogenic additives have little or no effect on the rates of sedimentation of carbon black particles. On the other hand, the ionogenic additives, CMC and gliadin, produce decreases in sedimentation rate in order of their charge. Adsorption measurements show that PVP is highly substantive to carbon black and relatively nonsubstantive to cotton, in contrast to the behavior of CMC, which is known to be highly substantive to cotton. Evidence of interaction between the nonionogenic additives and detergent is presented.

The ionogenic additives, therefore, differ from the nonionogenic additives in their specific effects on the surface charge of cotton, on the rate of sedimentation of carbon black, and in their adsorption on cotton, and it is concluded that their modes of action in preventing soil redeposition are different. The ionogenic additives apparently influence whiteness-retention action by their effect on the surface of the cotton, probably through increase in electrostatic repulsion between fabric and soil. On the other hand, the nonionogenic additives apparently act at the surface of the carbon test soil, possibly through reduction in van der Waals' attraction between fabric and soil.

Acknowledgments

The authors are indebted to Miss Geraldine Secor for the micro-Kjeldahl determinations. They also wish to express gratitude to Dr. H. P. Lundgren for his advice and encouragement during the course of this work.

Literature Cited

1. Bartholomé, E., and Buschmann, K. F., *Melliand Textilber.* **30**, 249 (1949).
2. Binney & Smith Co., Technical Bulletin on Carbon Blacks, Bone Blacks, Iron Oxide Pigments and Black Dispersions, New York.
3. Compton, J., and Hart, W. J., *Ind. Eng. Chem.* **43**, 1564 (1951).
4. Doscher, T. M., *J. Colloid Sci.* **5**, 100 (1950).
5. Fong, W., and Lundgren, H. P., TEXTILE RESEARCH JOURNAL **23**, 769 (1953).
6. Forziati, F. H., Stone, W. K., Rowen, J. W., and Appel, W. D., *J. Research Natl. Bur. Standards* **45**, 109 (1950).
7. Goette, E. K., *J. Colloid Sci.* **4**, 459 (1949).
8. Greiner, L., and Vold, R. D., *J. Phys. & Colloid Chem.* **53**, 67 (1949).
9. Hart, W. J., and Compton, J., TEXTILE RESEARCH JOURNAL **23**, 164 (1953).
10. Kling, W., and Lange, H., *Kolloid-Z.* **127**, 19 (1952).
11. Mankowich, A. M., *Ind. Eng. Chem.* **44**, 1151 (1952).
12. Merrill, R. C., and Getty, R., *Ind. Eng. Chem.* **42**, 856 (1950).
13. Nieuwenhuis, K. J., *J. Polymer Sci.* **12**, 237 (1954).
14. Powney, J., and Noad, R. W., *J. Textile Inst.* **30**, T157 (1939).
15. Ray, L. N., and Hutchison, A. W., *J. Phys. & Colloid Chem.* **55**, 1334 (1951).
16. Saito, S., *Kolloid-Z.* **133**, 12 (1953).
17. Scholtan, W., *Makromol. Chem.* **11**, 131 (1953).
18. Sookne, A. M., and Harris, M. J., TEXTILE RESEARCH JOURNAL **11**, 307 (1941).
19. Stackelberg, M. v., Kling, W., Benzel, B., and Wilke, F., *Kolloid-Z.* **135**, 67 (1954).
20. Stubblebine, W., A Study of the Electrophoretic Mobility of Carbon, Cotton, and Wool in Aqueous and Nonaqueous Detergent Solutions, Ph.D. thesis, Penn. State College (1942).
21. Urbain, W. M., and Jensen, L. B., *J. Phys. Chem.* **40**, 821 (1936).
22. Vold, R. D., and Konecny, C. C., *J. Phys. & Colloid Chem.* **53**, 1262 (1949).
23. Wagg, R. E., *J. Textile Inst.* **43**, T325 (1952).
24. Weatherburn, A. S., Rose, G. R. F., and Bayley, C. H., *Can. J. Research* **F28**, 363 (1950).

(Manuscript received June 25, 1954.)

The Influence of Chemical Treatment on the Properties of Wool

I. Alkali Solubility as a Measure of Sulfuric Acid Degradation

J. H. Dusenbury,* E. H. Mercer,† and J. H. Wakelin‡

Textile Research Institute, Princeton, New Jersey

Abstract

The view that the cortex of the wool fiber consists of a resistant fraction, the paracortex, and a less resistant fraction, the orthocortex, which extend in the form of two twisted hemicylinders from one end of the fiber to the other, is used to explain the mechanism of the alkali-solubility test on acid-damaged wool. The effects of acid damage on several single-fiber properties and on the resistance of fabrics to flex abrasion have been measured for correlation with alkali-solubility data.

During the initial exposure of the wool to acid damage, alkali solubility is observed to increase rapidly, corresponding to damage chiefly to the orthocortex; during the later stages, as the damage proceeds into the paracortex, the alkali solubility increases at a much slower rate with time of exposure. The decreases observed in the values for physical properties of the wool with increasing exposure to acid correspond generally with the changes in alkali solubility.

Wool treated with formaldehyde, either preceding or following a series of progressive exposures to acid, exhibits greatly decreased alkali solubility, but fails to show a corresponding improvement in physical properties. It is suggested that the acid acts to degrade the wool fiber by hydrolyzing peptide bonds, and that the formaldehyde treatments decrease alkali solubility by a cross-linking mechanism that does little to improve the physical properties of the wool.

A good correlation was found between the flex-abrasion resistance of the variously treated fabrics and the energy to break of the corresponding single fibers. The product of breaking stress and breaking extension, a fiber property related to energy to break, was also found to correlate well with the fabric flex-abrasion resistance.

Introduction

The alkali-solubility test was originally described by Harris and Smith as a method for determining oxidative damage to wool [7]; it has also been used as a measure of damage caused by acid and other chemical treatments [1, 11, 12, 14]. Little work has been published on the correlation of the results of this chemical test for damage with changes in the measured physical properties of single fibers and fabrics. It also appears that little attention has been paid to the problem of what part of the individual fibers is damaged and subsequently extracted by the alkaline solvent. Wool fibers are far from homogeneous in composition, and the several components may be expected to differ greatly in their resistance to chemical attack. It seems likely, therefore, that in the alkali-solubility test certain components will be extracted preferentially and thus determine the major portion of the actual loss in weight. The preferential attack on these components should also affect changes in single-fiber properties and in fabric properties.

The components exhibiting the greatest resistance to dissolution in alkali are the cortical cell membranes and the superficial layer of the cuticle, the epicuticle. Together these constitute about 8%–10% by weight of the fiber, and this figure is likely to determine an upper limit (*ca.* 90%) for the alkali solubility after severe damage. However, for the more usual forms of damage the structural factor likely to be relevant is the division of the cortex of the wool fiber into two more or less equal halves differing in degree of keratinization. These two halves have been designated dye accessible and nondye accessible [8] and the ortho- and paracortex [13]. Many experiments have shown that the orthocortex is more susceptible to attack by a great variety of

* Assistant Director of Research, Textile Research Institute.

† Present address: The Chester Beatty Research Institute, The Royal Cancer Hospital, London, England.

‡ Research Associate, Textile Research Institute.

chemicals and that it is also preferentially extracted by solvents capable of solubilizing keratin. Accordingly, any chemical treatment that preferentially attacks the orthocortex might be expected to sensitize preferentially the orthocortex for subsequent removal by alkali.

Preparation and Testing of a Graded Series of Damaged Wools

The Acid-Damaged Series

For quantitative studies it is desirable to have a smoothly graded series of damaged wools which can be reproduced at will. For this purpose a worsted fabric in a ready-to-dye state made from the master wool type WC-4 was chosen.* The alkali solubility of this material was about 6%, a typical value for untreated wool. A hot water extract of the fabric showed a pH value of 6. Accordingly, it was considered to be initially neutral.

Two replicate series of progressively damaged samples (hereinafter referred to as Series No. 1 and Series No. 2) were prepared by treatment with acid in the following way: fabric swatches 10 in. by 15 in. (weighing 26.9 g.) were first soaked in an aqueous sulfuric acid solution of concentration 1.2 g./l. for 2 hrs. at room temperature. This corresponds to 4.5% acid on the weight of the fabric (o.w.f.) or an initial pH of 1.6—an acid concentration that might be used to apply an acid dyestuff to wool. This presoaking allowed the wool to take up about one half of its total possible combining weight of acid. The fabric was then transferred to a boiling solution of the same acid concentration, boiled for a predetermined time under reflux, removed, washed in water, and dried. Samples were treated for varying times up to 24 hrs. The equilibrium weight of the wool on heating in an oven at 110°C was used as a basis for determining the weight loss on subsequent treatment in alkali.

The alkali solubilities were determined by the standard procedure of Harris and Smith [7]; that is, the loss in weight was determined on short, loose pieces of yarn taken from the treated fabrics after they had been exposed for 1 hr. to 0.1*N* NaOH at 65°C and at a solution-to-fiber ratio of 100:1. Prior to alkali exposure, the samples were soaked in a dilute aqueous solution of sodium bicarbonate at room temperature in order to "neutralize" any excess acid from the prior acid treatments. Sintered glass crucibles were used as filters and proved satisfactory even in those cases of the more heavily damaged wool where exposure to alkali degraded the wool to a gel.

Determinations of alkali solubility were made on fabrics as well as on short lengths of yarn from these fabrics. As observed previously by other workers, larger alkali-solubility values were observed for the yarns. There are also indications that the values obtained by carrying out the standard test are not truly equlibrium values, as implied by the use of the word "solubility."

TABLE I. Alkali Solubility of Yarns Removed from Treated Fabrics

Time of treatment (hrs.)	Alkali Solubility (%) H_2SO_4 Series No. 1	H_2SO_4 Series No. 2	H_2SO_4 followed by HCHO Series No. 1	H_2SO_4 followed by HCHO Series No. 2	HCHO followed by H_2SO_4
0	5.6	8.8	−0.1	1.5	1.5
0.5	13.3				
1.0	19.0				
1.5	26.0				
2.0	28.1	28.9	3.8	3.7	13.9
2.5	32.1				
3.0	43.2				
4	53.7		5.9	4.7	14.9
5	59.9				
6	62.5	62.5			
7	65.4				
8	64.2	63.7	6.3	6.5	22.6
9	65.2				
10	68.0				
11	71.1				
12	71.5	68.2	6.5	7.4	29.1
13	73.4				
14	73.4				
15	74.4				
16	74.3	72.7	10.9	8.4	28.9
17	75.4				
18	76.1				
19	77.3				
20	80.8		10.6		
21	81.5				
22	82.5				
23	81.7				
24			15.5		
Pooled variance (σ^2_p)	1.857	0.642	2.113	1.735	2.080
Standard deviation (σ_p)	1.4	0.8	1.5	1.3	1.4

*A U. S. Rambouillet wool of 64's grade, one of four types studied on the first four-year phase of the Wool Research Project at Textile Research Institute.

TABLE II. SINGLE-FIBER PROPERTIES (FIBERS REMOVED FROM TREATED FABRICS) *

Time of treatment (hrs.)	Number of fibers tested: Series No. 1	Number of fibers tested: Series No. 2	Elastic modulus (g. cm.$^{-2}$ for 100% extension) $\times 10^{-6}$: Series No. 1	Elastic modulus: Series No. 2	Stress at 20% extension† (g cm.$^{-2}$) $\times 10^{-6}$: Series No. 1	Stress at 20% extension†: Series No. 2	Stress at break (g. cm.$^{-2}$) $\times 10^{-6}$: Series No. 1	Stress at break: Series No. 2	Extension at break (% of fiber length): Series No. 1	Extension at break: Series No. 2	Energy to break (g. cm.$^{-2}$ normalized to both unit length and unit area) $\times 10^{-4}$: Series No. 1	Energy to break: Series No. 2
(a) Fabric Treated with H_2SO_4												
0	16	10	10.4 (17)	11.0 (12)	0.390 (7)	0.414 (4)	1.037 (21)	1.079 (12)	51.9 (16)	49.1 (5)	26.9 (27)	26.1 (14)
2	15	10	7.5 (20)	8.3 (26)	0.288 (7)	0.344 (21)	0.613 (29)	0.726 (37)	44.2 (25)	41.4 (27)	15.1 (31)	16.5 (42)
4	14	10	6.6 (30)	6.1 (15)	0.238 (18)	0.225 (8)	0.436 (36)	0.420 (18)	39.3 (26)	41.6 (8)	10.3 (42)	10.0 (16)
8	15	10	5.2 (22)	5.4 (15)	0.197 (10)	0.208 (10)	0.309 (29)	0.363 (30)	36.3 (21)	38.5 (20)	7.1 (37)	8.5 (33)
12	—	10	—	4.4 (22)	—	0.163 (10)	—	0.188 (41)	—	23.7 (58)	—	3.5 (71)
16	12	10	3.4 (21)	3.4 (23)	0.133 (16)	0.144 (5)	0.171 (35)	0.168 (40)	30.1 (38)	26.0 (52)	3.7 (54)	3.3 (65)
(b) Fabric Treated with H_2SO_4 Followed by HCHO												
0	16	—	11.2 (11)	—	0.405 (4)	—	0.744 (22)	—	38.0 (20)	—	16.5 (26)	—
2	13	10	6.9 (15)	7.4 (14)	0.304 (8)	0.314 (5)	0.499 (32)	0.434 (37)	34.1 (30)	28.4 (44)	10.6 (39)	8.5 (50)
4	16	10	7.0 (13)	5.8 (17)	0.266 (5)	0.262 (3)	0.453 (30)	0.362 (36)	35.6 (32)	28.4 (47)	9.9 (41)	7.1 (54)
8	14	10	5.1 (19)	5.0 (11)	0.208 (13)	0.225 (4)	0.331 (46)	0.343 (26)	30.8 (53)	33.7 (28)	7.0 (59)	7.3 (36)
12	—	10	—	4.6 (17)	—	0.193 (12)	—	0.285 (27)	—	31.8 (32)	—	5.9 (41)
16	13	10	2.9 (27)	3.2 (16)	0.156 (6)	0.152 (10)	0.150 (33)	0.193 (40)	18.2 (56)	26.3 (58)	2.7 (45)	3.6 (66)
(c) Fabric Treated with HCHO Followed by H_2SO_4‡												
0		16		11.2 (11)		0.405 (4)		0.744 (22)		38.0 (20)		16.5 (26)
2		10		7.8 (16)		0.298 (7)		0.598 (16)		42.8 (6)		14.1 (14)
4		10		8.3 (19)		0.343 (10)		0.581 (37)		35.0 (38)		12.7 (48)
8		10		5.9 (14)		0.234 (4)		0.369 (25)		35.5 (33)		8.5 (37)
12		10		4.8 (16)		0.201 (10)		0.249 (33)		27.3 (45)		5.1 (54)
16		10		4.5 (31)		0.188 (31)		0.259 (47)		31.6 (35)		5.8 (59)

* Numbers in parentheses following mean values are coefficients of variation (%) for the mean values.
† In some cases mean values are for a smaller number of fibers than listed because some of the fibers broke at less than 20% extension.
‡ Data at zero hours taken from Series No. 1 data where fabric was treated only with HCHO.

Formaldehyde Treatment

Samples of undamaged and the damaged wools of both Series No. 1 and No. 2 were treated in an aqueous formaldehyde solution of concentration 7.4 g./l. for 18 hrs. at 60°C. This concentration corresponds to 28% formaldehyde o.w.f. In one other case the treatment in formaldehyde preceded that in sulfuric acid. The pretreatment with formaldehyde was carried out at pH 6; in the case of formaldehyde following sulfuric acid, the pH was about 4.5.

Chemical Properties (Alkali Solubility)

The alkali-solubility values obtained for all of the series of damaged wools, with and without the formaldehyde treatments, are shown in Table I. It may be noted that the reproducibility of measurements within and between the two series is good.

For convenience of comparison and to aid in understanding the reaction, in Figure 1 the logarithm of the alkali *in*solubility (or weight percentage of wool remaining after exposure to alkali) is plotted against time of exposure to acid. The more extensive data of Series No. 1 are shown for the sulfuric acid and for the sulfuric acid-formaldehyde treatments, as well as the data for the case of the formaldehyde treatment preceding acid exposure. The lines above and below the experimental mean values indicate the limits of the standard deviation about the mean values of the measurements.

Single-Fiber Properties

Force-extension data were obtained on single fibers removed from the treated fabric samples, and the following properties were measured using techniques described elsewhere [5]: elastic modulus, stresses at the 20% and at the breaking extensions, the extension at break, and the energy to break per unit volume of fiber. Since wet testing was found to emphasize differences between differently treated fibers more than testing at 65% R.H. and 70° F, the fibers were all tested at 70°F in an aqueous borate buffer solution of pH 9.2 after an overnight presoaking.

The values obtained for the single-fiber properties are shown in Table II. When the coefficients of variation for the mean values are considered, the agreement between the Series No. 1 and Series No. 2 values is excellent. As observed previously in this laboratory, the stress at 20% extension shows a lower variance than most of the other parameters.

For more ready comparison of the single-fiber properties with the alkali-insolubility values, the logarithm of a single-fiber property, expressed as a percentage of the value for the undamaged wool, is plotted against time of exposure to acid. For single fibers withdrawn from fabrics treated in Series No. 2, the effect of time of exposure on the elastic modulus, the stress at 20% extension, the stress at break, and the energy to break are shown in Figures 2, 3, 4, and 5, respectively.

Fabric Properties

The resistance of fabric to flex abrasion, measured by the Stoll flex-abrasion test at 70°F and 65% R.H., was used to evaluate changes in fabric behavior due to chemical treatment [2]. The values obtained for flex-abrasion resistance for all the series of treated fabrics are listed in Table III. Two observations may be made regarding the results shown: first, the reproducibility of the measurements is good, and second, there appears to be no preferential resistance to abrasion when one weave direction is compared to the other.

In Figure 6 the logarithms of the values for relative abrasion resistance for the Series No. 2 sulfuric acid and sulfuric acid-formaldehyde treatments and the formaldehyde-sulfuric acid treatments are plotted against time of exposure to acid. In general, the

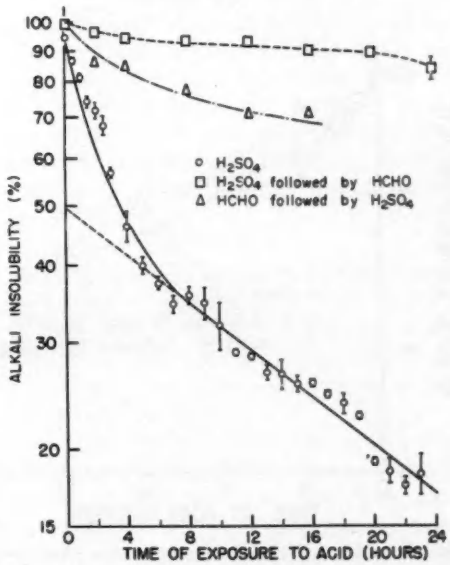

FIG. 1. *Alkali insolubility of yarns from treated fabrics.*

results of this test on the treated fabrics correspond to the results of tests on single fibers from these same fabrics. The correlation between fiber and fabric properties will be considered later in this paper.

Microscopic Observations

Fibers taken from the fabric treated for 6 hrs. with sulfuric acid were examined under the microscope at different time intervals of exposure to the alkaline solution used for determining alkali solubility. About 60% of the original weight is lost by exposure to alkali after 6 hrs. in acid. The microscopic observations, made with both unpolarized and polarized light, show that a pronounced preferential attack by the alkali is taking place on one side of the fibers.

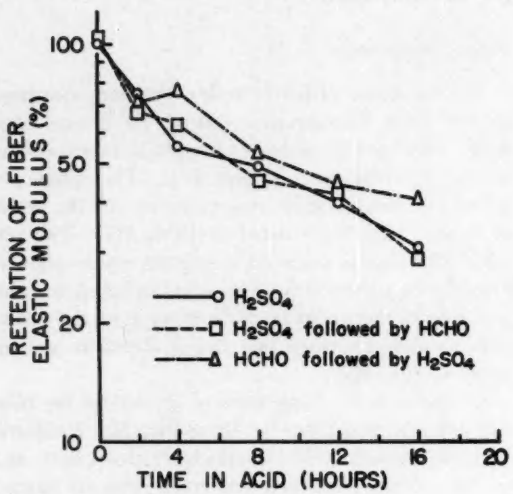

FIG. 2. *Effect of H_2SO_4 treatments on fiber elastic modulus.*

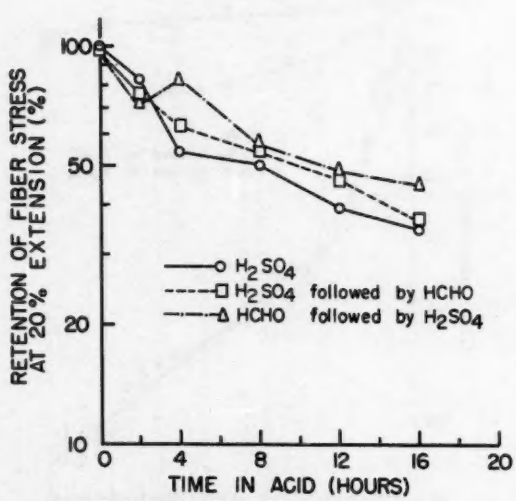

FIG. 3. *Effect of H_2SO_4 treatments on fiber stress at 20% extrusion.*

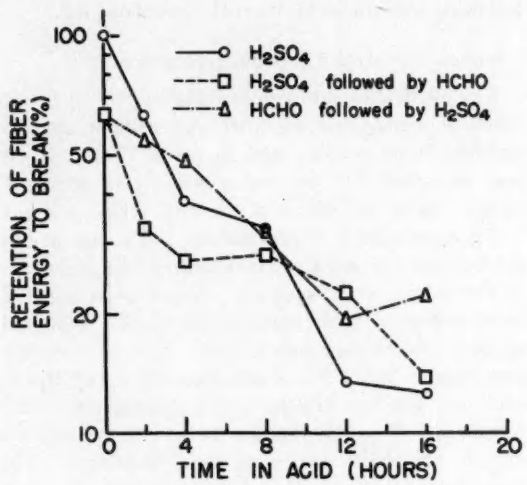

FIG. 4. *Effect of H_2SO_4 treatments on fiber breaking stress.*

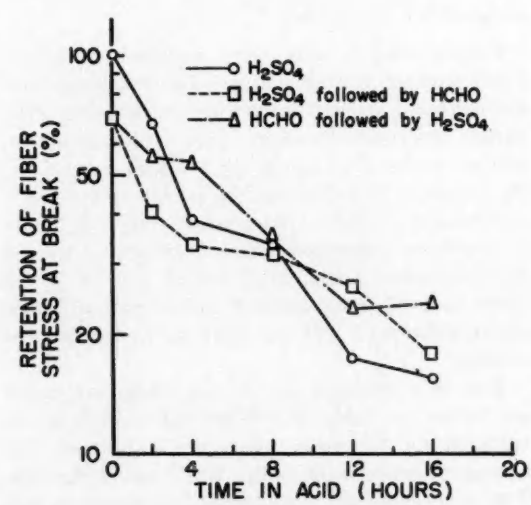

FIG. 5. *Effect of H_2SO_4 treatments on fiber breaking energy.*

TABLE III. STOLL FLEX–ABRASION RESISTANCE OF TREATED FABRICS *

Time of treatment (hrs.)	Fabric treated with H_2SO_4 Series No. 1† Warp	Fabric treated with H_2SO_4 Series No. 1† Fill	Fabric treated with H_2SO_4 Series No. 2‡ Warp	Fabric treated with H_2SO_4 Series No. 2‡ Fill	Fabric treated with H_2SO_4 followed by HCHO Series No. 1† Warp	Fabric treated with H_2SO_4 followed by HCHO Series No. 1† Fill	Fabric treated with H_2SO_4 followed by HCHO Series No. 2‡ Warp	Fabric treated with H_2SO_4 followed by HCHO Series No. 2‡ Fill	Fabric treated with HCHO followed by H_2SO_4‡ Warp	Fabric treated with HCHO followed by H_2SO_4‡ Fill
0	6807	6365	3480	3353	2075	2072	1251	1143	1251	1143
1	4234	4533								
2	3397	3116	1794	2281	1671	1660	1064	1063	1890	1675
3	2736	2660								
4	2294	2155	1006	960	1111	1378	834	852	1662	2218
8	1233	1079	746	755			582	605	1044	1025
12			455	375	632	517	459	394	698	843
16	267	387	181	182			305	218	586	481
Pooled variance (σ^2_p)	23464	28191	15246	8356	3679	22280	4388	1849	10667	8210
Standard deviation (σ_p)	153	168	123	91	61	149	66	43	103	91

* Cycles to failure (with 3-lb. tension, 1-lb. load).
† Test specimens were 1½ in. frayed strips.
‡ Test specimens were 1-in. frayed strips.

At the beginning of exposure to the alkali, a preferential swelling takes place on one side of the fiber accompanied by a simultaneous decrease in birefringence on that side. At later stages of alkali attack, the undissolved residue consists of the tubelike cuticle containing within it the mostly unchanged, still birefringent half of the fiber and, on the other or swollen side, only flimsy remnants of cortical cell membranes, most of which are dissolved away. This is strong indication that the alkali preferentially extracts the orthocortex of the fiber, leaving behind the more resistant cuticle and paracortex.

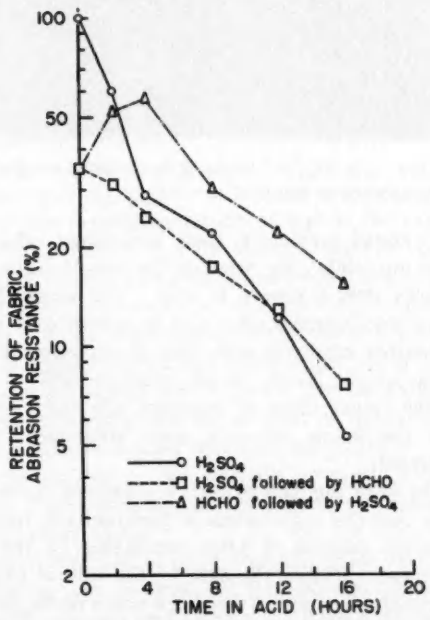

FIG. 6. *Effect on fabric abrasion resistance of H_2SO_4 treatments on fiber breaking energy.*

This effect is shown in Figure 7, which is a photomicrograph of a wool fiber after 20 min. in alkali following 6 hrs. in acid. The unpolarized light picture (top of Figure 7) shows the remaining paracortex crossing from one side of the fiber to the other. The picture taken with polarized light of the same portion of the fiber (bottom of Figure 7) shows how the birefringence exhibited by the fiber is a property of the remaining undissolved paracortex.

Discussion

It has been shown by Mercer [13] that the ortho- and paracortex of the wool fiber differ from one another in chemical reactivity. The results reported here suggest strongly that the orthocortex is more readily removed after prior sensitizing by an aqueous sulfuric acid treatment.

For the fabric series treated with acid, a strong correlation was found between alkali solubility and the physical property measurements. This may be seen by comparing the "H_2SO_4" curve of Figure 1, where alkali insolubility decreases smoothly with increasing times of acid exposure, with the correspond-

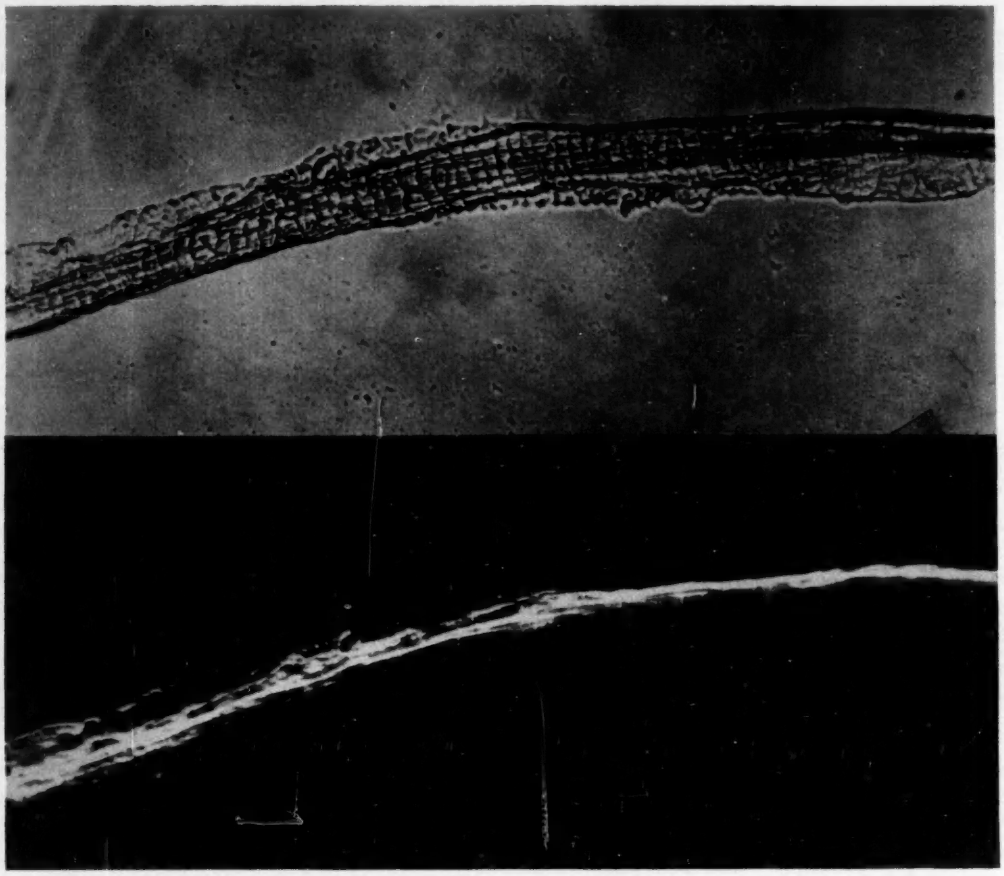

FIG. 7. *Photomicrograph of a single wool fiber treated 6 hrs. with H_2SO_4, followed by 20 min. in alkali.* Top—*unpolarized light;* bottom—*polarized light.*

ing curves for measurements of single-fiber properties shown in Figures 2, 3, 4, and 5. There is a similar good correlation with the fabric property, flex-abrasion resistance, as may be observed from inspection of the "H_2SO_4" curve of Figure 6.

The curve drawn through the experimental points for "H_2SO_4" in Figure 1 was calculated from the equation:

$$(\text{Wool})_t/100 = 0.451\ \exp(-0.477t) + 0.493\ \exp(-0.0441t),$$

where $(\text{Wool})_t$ is the percentage of wool found insoluble by the alkali-solubility test after t hours of exposure to acid. The values of the constants in the equation were obtained by a least-mean-squares analysis of the experimental data.

As stated previously, these percentage values for alkali insolubility are based on the weight of the wool samples after exposure to acid. The weight losses of the wool samples after acid treatment were found to increase regularly with time of exposure to acid. These weight losses, of the order of 10% to 15% for the longer times of exposure, are much smaller than the losses observed after subsequent alkali treatment.

The fit of the data to such a calculated curve suggests that the orthocortex is preferentially removed by alkali because of prior sensitizing by the acid treatment. Fitting the data by the sum of two exponentials also implies that the kinetics of the process is first order with respect to each of the parts of the cortex. The ratio of the exponents indicates that

the orthocortex becomes sensitized at a specific rate about 11 times greater than that for the paracortex. The extrapolation of the line through the latter portion of the experimental points to the zero of time gives an intercept value that indicates that the orthocortex and paracortex in this sample are present in about equal amounts by weight.

This result, in combination with the microscopic observations reported previously, indicates the following mechanism. During exposure to the acid a damaging reaction proceeds at different rates in the two segments of the cortex "sensitizing" them in different degrees towards alkaline attack. When subsequently "developed" in an alkaline solution, the damaged material is removed mainly from the orthocortex which has been the more sensitized. As this fraction of the cortex becomes exhausted, the alkali solubility increases much less rapidly with time of exposure to acid, corresponding to the removal of the more slowly attacked paracortex. The damage to the wool is also reflected in the progressive decrease in the values for the physical properties of the single fibers and for the flex-abrasion resistance of the fabrics.

When the fabrics were given a pretreatment or a posttreatment with formaldehyde, a large decrease in alkali solubility, or increase in alkali insolubility, was observed. This is readily seen by reference to Figure 1. The physical properties of single fibers from these same fabrics are shown in the corresponding curves of Figures 2, 3, 4, and 5; the effect of the formaldehyde treatments on the fabric-abrasion resistance is shown in Figure 6.

The treatment with formaldehyde thus appears to reverse the deleterious effects of acid in the case of the alkali-solubility test for damage, but the results of the physical tests on the same treated wools indicate that no such repair of damage has, in fact, occurred. There is an indication that the pretreatment with formaldehyde affords some protection at 2 and 4 hrs. of subsequent acid exposure, but the extent of protection is slight and not as great as the improvement in alkali solubility would appear to show. The observation that a formaldehyde treatment will decrease alkali solubility has been made previously by several other workers [4, 9, 15, 16], but little work has been reported to show that the effect may be a misleading one in terms of the physical properties of wool. Brown and Harris [3] have used Speakman's 30% index to study the changes in physical properties of wool subjected to sulfoxylate-formaldehyde treatments; they have shown that a decrease in alkali solubility is not always accompanied by an improvement in physical properties. Lees and Elsworth [12] caution that "the results of alkali solubility tests can be adequately interpreted only if the treatment to which the sample has been subjected is known or can be safely presumed."

The formaldehyde probably acts to form cross-links between polypeptide chains in the wool fiber. The number of these cross-links may be appreciable compared with the number of naturally occurring disulfide cross-links provided by cystine. Such an additional cross-linking process, where the cross-links would be relatively stable to alkaline attack, is the probable cause of the decrease in alkali solubility. That is, it is probably more difficult for the alkali to remove more highly cross-linked polymer molecules from the wool fiber matrix. Where no formaldehyde treatment is involved, the acid probably acts chiefly to hydrolyze peptide bonds in the fiber, leading to increases in alkali solubility. This is reflected in the decrease in single-fiber properties. The cross-linking reaction prevents dissolution by alkali, but fails to repair the point of actual damage, the peptide link broken by acid hydrolysis.

At this time the exact chemical nature of these formaldehyde cross-links is unknown. For example, it cannot be stated with certainty that adjoining peptide chains become linked by new covalent bonds as a result of the formaldehyde treatment. If such new primary bonds are formed, there may well be more than one type.

Most conditions of acid damage likely to be met in textile practice will concern alkali solubilities of less than 50%. In terms of the above discussion, this means that the important damage is likely to be confined largely to the orthocortex whose properties are therefore of special concern when preventive or recuperative measures are contemplated.

A good correlation has been found in this work between a single-fiber property (the breaking energy) and a fabric property (resistance to flex abrasion). This implies that the capacity of a fabric to withstand flex abrasion is related to the ability of its constituent fibers to absorb energy prior to breaking. Figure 8 shows a log-lot plot of flex-abrasion resistance *versus* single-fiber breaking energy for the Series No. 2 acid and acid-formaldehyde treatments and for the formaldehyde-acid treatments. The line

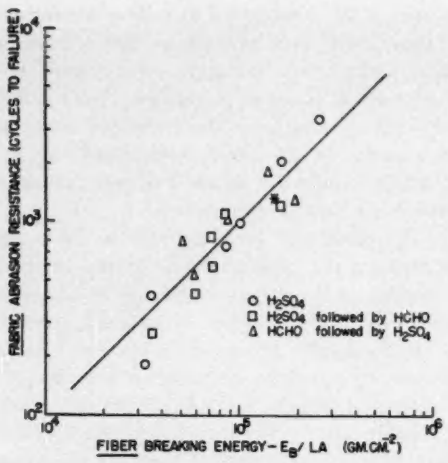
FABRIC ABRASION RESISTANCE (CYCLES TO FAILURE)
FIBER BREAKING ENERGY – E_B/ LA (GM.CM.$^{-2}$)
H_2SO_4
H_2SO_4 followed by HCHO
HCHO followed by H_2SO_4

FIG. 8. *Fiber abrasion resistance* vs. *fiber breaking energy (Series No. 2).* * *(Fiber data from Series No. 1.)*

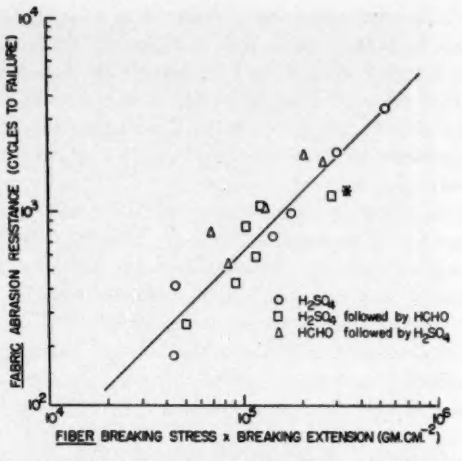
FABRIC ABRASION RESISTANCE (CYCLES TO FAILURE)
FIBER BREAKING STRESS x BREAKING EXTENSION (GM.CM.$^{-2}$)
H_2SO_4
H_2SO_4 followed by HCHO
HCHO followed by H_2SO_4

FIG. 9. *Fabric abrasion resistance* vs. *fiber breaking stress × breaking extension (Series No. 2).* * *(Fiber data from Series No. 1.)*

drawn through the points has a slope of unity, and the fit of the data to it indicates that there is a direct proportionality between *fabric* abrasion resistance and *fiber* breaking energy.

Hamburger [6, 10] has shown that a relationship similar to this one exists for a comparison of the abrasion resistance and energy to break of low-twist filament yarns of several textile materials. In his study, the yarns were mechanically conditioned to remove secondary creep prior to the determination of breaking energy. In this study, such a prior conditioning would appear unnecessary. This may be due to the fact that the fibers were tested wet where the secondary creep consideration is not of such importance. Furthermore, the relationship in this work is between textile materials of widely different constructions—that is, between fibers and fabrics.

Another property that is a close approximation of fiber breaking energy is the product of the breaking stress and breaking extension. Hence, this property, which was measured in all cases, should be related to fabric flex abrasion in the same way, and the log-log plot of Figure 9 shows that this is indeed the case. The fit of the data to the line of unit slope drawn through the points indicates that there is a direct proportionality in the case of these experiments between *fabric* flex-abrasion resistance and the product of *fiber* breaking stress and breaking extension.

Acknowledgment

This work has received the support of several industrial sponsors and the International Wool Secretariat in connection with the Wool Research Project at Textile Research Institute.

The authors wish to express their thanks to Mr. Edward B. Jeffries for performing most of the alkali-solubility determinations, to Mrs. Carol B. Piper and Miss Edith T. L. Voong for single-fiber measurements, and to Miss Dorothy F. O'Reilly for obtaining the photomicrographs shown here. Especial thanks are due Mr. Werner von Bergen of the Forstmann Woolen Company for many helpful discussions during the course of the work and to Mr. Claude S. Clutz of that company for providing the data on the flex-abrasion resistance of the treated fabrics.

Literature Cited

1. Am. Soc. Testing Materials, Committee D-13, "Tentative Method of Test for Alkali-Solubility of Wool" (D 1283–53T), 1953, in 1953 Supplement to Book of ASTM Standards, Part 7, p. 130.
2. Am. Soc. Testing Materials, Committee D-13, "Tentative Methods of Test for Resistance to Abrasion of Textile Fabrics" (D 1175–51A), 1951, in 1952 Book of ASTM Standards, Part 7, p. 156.
3. Brown, A. E., and Harris, M., *Ind. Eng. Chem.* **40**, 316 (1948).
4. Brown, A. E., Hornstein, L. R., and Harris, M., TEXTILE RESEARCH JOURNAL **21**, 222 (1951).

5. Evans, T. F., and Montgomery, D. J., TEXTILE RESEARCH JOURNAL **23**, 689 (1953).
6. Hamburger, W. J., TEXTILE RESEARCH JOURNAL **15**, 169 (1945).
7. Harris, M., and Smith, A. L., *J. Research Natl. Bur. Standards* **17**, 577 (1936); *Am. Dyestuff Reptr.* **25**, 542 (1936).
8. Horio, M., and Kondo, T., TEXTILE RESEARCH JOURNAL **23**, 373 (1953).
9. Kann, A., U. S. Patent 787,923 (1905).
10. Kaswell, E. R., "Textile Fibers, Yarns, and Fabrics," New York, Reinhold Publishing Corp., 1953, p. 305.
11. LaFleur, K. S., TEXTILE RESEARCH JOURNAL **19**, 497 (1949).
12. Lees, K., and Elsworth, F. F., *J. Soc. Dyers Colourists* **68**, 207 (1952).
13. Mercer, E. H., TEXTILE RESEARCH JOURNAL **23**, 388 (1953).
14. Ryberg, B. A., *Am. Dyestuff Reptr.* **29**, P588 (1940).
15. Speakman, J. B., and Peill, P. L. D., *J. Textile Inst.* **34**, T70 (1943).
16. Stoves, J. L., *Trans. Faraday Soc.* **39**, 294 (1943); *J. Soc. Dyers Colourists* **63**, 65 (1947).

(Manuscript received June 16, 1954.)

A Multiple-Unit Stress Relaxometer

Walter J. Thorsen

Western Utilization Research Branch, Agricultural Research Service, U. S. Department of Agriculture, Albany, California

Abstract

The application of an improved resistance-wire strain gage [3] to a multiple-unit instrument for the measurement of stress relaxation in single fibers is described. Forces are autographically recorded with a precision and accuracy of better than 3 mg. or ½% of full scale. The instrument is stable over long periods and is designed to record directly in units of stress, the scale being identical for all fibers.

Introduction

The measurement of stress relaxation in single fibers, particularly when carried out in selected environments affecting structure, offers valuable insight into the correlation of mechanical properties with structure. The technique, however, presents problems not ordinarily encountered in stress measurements. Not only is a stress-measuring device required which is highly sensitive to small forces, but the device must also be stable in order to measure forces over extended periods of time. Moreover, provisions for easy mounting of the fiber and means for accurate fiber elongation are required, and it should be possible to immerse the fiber in liquid media maintained at a constant temperature. Since experiments are frequently of long duration a multiple-unit apparatus is highly desirable. Kubu [1] described the application of a differential transformer to a multiple-unit stress relaxometer. This paper describes the application of an unbonded-resistance-wire strain gage reported in a previous paper [3] to a multiple-unit stress relaxometer.

Constructional Details

General

The apparatus consists of a row of 12 single-fiber units mounted between a thermostatted gage chamber (on top) and a main control chamber (Figure 1). The associated recording potentiometers are seen to the right. The battery power supply with its volt-

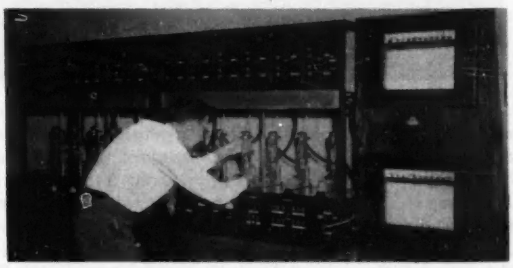

FIG. 1. *General view of stress relaxometer and associated single-point and multiple-point recorders. Fiber is being mounted in jacketed cylinder.*

age regulator is shown in Figure 2. Equipment for thermostatting the fiber units and gage chamber is not shown.

Fiber Mounting

Each fiber is attached to glass hooks and mounted vertically inside a glass cylinder surrounded by a water jacket, the lower end fixed to a stopper at the base of the cylinder and the upper end coupled to a glass rod which is suspended from the gage chamber (Figure 3). The lower hook is formed from a small glass rod which is inserted into a hole in the stopper.

The glass rod which is suspended from the gage chamber transmits the fiber tension directly to a strain gage. Elongation of the fiber is accomplished by lowering the jacketed cylinder with an elongating mechanism, which is seen in Figure 3, supporting the cylinder. In this manner the fiber can be surrounded with the selected solvent and thermostatted at the desired temperature. The stoppers are provided with "T" drain tubes to permit draining of the solvent into either a common drain pipe or a beaker for analysis. Pinch clamp valves allow rapid drainage and minimize fiber exposure to air. The water jackets are connected in four series-parallel circuits to reduce the pressure drop.

Elongating Mechanism

The jacketed cylinder is clamped to a vertical rod protruding from the elongating mechanism. For rapid elongations this clamp may be lowered to a pre-set stop clamped on the rod. For high-precision slow elongations, such as the initial unkinking of a fiber before a run, or the study of uncrimping forces, a screw mechanism is needed. This consists of a worm-driven gear threaded on the vertical rod. The worm gear is connected to a control rod which extends to the front of the instrument and is turned by a crank. The vertical rod and gear have a metric thread and the worm gear ratio is such that each

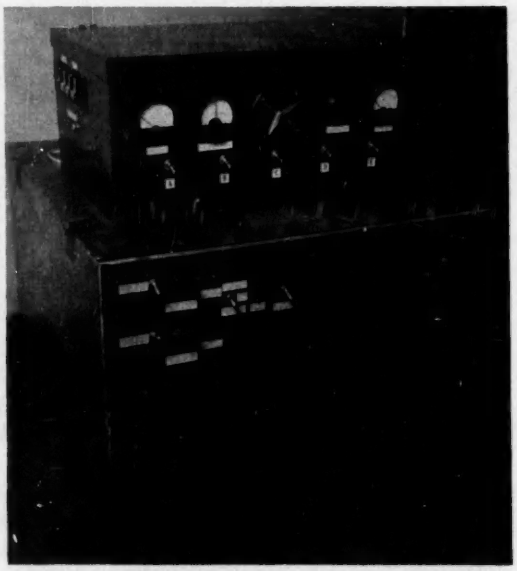

FIG. 2. *Battery power supply and output voltage regulator. Meters on the voltage regulator indicate the input and output voltages and standard cell current. Center dial indicates position of rheostat* R_{bat}. *Switch* A *connects resistor in series with standard cell during initial adjustments of multi-turn potentiometer. Switches* B *and* D *reset the stepping relay,* C *overrides the interval timer, and* E *is the main power switch. For a detailed discussion of this equipment see* [3].

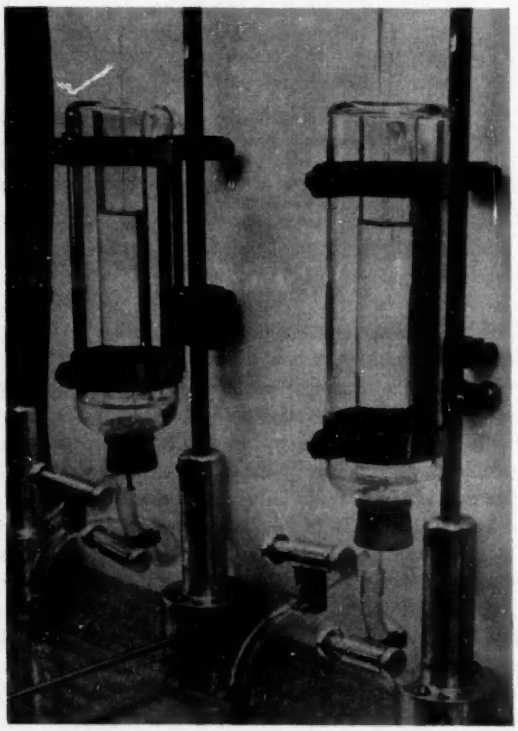

FIG. 3. *Jacketed cylinders which allow fibers to be thermostatted and surrounded with selected solvent. Cylinders are supported by elongating mechanism which permits accurate elongation of fibers to any predetermined amount.*

turn of the control rod raises or lowers the vertical rod 0.2 mm.

Gage Chamber

The gage chamber accommodates 12 gages, one for each fiber assembly, and the gages are positioned above the jacketed cylinders. The chamber is lined with sheet copper which in turn has 0.5-inch copper tubes clamped to it and spaced about 2 in. apart. Water thermostatted at about 38°C is circulated through the tubing; control to ± 0.02°C is satisfactory. The thermostat is located in the water stream inside the chamber so that the temperature of the water flowing through the coils is controlled rather than the external water bath. Thus temperature fluctuations due to ambient temperature changes are eliminated.

The chamber walls are insulated against heat loss to permit good temperature regulation. An exterior layer of fibrous insulating material is used on all walls except the top and front, which are wood and micarta, respectively. These materials provide sufficient thermal insulation. The top of the chamber consists of a plywood section on hinges to provide access to the gages. The container for the thermostat is attached to this section. The gage chamber is supported by 1-inch angle iron, which is used throughout as a framework. This rigid framework is necessary, since the gages are sensitive to small deflections, and at the same time it facilitates shielding of all circuitry. Although shielding is not absolutely necessary, it reduces A-C pickup and enables the response of the potentiometers to be maintained at a maximum. Metal conduit is used to bring the wires from the gage chamber to the lower chamber, which in turn are shielded by the base plate and sheet metal walls. Both switching panels are laminated plastic and are shielded by an inner lining of sheet metal directly behind the panels.

Electrical Circuit

A diagram of the complete electrical circuit is shown in Figure 4. The ON–OFF switches, fine and coarse balance switches, precision zero output potentiometers (3 ohm), input voltage rheostats, and attenuators (multiturn potentiometers, 5,000 ohm, ± 0.1% linearity) are mounted on the upper panel. The attenuators, which are connected across the outputs of the gages, are adjusted so that fibers of different diameters will produce equal gage outputs with equal fiber stresses. Thus, when the input voltage rheostats are adjusted to give identical outputs per gram force and the precision zero output potentiometers are set so that all gages have a common zero force reading, the records are in known units of stress with scales identical for all fibers. The relation between the stress and chart deflection is expressed by the equation:

$$\frac{\dfrac{\text{dynes}}{\text{chart inch}}}{\text{cm.}^2} = \frac{980}{\text{input volts} \times C \times A_M} = \frac{\text{constant}}{\text{input volts}},$$

where C = chart in./g./gage input volt, without attenuation, and A_M = cross-sectional area in cm.² established as a minimum.

The stress per chart inch is immediately obtained from a measurement of the input voltage. In order to adjust the attenuators rapidly, tables of attenuation *vs.* diameter are used. For example, one for use with small fibers has 100% output listed for a fiber of minimum cross-sectional area $A_M = 1.33 \times 10^{-6}$ cm.² (13.0 μ) and all larger fibers attenuated in relation to their area A_f—*i.e.*, attenuation $\delta = 1 - A_f/A_M$, and A_f/A_M is tabulated since the attenuator dials may be set to this figure directly. Use of the attenuators and precision zero output potentiometers eliminates 600 subtractions and multiplications in the calculation of one 12-fiber run (25 points calculated per fiber). The use of more than one attenuation table allows the stress range to be changed during an experiment.

Gage output, shorting, and tapping switches are mounted on the lower panel, as well as the voltmeter,

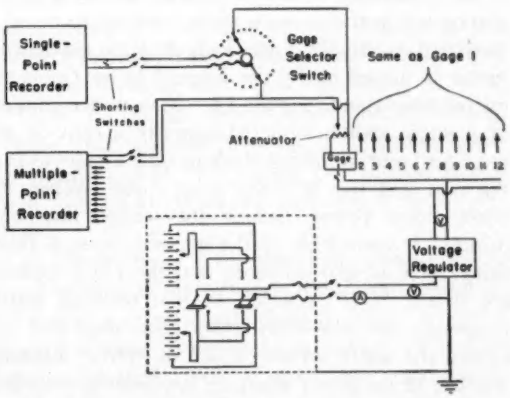

FIG. 4. *Circuit diagram of stress relaxometer and battery power supply.*

ammeter, fuses, input, and output cable receptacles. The frame of the relaxometer and one side of the battery are grounded. The input and output cables are shielded and the battery box is constructed of steel. As seen in Figure 4, the gage outputs may all be switched to the multiple-point recorder or individually switched to the single-point recorder. The gage shorting switches are provided to cause unused points on the multiple-point recorder to read zero, since chart reading is much easier when stray points are eliminated.

Voltage Supply

Three 8-volt, 80-ampere-hour truck batteries are used. Since the instrument input voltage must remain constant, the voltage regulator described previously [3] was modified and used (Figure 2). This modification was to change R_{bat} to 0.5 ohm and the steps to 0.4 ohm. If no regulator is used, manual adjustment of the rheostat every hour is satisfactory. For continuous long range experiments two sets of batteries are employed (Figure 4); when one set is low the other can be switched in without interrupting the current.

Recorders

A single- and a multiple- (12) point recorder is used. Each has a 1.0 mv. span and two-second pen speed (full chart travel time), and uses a high gain amplifier [2]. The 1.0-mv. span was chosen instead of a 2.5-mv. span employed previously [3] due to the fact that the attenuators reduce the gage sensitivity considerably.

An additional electro-mechanical device was incorporated in the multiple-point recorder to cause it to record exactly 12 points each time the chart drive motor is turned on by the interval timer (mounted on recorder stand, Figure 1). This device consists of a micro switch mounted opposite a cam on the recorder point switching shaft in such a manner that the cam will trip it every point cycle. When the chart motor power (which also drives the point printer) is turned on by the interval timer, a time-delay relay is also activated and the relay contacts are in the "ON" position so that printing starts. However, the time-delay relay soon trips and activates the micro switch, which is "ON," allowing it to cut off the motor when the last point is recorded. When the timer turns off the current the time delay relay is reset back to the "ON" position. Thus the cycle can be repeated.

Operating Procedure

The gages are usually warmed up about 12 hrs. beforehand. The water jackets are brought to the desired temperature and the fibers are mounted. Whatever solution is desired as a fiber environment is added and the fibers are allowed to soak. If it is desired to have all forces recorded as unit stresses the attenuators are set. Gage No. 1 is switched to the single point recorder and is "balanced" to zero voltage output. Then the water jacket is lowered until a small tension is applied to the fiber, usually just enough to unkink it. The same procedure is repeated for the rest of the gages. The stops are clamped on the elongating mechanism rod below the jacket clamp the distance that the fibers are to be elongated. The single-point recorder chart drive is started and fiber No. 1 is elongated. After 10 min., for example, gage No. 1 is switched to the multiple-point recorder and gage No. 2 is switched to the single-point recorder. The multiple point is set to record every 3 min. This procedure is repeated until all 12 fibers are elongated. In this manner the stress in each fiber will be continuously recorded for the first 10 min. and thereafter at intervals of 3 min. For periods lasting more than 24 hrs. recordings at 30-minute intervals are sufficient.

Acknowledgment

The author wishes to acknowledge the assistance of Mr. Morris F. Pool and Mr. Andrew Yeiser of this Laboratory, and the precision machine work performed by Mr. Ernst Aeschlimann of our machine shop. Special thanks are due to Dr. Harold P. Lundgren for his encouragement and suggestions.

Literature Cited

1. Kubu, E. T., TEXTILE RESEARCH JOURNAL **22**, 765 (1952).
2. Minneapolis-Honeywell Regulator Co., servo-amplifier type 12X, No. 354574, Instrumentation Data Sheet No. 10.20–4.
3. Thorsen, W. J., TEXTILE RESEARCH JOURNAL **24**, 407–13 (1954).

(Manuscript received May 4, 1954.)

Properties of Apparel Wools

VIII. The Aging of Worsted Yarn*

Harris M. Burte†

Textile Research Institute, Princeton, New Jersey

Abstract

Mechanical properties derived from the force-extension curve, and including tensile recovery, have been measured for single strands of steamed worsted yarn throughout their aging at 65% R.H. and 70°F. None of these properties appears to change significantly throughout an aging period of several months.

Measurements on single strands of unsteamed yarn which are permitted to untwist prior to test indicate a progressive change in physical properties with time of aging. This is caused by a slow setting-in of the twist similar to that provided rapidly by a steaming treatment.

Introduction

Since there is a widespread belief that aging yarn prior to weaving has beneficial effects on the weaving, an investigation of worsted yarn aging has been one of the objects of the Wool Research Project. The results of the processing trials at the Forstmann Woolen Company indicated that aging the yarn did increase the loom efficiency during weaving [3]. Experiments at the Textile Research Institute have been directed toward an investigation of the aging mechanism by determining which properties of the yarn change during aging. This paper presents the results of measurements of several tensile mechanical properties of the yarn; for yarn tested without loss of twist, none of the mechanical properties so far investigated are affected by aging.

Sampling and Experimental Methods for Steamed Yarns

The Wool Research Project was concerned with an evaluation of the properties and processing of four wools: an Australian 70's grade Merino, a New Zealand 58's grade crossbred, a U. S. 64's grade Rambouillet, and a U. S. 58's grade crossbred. A summary of the processing operations is given in the first paper of this series [3]. The two fine wools were spun into 1/40 worsted count yarns; the two medium wools were spun into 1/37 worsted count yarns; all singles yarns had a Z twist of 13 to 14 turns per inch. The singles yarns were twisted into 2-ply yarns (2/40 and 2/37) with an S twist of 12 to 13 turns per inch. During the mill processing, the 2-ply yarns were aged after steaming to set the twist but before rewinding or warping. The experiments on 2-ply yarns were performed on yarns sampled at this stage in processing.

Partially filled bobbins of the 2-ply yarns were doffed from the twisting frame at the mill, given a normal steaming to set the twist, and brought to the Textile Research Institute where they were allowed to age in a conditioned room maintained at 65% R.H. and 70°F. At various times after processing, samples were removed from the bobbins and tested at 65% R.H. and 70°F, using the Instron tensile tester [2]. Two types of experiment were performed.

(*a*) *Single-strand force-extension curve.*—Single-strand samples of 10-inch gage length were extended to break at a constant rate of 12 in./min. Figure 1 shows a typical force-extension curve; little fiber slippage occurred as these yarns were extended to break. The parameters measured from the curve were the Hookean slope, which is the slope of the

* A report of work done under contract with the U. S. Department of Agriculture and authorized by the Research and Marketing Act of 1946. The contract is being supervised by the Western Utilization Research Branch of the Agricultural Research Service. Other phases of the project are sponsored by the American Wool Council; the International Wool Secretariat; the National Wool Trade Association; the Office of Naval Research, Department of the Navy; and by a number of American wool manufacturers.

Parts I–VII appeared in the Feb., 1952, July, 1952, July, 1953, Oct., 1953, July and August, 1954, issues, respectively.

† At present on active duty in the United States Air Force.

early linear region where the force is rapidly increasing, the breaking strength, and the breaking extension. For successive samples from a single bobbin, these parameters had coefficients of variation in the range from 10% to 20%.

(*b*) *Tensile recovery.*—Single-strand samples of 10-inch gage length were extended to 15% extension at a constant rate of 12 in./min. and were immediately allowed to contract at the same rate. After a very short time (8–9 sec.) at no load, they were re-extended to break. Figure 2 presents the force-extension curve for a typical cycle of extension, contraction, and re-extension: *OA* is the initial extension; *OB* is the initial set, the unrecovered extension remaining after a single cycle of extension and contraction; *BC* is the tensile recovery during the period of 8–9 sec. before the second extension. Note that due to a condensation of the yarn structure, the extension and contraction curves leave and approach the extension axis almost asymptotically. This is similar to the influence of crimp on the stress-strain curves of single fibers (see Figure 12 in reference [3]). The linear portions of the extension curves were extrapolated to the extension axis to give *O*

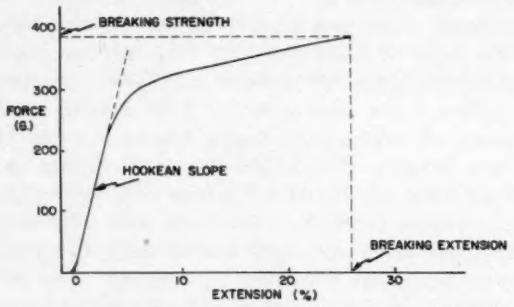

FIG. 1. *Typical force-extension curve for steamed 2/37 worsted yarn made from the New Zealand medium wool; rate of extension = 12 in./min.; gage length = 10 in.*

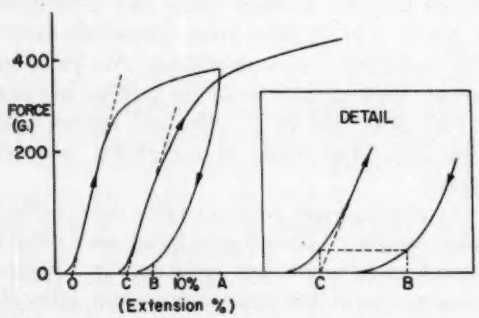

FIG. 2. *Typical tensile recovery measurement for steamed 2/37 worsted yarn made from the New Zealand medium wool; rate of extension = 12 in./min.; gage length = 10 in.*

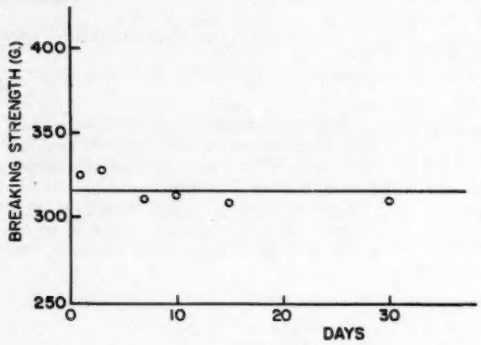

FIG. 3. *The effect of yarn aging on the single-strand breaking strength of steamed 2/40 worsted yarn made from the U. S. fine wool.*

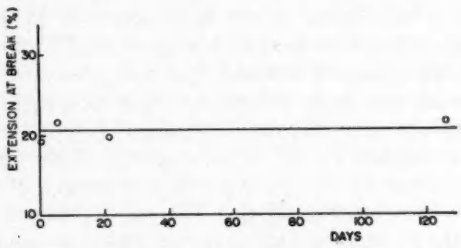

FIG. 4. *The effect of yarn aging on the single-strand breaking extension of steamed 2/37 worsted yarn made from the U. S. medium wool.*

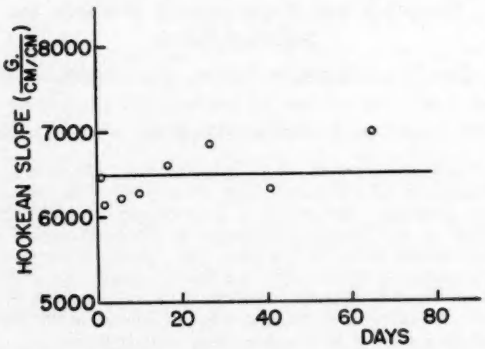

FIG. 5. *The effect of yarn aging on the single-strand Hookean slope of steamed 2/37 worsted yarn made from the New Zealand medium wool.*

and C, the points at which it was assumed the curves would start if this effect of condensation of the yarn structure did not exist; the nonlinear recovery curve, however, cannot be easily extrapolated. The detail drawing in Figure 2 shows the construction that was used to obtain the point B.

The property considered in this work was the initial set OB, expressed as a percentage of the initial gage length. The initial extension (nominally 15% of the initial gage length) varied slightly from sample to sample. There is an approximately linear relation between the initial set and the initial extension, and all values of the set were corrected to an initial extension of 15%. For successive samples from a single bobbin, all tested on the same day, the coefficient of variation of corrected values of the initial set was less than 5%.

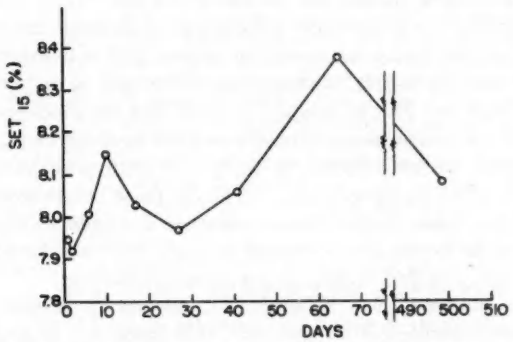

FIG. 6. *The effect of yarn aging on the initial set after a single extension to 15% of steamed 2/37 worsted yarn made from the New Zealand medium wool.*

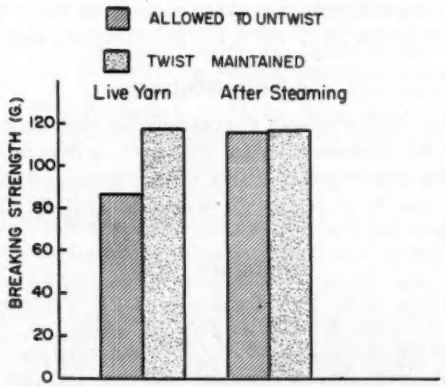

FIG. 7. *The effect of twist liveliness on the physical testing of wool yarn.*

Results for Steamed Yarns

The experiments described above were run on yarn from each of the wools. The response to aging, insofar as these mechanical properties were concerned, was the same for the four wools. Figures 3, 4, and 5 present representative data which show that the breaking strength, the breaking extension, and the Hookean slope were not affected by aging for several months. Each point is the average of 10–20 samples from each of two bobbins. The data have been analyzed statistically, and for none of these properties does the average on any one day differ from that on any other day. Figure 6 shows representative data for the initial set after an extension to 15% as a function of aging time (time after processing). Each point is the average of 5 samples from each of two bobbins. Although there were significant differences between the averages on various days (for example, the mean value on day 65 was significantly high), this was an erratic effect, and no steady progression with aging time was found. It is probable that this erratic day effect may be attributed to slight differences in the relative humidity or temperature of the laboratory among the times of testing. The very low sampling variance of the initial set enabled the detection of quite small differences due to changes in relative humidity of only a few percent, and the conditioned laboratory used could easily have varied by $\pm$ 2% R.H.

It is concluded that none of these simple tensile mechanical properties of the steamed plied yarns shows any detectable change due to aging.

Some Experiments with Unsteamed Yarn

Experiments were also performed to study the mechanical properties of single yarn and unsteamed

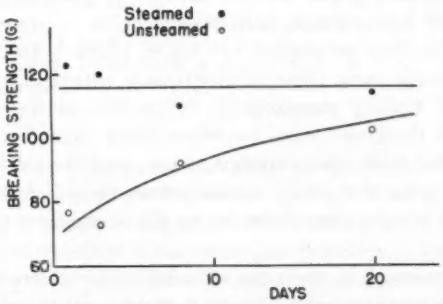

FIG. 8. *The effect of yarn aging on the breaking strengths of steamed and unsteamed 1/42 worsted yarn made from the Australian fine wool. The yarn samples were allowed to untwist before testing.*

yarn. During the testing of unsteamed yarn, great care must be taken to prevent any loss of twist during the transfer of the yarn sample from the bobbin to the testing machine. Figure 7 shows the results of measurements of the force-extension curves of "live" unsteamed yarn and of the same yarn after the twist had been set by steaming. Two experimental procedures were used; in one, 30-inch lengths of yarn were removed from the bobbin, held at one end, and allowed to untwist; in the other, no twist was lost while transferring the samples from the bobbin to the testing machine. While the steamed yarn showed no tendency to lose any twist, the spontaneous loss of twist in the unsteamed yarn caused a decrease of the breaking strength and the Hookean slope.

Figure 8 shows the results of an aging experiment on steamed and unsteamed single yarn where the yarn samples were allowed to untwist before testing. The increase in breaking strength of the unsteamed yarn can be attributed to a slow setting-in of the twist similar to that provided rapidly by a steaming treatment. Thus, as the aging of the unsteamed yarn proceeded, the yarn progressively lost less twist while being transferred from bobbin to tester, and the breaking strength increased. For the steamed yarn, which showed no tendency to lose twist, the breaking strength showed no statistically significant change with aging. Samples of unsteamed or steamed yarn, tested so that no twist was lost while the yarn was transferred from the bobbin to the tester, were found to be unaffected by aging. Both gave results identical with those shown in Figure 8 for the steamed yarn.

Discussion

Another paper in this series [1] presents data which indicate that, with the exception of crimp, the mechanical properties of single fibers withdrawn from the yarns show no progression with aging time. This finding complements the results of the yarn tests described here, for when these yarns are extended little fiber slippage occurs, and the mechanical properties under consideration should show essentially the same behavior as the single-fiber properties.

Inasmuch as the ratio of yarn breaks to length of yarn woven is relatively small, there is the possibility that aging has an effect on only a small fraction of the total length of yarn strand, say, at widely separated weak places, and that its contribution to the average of the properties measured here is too small to be detected. It is difficult, however, to conceive of an aging mechanism which will affect widely separated places along the yarn strand without also affecting the properties of the remainder of the strand.

The mill processing results have indicated that aging these steamed yarns has a beneficial effect on weaving. Since it has been shown that the simple force-extension properties do not change during aging, attention must be focused on other properties, such as the frictional properties or the behavior under conditions of impact, or rapidly repeated loading.

Summary

Bobbins of worsted yarn were allowed to age under controlled conditions (65% R.H., 70°F), and samples were tested at various times after processing. The properties measured include those obtained from the single-strand force-extension curve and the initial set remaining after a 15% extension.

If the testing technique for unsteamed yarn prevents any loss of twist, it is found that the Hookean slope, the breaking strength, and the breaking extension are not affected by aging. If unsteamed yarn is given an opportunity to lose its twist before testing, these properties are affected by aging. The aging causes a slow setting-in of the twist similar to that provided rapidly by a steaming treatment.

Steamed yarn showed no tendency to untwist, and mechanical tests showed that aging for several months did not affect the Hookean slope, the breaking strength, the breaking extension, or the initial set remaining after a 15% extension. Since aging steamed yarn does appear to provide an increase in weaving efficiency, the effect of aging on other properties of the yarn will have to be investigated.

Acknowledgment

The author wishes to acknowledge with appreciation the assistance of Mr. Walter O. Seifert in some of the experimental phases of this work and of Dr. Thomas F. Evans in the statistical analysis of the data.

Literature Cited

1. Evans, T. F., and Montgomery, D. J., TEXTILE RESEARCH JOURNAL **23**, 689–701 (1953).
2. Hindman, H., and Burr, G. S., *Trans. Am. Soc. Mech. Engrs.* **71**, 789–96 (1949).
3. von Bergen, W., and Wakelin, J. H., TEXTILE RESEARCH JOURNAL **22**, 123–37 (1952).

(Manuscript received May 27, 1954.)

Mechanics of Elastic Performance of Textile Materials

Part XI: Factors Affecting the Translation of Certain Mechanical Properties of Cordage Fibers and Yarns into Cordage Strands and Ropes*

M. M. Platt, W. G. Klein, and W. J. Hamburger†

Fabric Research Laboratories, Inc., Boston, Massachusetts

Abstract

This paper is concerned with the quantitative analysis of some of the factors which determine the strength of cordage strands and plied yarns. When integrated with the analyses covered in Part IX of this series [1], a complete picture is given of the effects of the factors considered on translation of the strength of cordage fibers into singles yarns, strands, or plied yarns and, by direct projection, into cordage ropes. The problem is solved by a combined mechanical-statistical analysis similar in type to that given previously [1], assuming simplified idealized geometrical forms and a normal distribution of yarn properties. It is shown that such assumptions produce results which agree, within the limits of engineering accuracy, with experiment. Checks were available for: 9-rope strands of varying twist structure, all made of Manila abaca fiber; a small Sansevieria 3-ply rope; and small size bundles of Manila abaca fiber used as laboratory models to illustrate the effect of the number of singles in a strand or plied yarn. The factors which are analyzed mathematically for their mechanical effects include: singles yarn twist; strand or plied yarn twist; number of singles which are stranded; elastic properties of the singles yarns; and uniformity of the mechanical properties of the singles yarns.

Significant losses occur in the translation of the strength of the yarns into the strands and ropes, efficiencies of the order of 75% being theoretically calculated and experimentally verified. However, the major cause of the low over-all 40% translation of fiber strength into strands and ropes resides in the low fiber-to-yarn translation of only 55%. The losses from yarns to strands are indicated to result from both low uniformity of yarn elongation to break and inclination of yarns to the strand and rope axes, these effects being equal in magnitude for most of the structures studied. The coefficients of variation of yarn rupture elongation of about 10% for the yarns examined in this work appear, on the basis of the inherent variability of 20%–30% for their constituent fibers, to be the result of nonuniformities created by processing. Such levels of nonuniformity do not lend themselves, at present, to significant reduction by alterations of manufacturing techniques. Thus, it appears that improvements in yarn-to-strand or -plied yarn translational efficiencies can be practically accomplished only by strand and rope twist reductions or by the use of more extensible fibers and yarns.

Results of the simplified geometric analyses are checked by comparison with the results of a more precise geometrical analysis of plied structures as developed by Chow [4]. Differences between the results of the two approaches are shown to be negligible for practical ranges of twisted structures, justifying the assumptions leading to the simplified analyses.

The results, which are presented graphically over a range of the variables in excess of those presently used in cordage structures, are immediately applicable to the engineering calculations of strength of cordage structures, tire cord, and sewing threads. The limits of applicability are defined by the validity of the assumed simplified geometry.

PREVIOUS work [1] has shown how the translation of strength from fiber to singles yarn of cordage type can be predicted with considerable accuracy from a combination of the effects of inherent fiber properties and yarn geometry. This work is extended herein to higher-order cordage structures such as strands, plied yarns, and ropes on the basis of a similar analysis. To effect such an analysis, a method has been developed for treating the statistically difficult range where the sampling is too small to utilize large-sample approximations and yet large enough so that small-sample methods are

* The preceding parts in this series appeared in the following issues of Textile Research Journal: I, Feb. 1948; II, Dec. 1948; III, Jan. 1950; IV and V, Aug. 1950; VI, Oct. 1950; VII, May 1951; VIII, Mar. 1952; IX, Oct. 1952; X, Nov. 1952.

† The authors acknowledge the support of the United States Navy, Office of Naval Research, and the Bureau of Ships, in sponsoring the research, part of which is covered in this paper.

too cumbersome. Such intermediate sample sizes are represented by the case of plied yarns, strands, and ropes. The results are presented graphically in a manner which is immediately applicable with engineering accuracy to many cordage structures.

In a previous publication [1] an analysis was made of the factors which affect the translation of fiber strength into singles yarns on the basis of inherent fiber properties and yarn geometry. The basic load equation derived in that work is

$$P_y = 2\int_o^{R_y} \pi b\left(\frac{a}{b} + e_y \cos^2\theta_y\right)\cos^2\theta_y N_{fu} r\, dr, \quad (1)$$

where P_y is the load supported by the yarn, a and b are constants found from the fiber stress-strain relationship, e_y is the yarn elongation corresponding to any yarn load P_y, θ_y is the helix angle at any point in the yarn cross section, N_{fu} is the fraction of fibers unbroken at an elongation $e_y \cos^2\theta_y$ [2], and r is the radial distance from the yarn center. Important assumptions in the analysis leading to equation (1) were: (*a*) the number of fibers in any element of yarn cross-sectional area $2\pi r\, dr$ is sufficiently large so that N_{fu} might be defined uniquely and continuously as a function of both the strain in the fiber and the standard deviation of fiber rupture elongations, under the assumption of a normal distribution of fiber rupture elongations; and (*b*) the fiber diameter is sufficiently smaller than the yarn diameter so that θ_y might be defined continuously as a function of r. Clearly, neither of these assumptions is valid for a plied yarn consisting of two or three or even seven singles yarns, where the singles yarn assumes the role of the fiber and the plied yarn that of the singles in the above expression; nor is it obvious just how many units or what diameter ratios are necessary to make these assumptions valid. Thus, the above integral must be replaced by a summation for the case of plied structures. In addition, since the plying operation may introduce excess fiber lengths into the constituent singles yarns, the term $e_y \cos^2\theta_y$ in equation (1) above is not necessarily the true strain on the fiber and must be modified to include crimp.

The present analysis is divided into four parts: (*I*) the geometric effects of ply and yarn twist in various configurations on strength translation; (*II*) the effects of yarn variability on strength translation; (*III*) the combined effects of geometry and variability on strength translation and comparison with experiment; (*IV*) examination of assumptions.

I. Effects of Ply Twist

A. Determination of Ply Helix Angle

The axial load transmitted by a yarn inclined at an angle θ_p to the plied yarn axis is given by the expression

$$P = P_y \cos\theta_p, \quad (2)$$

where P is the load parallel to the plied yarn axis and P_y is the load in the inclined yarn. Thus, each yarn in a plied yarn or strand contributes a supporting load equal to its own load multiplied by the cosine of its angle of inclination with the plied yarn axis. This angle of inclination of the yarn is taken to be that obtained from the expression [3]

$$\tan\theta_p = 2\pi N_p R_p, \quad (3)$$

where N_p is the turns per unit length of the plied yarn and R_p, the plied yarn helix radius, is the distance from the center of the plied yarn to the center of mass of the given singles yarn. It will be shown later, when the various assumptions are examined, that this definition leads to results that are in good agreement with the length-twist relationships that exist in the yarns of plied and stranded structures.

Three specific examples will illustrate the method of determining the angles of inclination, θ_p. By definition, R_y = yarn radius; R_p = helix radius of plied yarn, the distance from the center of the plied yarn to the center of mass of the singles yarn in question; θ_p = plied yarn helix angle, the angle between the axis of the singles yarn in question and the plied yarn axis.

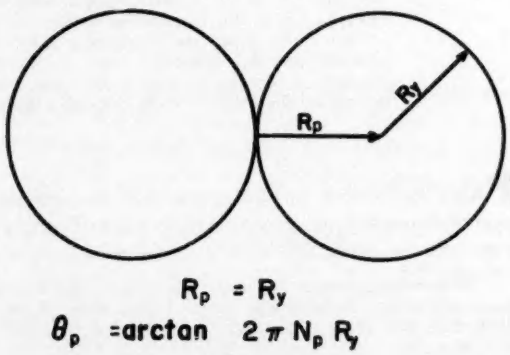

FIG. 1. *Two-ply yarn.*

Example 1.—A 2-ply yarn, yarns of circular section (see Figure 1).

$$R_p = R_y,$$
$$\tan \theta_p = 2\pi N_p R_y.$$

Example 2.—A 3-ply yarn, yarns of circular section (see Figure 2).

$$R_p = \tfrac{2}{3}\sqrt{(2R_y)^2 - (R_y)^2} = 1.155R_y,$$
$$\tan \theta_p = 2.310\pi N_p R_y.$$

Example 3.—A 15-yarn strand consisting of a single core yarn surrounded by 14 wedges (see Figure 3). Since all 15 units are of about the same area, each has an area $\pi R^2/15$. For the circular core the area is πr_c^2 so that

$$r_c^2 = \frac{R^2}{15},$$

and, thus,

$$r_c = 0.258R.$$

The core yarn obviously is inclined zero degrees to the strand axis. Now consider one of the yarns in the external ring. Its shape and dimensions are as shown in Figure 3b. For 14 units in the outer ring, the angle $\alpha = 12.85°$. By taking moments about the center of the strand, it can be shown that R_p, the distance between the center of the strand and the center of mass of each of the external yarns, is

$$R_p = 0.694R,$$

and, thus,

$$\tan \theta_p = 2\pi N_p(0.694)R$$
$$= 1.388\pi N_p R.$$

Similar analyses can be made for any structure after the geometric configuration has been defined or approximated. Thus, from the geometric configuration and the turns per unit length of the ply, an angle can be found whose cosine is the load transmission factor from singles yarn to plied yarn.

While this very simple relationship exists between plied yarn twist, helix radius, and load transmission, there may, depending on processing, be two other important effects of ply twist. These are a change in singles yarn helix angle, and an introduction of excess lengths into the yarns. These factors will now be investigated on the basis of two assumptions:

(*1*) The helix angle at any point in the yarn as it lies in the ply can be determined from

$$\tan \theta_{yp} = 2\pi N_{yp} r_y,$$

where N_{yp} is the number of turns per unit length of the yarn as it lies in the ply. That is, the angles between fiber and yarn axes are not affected by the fact that the yarn axis is itself helical. As is shown later, this assumption introduces negligible errors into the results of the mechanical analysis.

(*2*) Excess fiber lengths are created by a reduction in yarn helix angle, and can be expressed as the difference between the fiber path length required for the initial singles helix angle and the length required for the final singles helix angle.

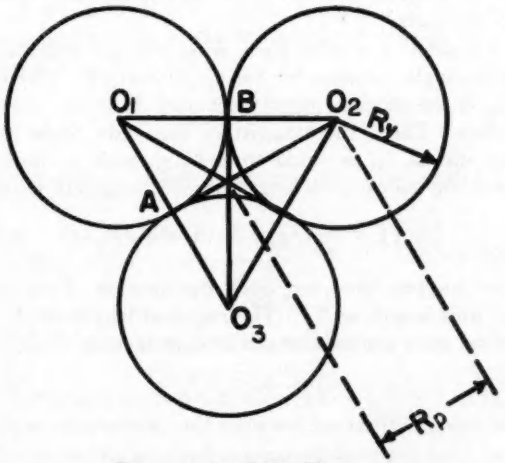

FIG. 2. *Three-ply yarn.*

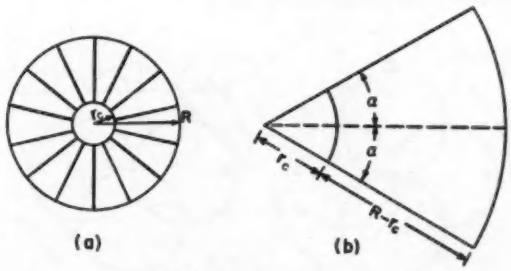

FIG. 3. *Fifteen-yarn strand.*

B. Changes due to Plying in Helix Angle of Singles Yarns

The helix angle at any point in a singles yarn has been defined [2] as $\tan \theta_y = 2\pi N_y r_y$, where N_y is the turns per unit length of the singles yarn and r_y is the radius to that point. When a yarn is plied, it is possible for the helix angles to be either increased, decreased, or unchanged, depending entirely upon the method of plying. In the case of pure twisting—that is, when the group of singles yarns can be considered to be clamped at both ends (see Figure 4a), twist can be considered to be inserted into the yarn on a turn-for-turn basis with ply twist. Whether this added twist is positive or negative depends upon whether the yarn and ply twists are in the same or the opposite sense (S on S, Z on Z, or S on Z, Z on S). The usual case is for twists in the opposite sense, so only this case will be considered. The total final equivalent twist in a singles in a strand will then be $N_{yo} - N_p$, where N_{yo} is the total turns originally in a given length of singles yarn and N_p is the total turns in the corresponding length of ply. But since the length of a helical path is (length of axis)/$\cos \theta$, where θ is the path helix angle, the singles yarn length is (ply length)/$\cos \theta_p$. Thus, if N_p is the number of plied yarn turns per unit length of plied yarn axis, $\frac{N_p}{1/\cos \theta_p} = N_p \cos \theta_p$ turns per unit length of singles axis are subtracted from the yarn by plying, and, thus,

$$\tan \theta_{yp} = 2\pi(N_{yo} - N_p \cos \theta_p) r_y, \qquad (4)$$

where N_{yo} is the original turns per unit length of the singles yarn. If, during the plying operation, a twist of N_{y1} turns per unit length of singles axis is added to the singles yarn, then

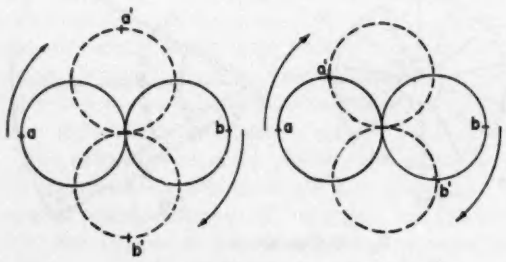

FIG. 4. left—*Pure twisting.* right—*Complete twist compensation.*

$$\tan \theta_y = 2\pi(N_{yo} - N_p \cos \theta_p + N_{y1}),$$

and the condition for perfect twist compensation, as shown in Figure (4b), should be

$$N_{y1} = N_p \cos \theta_p. \qquad (5)$$

This relationship does not seem to hold precisely in practice, although it is a good general guide. Discrepancies are discussed in more detail later, as are the results of Chow's [4] more precise mathematical analysis of the geometry of plied yarns as it affects equation (4) above.

C. Excess Lengths

If a singles yarn is partially untwisted by plying, the helix angle of any fiber in the yarn cross section will decrease in a manner described by equation (4) and, consequently, so will the required helical path length of each fiber. But unless there is opportunity for the excess lengths to be absorbed by yarn growth, the final total length of any fiber in a given length of yarn untwisted by plying will be the same as it was before untwisting. The % difference between the original length of fiber and the length required for the new helical path, based on original length, will be called the "excess length" or "crimp." Clearly, the excess length will vary from zero at the center of the yarn, where untwisting has no angular effect, to a maximum at the outside of the yarn. The magnitude of these excess lengths in yarns of *circular section* will now be analyzed.

Consider a singles yarn with original external helix angle defined by $\tan \theta_{yo} = 2\pi N_{yo} R_y$, where N_{yo} is the original yarn twist and R_y is the yarn radius. Then, the tangent of the helix angle at any radius, r_y, is equal to $2\pi N_{yo} r_y$, with a corresponding helical path length per unit length of yarn

$$\frac{1}{(\cos \theta_o)_r} = \sqrt{1 + (\tan^2 \theta_o)_r} = \sqrt{1 + 4\pi^2 N_{yo}^2 r_y^2}. \qquad (6)$$

Now untwist the yarn until the number of turns per unit length is N_y. The required length of the helical path per unit length of yarn is now

$$\sqrt{1 + 4\pi^2 N_y^2 r_y^2}, \qquad (7)$$

and the % difference between the two lengths is

$$\frac{\sqrt{1 + 4\pi^2 N_{yo}^2 r_y^2} - \sqrt{1 + 4\pi^2 N_y^2 r_y^2}}{\sqrt{1 + 4\pi^2 N_{yo}^2 r_y^2}} \times 100. \qquad (8)$$

Equation (8) defines the excess length, or the amount the fiber path must be extended before the

fiber bears any appreciable tensile load, and thus must be included as a part of the fiber extension term in any expression for yarn load.

In deriving the expression given by equation (1) for yarn load, e_f, the strain in a fiber, was taken as $e_y \cos^2 \theta_y$, where e_y is the yarn strain and θ_y is the helix angle for a given fiber. While $e_y \cos^2 \theta_y$ still expresses the total strain in the direction of the path, it does not define the part of the fiber strain which is load-bearing if any crimp is present. An expression for load-bearing fiber strain is derived as follows:

Let: l_y = the singles yarn length; l_f = total fiber length in a length l_y of yarn = $l_y/\cos \theta_{yo}$; θ_{yo} = yarn helix angle before untwisting; θ_y = yarn helix angle after untwisting; Δl_y = yarn extension; Δl_f = total fiber path extension due to Δl_y; $(\Delta l_f)_p$ = fiber path extension which is load-bearing; e_y = yarn strain = $\Delta l_y/l_y$; $(e_f)_p$ = load-bearing fiber strain.

From previous work [2],

$$\Delta l_f = \Delta l_y \cos \theta_y, \tag{9}$$

and it is clear that

$$(\Delta l_f)_p = \Delta l_f - l_y\left(\frac{1}{\cos \theta_{yo}} - \frac{1}{\cos \theta_y}\right), \tag{10}$$

where the subtractive expression on the right side of equation (10) represents the total crimp, or excess length created by the untwisting. Equation (10) assumes that the load required to straighten a crimped fiber is negligible compared to the load required to extend the same fiber in tension by an equal amount. Since

$$(e_f)_p = \frac{(\Delta l_f)_p}{l_f}, \tag{11}$$

then, by combining equations (9), (10), and (11),

$$(e_f)_p = \frac{\Delta l_y \cos \theta_y - l_y\left(\dfrac{1}{\cos \theta_{yo}} - \dfrac{1}{\cos \theta_y}\right)}{\dfrac{l_y}{\cos \theta_{yo}}}, \tag{12}$$

which, after simplification, becomes

$$(e_f)_p = e_y \cos \theta_y \cos \theta_{yo} - \left(1 - \frac{\cos \theta_{yo}}{\cos \theta_y}\right). \tag{13}$$

Since in the original expression for yarn load as a function of yarn strain, as given by equation (1), the term $e_y \cos^2 \theta_y$ represents the load-bearing strain in a fiber, $(e_f)_p$, the right side of equation (13) can be substituted in equation (1), resulting in

$$P_y = 2\pi \int_o^{R_y} b \left(\frac{a}{b} + e_y \cos \theta_{yo} \cos \theta_y - 1 + \frac{\cos \theta_{yo}}{\cos \theta_y}\right) \cos^2 \theta_y N_{fu} r \, dr, \tag{14}$$

or, in terms of r,

$$P_y = 2\pi \int_o^{R_y} b \left[\frac{a}{b} + e_y \left(\frac{1}{\sqrt{1 + 4\pi^2 N_{yo}^2 r^2}}\right) \times \left(\frac{1}{\sqrt{1 + 4\pi^2 N_y^2 r^2}}\right) - 1 + \frac{\sqrt{1 + 4\pi^2 N_y^2 r^2}}{\sqrt{1 + 4\pi^2 N_{yo}^2 r^2}}\right] \times \frac{1}{(1 + 4\pi^2 N_y^2 r^2)} N_{fu} r \, dr.$$

Reference to previous work [1], which gave general solutions for the maximum value of P_y in terms of the several parameters when $N_y = N_{yo}$, will indicate the complexity of the problem when N_{yo} and N_y are not equal. Even assuming that an analytic solution could be found, an extremely large number of curves would be required to give any sort of generality to the work. Accordingly, no general solution was found. Instead, a piecewise summation was used to obtain approximate solutions for several specific cordage structures.

The procedure is as follows: Divide the yarn cross section into five parts by inscribing four circles with radii $R_y/5$, $2R_y/5$, $3R_y/5$, and $4R_y/5$, and assume that each one of the rings so formed can be characterized by its properties at its mid-point (see Figure 5).

Let: p_i = load per unit weight supported at mid-point of the ith ring; r_i = radius to mid-point of

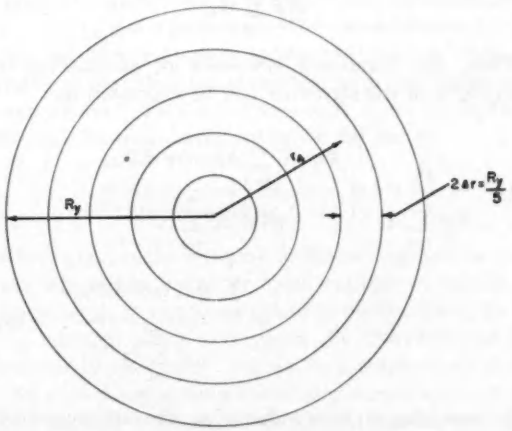

FIG. 5. *Division of yarn cross section for approximate solution.*

the ith ring; Δr = half-width of any ring; θ_i = helix angle at mid-point of the ith ring corresponding to the yarn twist, N_y; A_i = area of ith ring; $\bar{p}$ = average strength per unit weight of fiber; P_y = total yarn load.

Since the weight is proportional to the area, the load in the ith ring will be

$$P_i = Kp_iA_i,$$

where K is a constant. Then the total load supported by all the rings will be

$$P_y = \sum_{i=1}^{5} Kp_iA_i \cos^2 \theta_i N_{fu}. \tag{15}$$

This is entirely analogous to the expression

$$P_y = 2\int_o^{R_y} \pi f \cos^2 \theta_y N_{fu} r \, dr.$$

But

$$A_i = \pi[(r_i + \Delta r)^2 - (r_i - \Delta r)^2] = 4\pi r_i \Delta r,$$

and inspection of Figure (5) shows that $\Delta r = r_1$, so that

$$A_i = 4\pi r_1 r_i,$$

and thus

$$P_y = 4\pi r_1 K \sum_{i=1}^{5} p_i r_i \cos^2 \theta_i N_{fu}. \tag{16}$$

If the structure were 100% efficient, the load would be $\bar{p}$, the mean fiber strength per unit weight, multiplied by the total area, or

$$K\bar{p} \sum_{i=1}^{5} A_i. \tag{17}$$

Thus, the fractional efficiency of translation of strength of the structure can be expressed as

$$\eta = \frac{P_y}{K\bar{p}\sum_{i=1}^{5} A_i} = \frac{4\pi r_1 K \sum_{i=1}^{5} p_i r_i \cos^2 \theta_i N_{fu}}{\bar{p} 4\pi r_1 K \sum_{i=1}^{5} r_i}$$

$$= \frac{\sum_{i=1}^{5} p_i r_i \cos^2 \theta_i N_{fu}}{\bar{p}\sum_{i=1}^{5} r_i}. \tag{18}$$

By assuming a given value of e_y, the corresponding value of η can be found as follows: (a) calculation of $(e_f)_p$ for each ring from equation (13), utilizing the known geometry of the yarn to specify θ_{yo} and θ_y for each ring; (b) the determination of appropriate values of P_i corresponding to $(e_f)_p$ for each ring, from the fiber stress-strain curve; (c) the calculation of N_{fu} for each ring from $(e_f)_p$, the mean fiber rupture strain, e_m, and the coefficient of variation of fiber rupture elongation, V; (d) the summation of equation (18) for all rings. By successively repeating this procedure for different values of e_y, a maximum η can be found.

The values of p_i must in general be found directly from the average fiber stress-strain curve, since with excess lengths the range of fiber strains for any given yarn strain is so great as to make the linear approximation used and described previously [1] too inaccurate.

The stress-strain curve used here differs slightly in type from that employed in previous work in which a plot of average grams per denier *versus* strain was used. The modification in the present work is to express the stress ordinate as average grams per average denier. Both types of curves for a given sample of Manila abaca fiber are plotted in Figure 6. The fact that the curve formed by using the average grams per denier does not show the mean value of breaking stress occurring at the mean value of rupture elongation is a matter which required a modification factor in the theoretical calculation of yarn efficiency as described previously [1].

The reason for using the curve of average grams per average denier rather than the average of the grams per denier will become clear after observing the formation of each of these quantities, followed by comparison with the load expression in which they are used.

In forming a curve of average grams per denier *versus* strain, each fiber is weighed separately and the grams per denier of the fibers at given strains are averaged at enough different strains to delineate a curve. In plotting average grams per average denier, all fibers in the sample are weighed as a group, and the average load at various strains is divided by the average weight, in denier per fiber, of the whole original fiber sample. Expressed in analytic form, the procedure for finding the average grams per denier gives

$$f(e) = \frac{\sum_{n(1-N_{fu})+1}^{n} \left(\frac{p_i}{w_i}\right)}{n(N_{fu})}, \tag{19}$$

while the average grams per average denier is determined from

$$g(e) = \frac{\sum_{n(1-N_{fu})+1}^{n} \frac{p_i}{n(N_{fu})}}{W/n} = \frac{\sum_{n(1-N_{fu})+1}^{n} p_i}{W(N_{fu})}, \quad (20)$$

where n equals the total number of fibers tested, of total weight W. A simplification of equation (19) can be made by realizing that when the values of p_i/w_i are fairly symmetrically distributed, the average value $f(e)$ is very nearly $\sum p_i / \sum w_i$. Therefore,

$$f(e) = \frac{\sum_{n(1-N_{fu})+1}^{n} \left(\frac{p_i}{w_i}\right)}{n(N_{fu})} \doteq \frac{\sum_{n(1-N_{fu})+1}^{n} (p_i)}{\sum_{n(1-N_{fu})+1}^{n} (w_i)}. \quad (21)$$

What is desired is the total load supported by a bundle of fibers, $\sum p_i$, at any given elongation, in terms of the stress-strain curve parameters. From equation (21),

$$\sum p_i = f(e) \sum_{n(1-N_{fu})+1}^{n} (w_i),$$

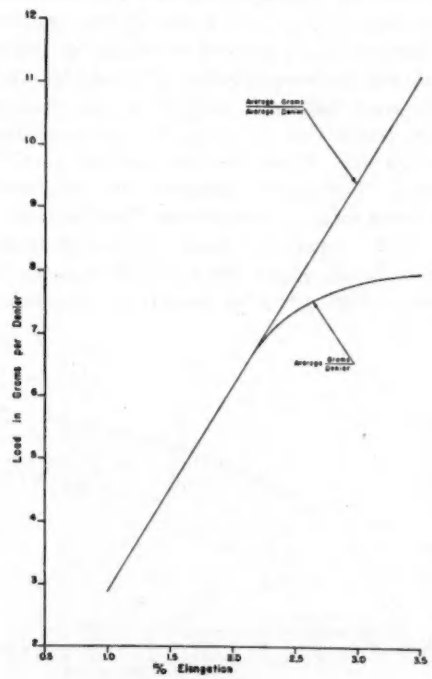

FIG. 6. *Average stress-strain curves for Manila abaca fiber.*

and from equation (20),

$$\sum p_i = g(e)W[N_{fu}(e)].$$

Thus, in order to find $\sum p_i$ from the $f(e)$ curve, it is necessary to know $\sum_{n(1-N_{fu})+1}^{n} (w_i)$ or the total weight of the unbroken fibers at any given strain, while use of the $g(e)$ curve requires only a knowledge of the total original weight of the bundle.

In the case where average fiber modulus is independent of tenacity, there would, of course, be no difference between equations (20) and (21), but in the general case such a dependence can be shown.

From Figure 6 it can be seen that the higher tenacity fibers have the lower modulus, or, in other words, that

$$\sum_{n(1-N_{fu})+1}^{n} (w_i) < N_{fu}W.$$

While results of previous calculations were compensated with a correction factor for the "drooping" characteristic of curves defined by equation (21), the more recent method is the more logical procedure in the sense that it properly expresses the load-carrying capacity of the aggregate structure. It offers the additional advantage that the average curve so defined has the same appearance as a single typical fiber stress-strain curve, while the former method introduces a distortion such that the average curve does not resemble any single given test curve. However, since experimental efficiencies are based on the mean breaking tenacity of the elements, it may, in some cases, be necessary to modify the theoretical efficiencies obtained by the use of the average grams per average denier curve so that they are consistent with the foregoing convention. This is conveniently done by multiplying theoretical efficiencies by the factor

$$\frac{g(e_m)}{\text{mean rupture tenacity}},$$

where $g(e_m)$ is the ordinate to the average grams per average denier curve at mean rupture elongation. In general, it has been found experimentally that for cordage fibers and yarns the above factor is extremely close to 1. Again, it is emphasized that this expression is not an arbitrary correction factor, but instead is necessary in order that theoretical and experimental efficiencies may be expressed on the same basis—namely, mean rupture tenacity.

Thus far a circular yarn cross section has been assumed. For singles yarns, or yarns removed from strands, this seems to be a good approximation, but examination of strand sections shows that a yarn lying in the strand has a cross section which may deviate considerably from a circular shape. An exact theoretical analysis of excess lengths for these distorted cases would be extremely complex geometrically and not particularly valuable practically because of the variety of shapes assumed by the yarns under different stranding conditions. Fortunately, the results are not so critically dependent on the exact shape of the yarn that certain rough approximations do not give satisfactory results. This aspect, together with deviations in results produced by differences in cross-sectional shape, is covered in a subsequent section dealing with comparisons between theory and experimental results.

II. Variability

It was pointed out in the "Introduction" that variability of elongation to break among singles yarns in a plied yarn cannot in general be treated in the same manner as variability among fibers in a yarn. A method is presented here, the results of which make it possible to predict the effects of variability on the strength of small groups of fibers or yarns. The results also define the minimum size of the sample for which the efficiency is essentially the same as that given by the large-sample approximation developed and utilized in earlier work [1]. The analysis applies equally to fibers, yarns, strands, or any elements which act as units in a large structure. For purposes of this analysis, a bundle of units is termed "parallel" if the geometry is such that all units are subjected to equal strains as a result of straining the group. Thus, 2- or 3-ply yarns of uniform geometry represent parallel bundles. The ply helix angle in this case necessitates the use of a geometric factor for efficiency calculations, which factor is independent of the statistical analysis which follows.

Suppose there exists a certain population of units, and the results of many tensile tests of such units are plotted as a distribution of elongations to break. Then, if from the same population tensile tests of bundles of two units are made, consider the distribution of elongations to break of the first break in each group. Since the lowest elongation unit is the controlling factor, a high elongation unit paired with a low one would give no weight to the high one in the distribution. Similarly, it is clear that as the number of units in the bundle becomes larger, the average elongation at which the first unit breaks becomes lower. A method for obtaining the theoretical distributions of first-unit breaks for various bundle sizes has been derived on the basis of a normal population of units, and is presented in Appendix *II*. These distributions are plotted in Figure 7. For present purposes, the only concern is the mean value of each of these distributions, and, accordingly, a curve of mean elongation at which first-unit break occurs *versus* bundle size has been plotted in Figure 8, with elongation generalized in

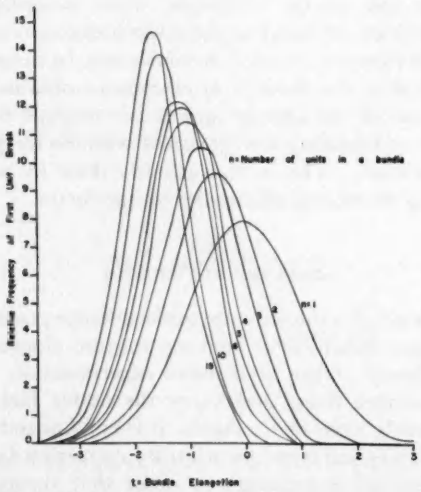

FIG. 7. *Distribution of first-unit rupture in a bundle* vs. *bundle elongation.*

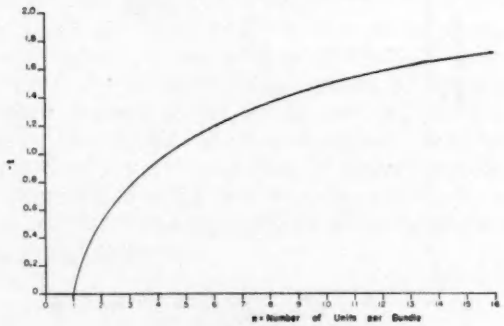

FIG. 8. *Mean value of* t vs. *bundle size for first-unit break.*

terms of t, the number of population standard deviations from the unit population mean.

A question now arises as to the utility of these mean elongation curves with respect to the strength of a bundle or plied structure. It is obvious that if a bundle of two units is loaded, the total load will seldom exceed that reached when the first one breaks, so that it can be said with certainty that the mean load for the first break in each bundle will also be very nearly the mean maximum bundle load. For example, if bundles of two units were tested, the mean breaking tenacity for the bundles would for a linear average stress-strain curve be that corresponding to an elongation of $e_m - 0.5\sigma$ (see Figure 8) on the average stress-strain curve for the population, where e_m is the mean breaking elongation for the population and σ is the population standard deviation of elongation to break. For the general case of nonlinear stress-strain curves, it would be necessary to find the mean of the distribution curves of Figure 7, with the abscissa scale, t, converted to stress in order to obtain the mean bundle tenacity. The results of efficiency at first-unit rupture are plotted as the solid lines of Figure 10. Here n is the number of units in the bundle and $m = b\sigma$, where σ is the standard deviation of the unit elongation to break and b is the slope of the assumed linear average stress-strain curve of the units in the region near rupture.

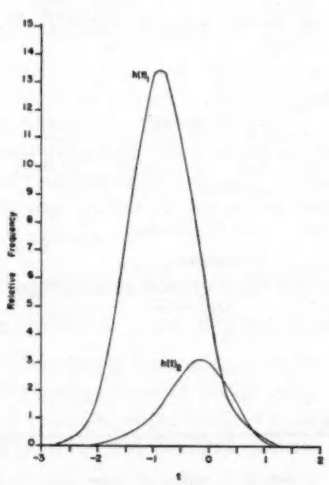

FIG. 9. *Relative frequency of maximum bundle load* vs. t. *In this case,* n = *4 and* m = *20.*

In attempting to extend this reasoning to larger size bundles, another problem is encountered—namely, that maximum load does not necessarily occur when the first unit breaks. In fact, for large numbers of units a very sizable portion may be broken before maximum bundle load is attained. This case has been discussed previously [1], and the results of this previous work together with the results for first-unit break bracket the middle sized groups. Thus, the problem is reduced to the specific solution of some examples of middle sized groups in order to extend the analysis of the effects of variability over the entire range from single units to infinitely large bundles. The important practical results of these calculations will be both the ability to predict the effects of number of units and also to define the minimum size which constitutes an "infinite" size for tensile strength purposes.

An elongation is chosen for the first unit to break, and the probability of having the maximum bundle strength occur at this point is calculated. A number of other elongations for first-unit rupture are chosen, and similar probabilities calculated. The results are plotted as a distribution of probability of occurrence of maximum load *versus* elongation at first-unit break.

Then similar sets of calculations are made for the cases where maximum bundle strength is attained when the second unit ruptures, third unit ruptures, etc. The method is outlined in detail in Appendix *I*, and the results for $n = 4$—*i.e.*, a bundle of 4 units—and $m = 20$ are plotted in Figure 9. The parameter m is a convenient one to describe bundles [5]. It is numerically equal to $b\sigma$ or $be_mV/100$, where b is the slope of the linear approximation to the average unit stress-strain curve near rupture, σ is the standard deviation of elongation to rupture, e_m is the mean rupture elongation, and V is the coefficient of variation of elongation to rupture of the units.

The relative areas under the curves of Figure 9 represent the relative frequencies of maximum bundle loads occurring at the first- and second-unit breaks. For this case, any break beyond the second has a very small probability of producing a maximum bundle load, and need not be considered. The average breaking elongation can be calculated by taking the weighted mean of all of the distribution curves—that is, the sum of each of the individual means multiplied by the area under the curve, divided by the sum of the areas. To find

the average breaking load, the mean breaking load for each configuration must be modified by the number of units intact. Strictly speaking, the total area should be numerically equal to unity, but since in calculating averages the same normalization constant appears in both numerator and denominator, formal normalization is unnecessary here.

The same procedure was followed for other values of n and m. Combining this information with both the translational curves for first-unit breaks and also the magnitude of bundle efficiencies for very large groups of units, a useful graphical representation can be made as follows: It is known that the efficiency decreases with increasing size of group, and thus must asymptotically approach the value found for very large sized groups. It is also known that for any size group the loss in efficiency can be no greater than that corresponding to the first-unit break, since the elongation at maximum load can be no smaller than that at which the first unit breaks. Thus, a curve for bundles showing translational efficiency plotted *versus* n, the number of elements in the bundle, must lie on or above the curve giving the efficiencies for which it is assumed that maximum strength is reached when the first unit breaks. Thus, the general shape and position of the translational efficiency curves are known, and, by calculation of only a few judiciously selected points, as above, a general set of curves showing translational efficiency of the bundle *versus* n, the number of units in the bundle, can be plotted. This has been done in Figure 10, where the curves are represented by the dashed lines. The solid lines of Figure 10 represent the results for first-unit break.

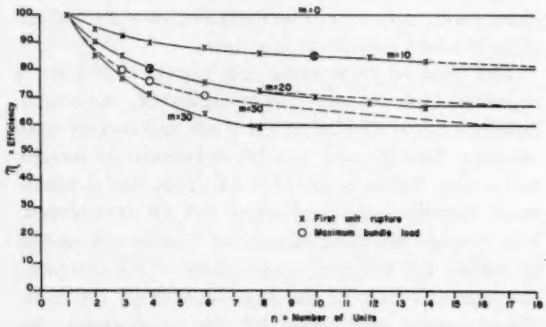

FIG. 10. *Efficiency* vs. *bundle size.*

There are three important points to note in these curves: (*1*) as n becomes smaller, the efficiency can be more nearly characterized directly by the curve of efficiency at first-unit break; (*2*) as n reaches about 15, the asymptotic value can be used with very little error, or, in other words, an infinite sample can be assumed; (3) with other factors remaining constant, the efficiency of translation is an inverse function of the number of units in the bundle for small numbers of units. These observations must be interpreted with caution because they apply only to translation of strength, although they are based on elongation. That is, it is proper to say that strengthwise a bundle of, say, 15 units from a given population will, on the average, translate to about the same extent as a bundle of 100, but it is not true that the distribution of breaking elongations will be the same, although the mean elongations may be close for the two cases. This can best be understood by following the steps of the derivation given in Appendix *I*.

The analysis of a plied yarn containing a core differs from that of a similar number of units in parallel, since in the former case any significant ply helix angle results in a different strain on the core yarn than on the exterior yarns. The statistical analysis must take this difference in strains into account. This has been done for 7-ply yarns, with the procedure outlined in Appendix *III*, and the results of the analysis are given by the efficiency curves of Figure 11. An interesting feature of these curves is the relative insensitivity of the

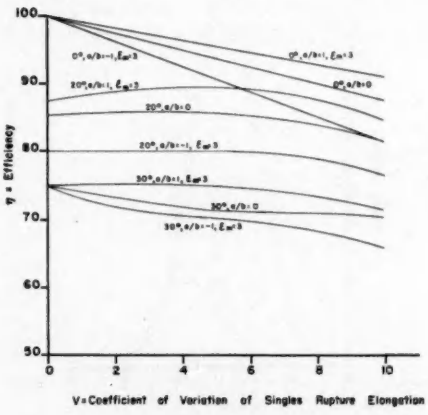

FIG. 11. *Theoretical translational efficiency of singles into 7-ply yarn* vs. *singles rupture elongation variability.*

results to unit variability for any significant ply helix angle. This is true only for the range of unit variabilities covered by the calculations. The cause of this apparent insensitivity resides in the somewhat improved degree of elongation balance between the core yarns and the exterior yarns with a small increase in unit variability. Such an effect would be difficult to demonstrate experimentally, since the magnitude of the effect is small. In the case of a large number of exterior yarns with a single-unit core, as discussed later, little error is introduced by assuming all units to be in parallel.

It is of interest to note that the curves of strength translation at first-unit break can also be interpreted as giving the average strength of the weakest link in chains composed of n links. Here the word "link" means simply some arbitrary length of fiber, yarn, or plied yarn. In parallel-type structures, all elements are at a known elongation, so that elongation has been chosen as a basic parameter. In series structures, all elements are at the same load, so that load must replace elongation in the statistical calculations. The solid curves of Figure 10, with m replaced by the coefficient of variation of breaking load, will give directly the efficiency of units in series, where the abscissa is the number of units in series. For example, it should be possible to determine the effect of gage length on tensile strength simply by knowing the mean strength and standard deviation of strength at some short length and assigning to this length a value of n equal to unity. The strength at any longer gage length could then be calculated from the efficiency curves given in Figure 10 if the only effects of gage length were statistical in nature. However, differences between specimens in the short gage length tests might be due to factors which would not have acted on a single long specimen, and would thus obscure the results—*e.g.*, local rate of loading, jaw penetration effects, etc.

III. Comparison of Theory with Experiment

A. Excess Lengths in Yarns Removed from Strand

It has been shown theoretically that the length of a fiber in a circular yarn should vary according to the inverse cosine of the angle it makes with the yarn axis, or, in terms of helical parameters,

$$l_f = l_y\sqrt{1 + 4\pi^2N_y^2r^2},$$

where l_f is the length of fiber corresponding to a length l_y of yarn, N_y is the number of turns per unit length of the yarn, and r is the fiber distance from the yarn center.

Tests have been performed in which a 20-in. length of yarn is placed under a constant tension, is completely untwisted, and all nonthroughgoing fibers are removed. Then one by one the taut fibers are cut, and the increased length of the yarn is measured several times during the cutting procedure. The % total fibers cut is plotted *versus* the % increase in length. The theoretical form of such a curve can be derived as follows:

Consider a circular yarn of radius R_y. Then the % fibers included to a radius r is

$$(\pi r^2/\pi R_y^2) \times 100 = 100r^2/R_y^2,$$

assuming a constant yarn density from the center outward. The length of a fiber at a radius r is

$$l_y\sqrt{1 + 4\pi^2N_y^2r^2},$$

and the % increase in length is

$$\frac{l_y\sqrt{1 + 4\pi^2N_y^2r^2} - l_y}{l_y} \times 100 = (\sqrt{1 + 4\pi^2N_y^2r^2} - 1)100. \quad (22)$$

For small values of $4\pi^2N_y^2r^2$, the quantity $\sqrt{1 + 4\pi^2N_y^2r^2}$ can be closely approximated by $1 + 2\pi^2N_y^2r^2$, so that the expression for % increase in length becomes

$$100(1 + 2\pi^2N_y^2r^2 - 1) = 200\pi^2N_y^2r^2.$$

The plot then becomes a straight line with slope

$$\frac{100r^2/R_y^2}{200\pi^2N_y^2r^2} = \frac{1}{2\pi^2N_y^2R_y^2}.$$

This can be expressed in terms of the yarn surface helix angle, θ_y, as 2 $\text{ctn}^2\,\theta_y$.

If a yarn is partially untwisted by, say, plying after having been spun to an initial twist which gives a helix angle θ_{yo}, it is clear that the distribution of absolute fiber lengths should still be the same as before untwisting. However, the plot of the theoretical length distribution for a yarn with the new lower angle θ_y will have a steeper slope. The difference in slopes for the original and untwisted yarns is a measure of the excess fiber lengths existing in the untwisted yarn. The distribution of these excess lengths with respect to radius was derived in section I*C*.

Figure 12 shows a plot of four theoretical distributions of fiber length together with the experimental results for a "soft"-twist yarn series. A detailed description of the nature of these samples will be given later. However, for convenience in following Figure 12, the symbol *YS* refers to a yarn (*Y*) *before* plying whose twist was "soft" (*S*). All three-letter symbols refer to yarns from strands, the first letter, *Y*, signifying that the test was performed on yarns, the second letter, *S*, that the original yarn twist was soft, while the strand twist was in turn either soft (third letter *S*), medium (third letter *M*), or hard (third letter *H*). Thus, as the designation of yarns from strands proceeds from *YSS* to *YSH*, the ***required*** fiber length should decrease, and thus the excess length should increase. In each case, experimental lengths of fibers in yarn removed from strands, as well as theoretical lengths, were determined using the singles twist as it lies in the strand. While experimental results of fiber length are not dependent upon the manner in which the singles yarns were untwisted from the strands, the twists to be used in calculating the theoretical lengths are so dependent.

The results of Figure 12 can be seen to agree with theory quite well so far as the trend is concerned. The four experimental curves are all nearly identical, irrespective of final twist, as would be expected for yarns of the same original twist. The theoretical distributions indicate the distribution which would be required in order that all the helical paths be exactly satisfied with no excess lengths, and thus that the excess lengths increase with increasing twist removal, achieved by increasing the strand twist. The discrepancy between theoretical and experimental curves for the original *YS* yarn is probably due to errors in both experiment and assumption: (*1*) *Experimental*—It is possible that not enough tension was exerted on the yarn when a large percentage of the fibers were still intact, so that the increase in length measured was too low. For example, at the 60% ordinate of Figure 12, the length increase is about 0.4% too low; on a 20-in. gage length this means 0.08 in., a small amount for a rough measuring and tensioning system. (*2*) *Theoretical*—The assumption that all fibers lie in perfect helices is clearly not true, since much darting has been observed. While this darting is of little consequence over the short lengths involved in yarn rupture, it will have a tendency to equalize fiber lengths over the longer lengths used in the investigation of fiber length distributions, and thus yield a steeper slope than that calculated. The long tails observed in the upper regions of the experimental curves are undoubtedly due to the tendency of a very few fibers in every yarn to be somewhat stray—that is, not really tightly bound within the yarn.

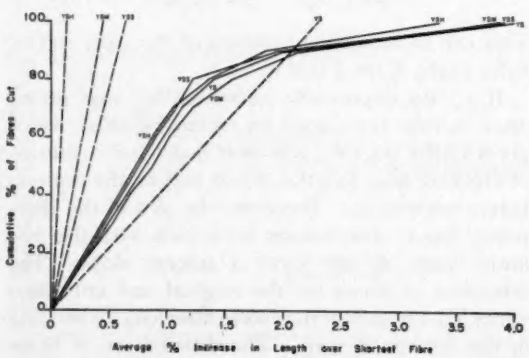

FIG. 12. *Distribution of fiber lengths.* —— *Experimental.* — — — *Theoretical, based on final yarn twist.*

If the above reasoning is true, then the major deviation between theoretical and experimental results has been explained on the basis of length, a consideration not valid for the short lengths involved in rupture, and thus tensile calculations should be based on the more accurate theoretical values and not on the experimentally obtained curves.

B. Strength of Yarns Removed from Strands

In Section I*C*, a theoretical analysis was made of the strength of yarns removed from strands on

TABLE I. TWIST STRUCTURE OF EXPERIMENTAL ABACA STRANDS *

Strand code	Singles yarn twist before stranding (turns/ft.)	Strand twist (turns/ft.)	Singles yarn twist as it lies in the strand (turns/ft.)
SSS	6.6Z	4.3S	3.5Z
SSM	6.6	5.4	2.9
SSH	6.6	6.9	1.7
SMS	11.0	3.8	9.0
SMM	11.0	4.8	8.4
SMH	11.0	6.0	8.0
SHS	15.0	3.9	13.4
SHM	15.0	3.9	13.4
SHH	15.0	4.3	13.3

* All yarns 300 ft./lb. nominal weight.

the basis of the creation of excess lengths due to untwisting in the stranding operation.

As part of the study of factors influencing the translational efficiency of cordage, a series of abaca fiber cordage strands of different twists made from yarns of different twists were produced at the Boston Navy Yard. Description of the pertinent nominal structure of these strands is given in Table I. In all cases, strands possess a single-core yarn surrounded by either thirteen or fourteen singles yarns in the exterior shell. For purposes of efficiency calculations of yarns removed from strands, there is negligible effect produced by changing the number of external yarns. Correspondingly, there is negligible difference in residual singles twist whether a core yarn or external yarn is used—*i.e.*, it is impossible to detect such differences experimentally.

In all cases, the singles twist as it lies in the strand was determined by cutting away all but one of the yarns in the strand, followed by untwisting of the single remaining yarn. Length growths were added to original strand lengths so that the twist per unit length of yarn could be determined. The foregoing procedure is obviously equivalent to removing a single yarn from the strand by "unwrapping"—*i.e.*, holding one end of the strand rigidly clamped, and rotating the free end of any yarn about the strand axis but not its own axis. By this latter technique, most of the yarns in any given length of strand can be used for twist determinations. As will be shown later, the twist of yarn determined by either of the two described procedures gives helix angles and excess lengths of yarns as they lie in strands substantially in agreement with those which result from the more rigorous analyses of Schwarz [3] and Chow [4]. Yarns removed from the strands described in Table I are designated as *YSS*, *YSM*, etc., the initial letter *Y*, for yarn, replacing the initial letter *S*, for strand.

The results of efficiency calculations for the full series of soft-, medium-, and hard-twist yarns removed from soft-, medium-, and hard-twist strands, together with the theoretical efficiencies, with and without consideration of excess lengths, are tabulated in Table II. These results were calculated by the summation procedures derived in section I*C*. The plus and minus values represent two standard errors of efficiency calculated using only the variance in experimental yarn strengths.

The experimental values of efficiency for the *YSS*, *YMS*, *YMM*, and *YMH* yarns are all quite close to the theoretical values computed for full excess lengths. In the case of yarns *YSM* and *YSH*, the theoretical values are too high since the residual yarn twists are sufficiently low that only the throughgoing fibers contribute any appreciable amount to the strength, although the nonthroughgoing fibers contribute more load in yarn *YSM* than in yarn *YSH*, since the residual twist in the former exceeds that in the latter. While no precise quantitative prediction of the strengths of these yarns can be made, it is possible to account for most of the discrepancies as follows: for the gage length to fiber length ratio employed in the determination of experimental efficiencies, approximately one-third of

TABLE II. COMPARISON OF THEORETICAL AND EXPERIMENTAL EFFICIENCIES OF YARNS FROM STRANDS

Yarn code *	Initial yarn twist (turns/ft.)	Final yarn twist (turns/ft.)	Yarn diameter (in.)	Efficiencies (%) Theoretical: No excess lengths	Theoretical: Full excess lengths	Experimental
YSS	6.6Z	3.5Z	0.125	58.8	54.0	53.6 ± 6
YSM	6.6	2.9	0.125	58.8	53.2	44.0 ± 5†
YSH	6.6	1.7	0.125	58.8	51.2	36.3 ± 5†
YMS	11.0	9.0	0.125	56.3	49.5	46.2 ± 4
YMM	11.0	8.4	0.125	56.3	47.0	46.2 ± 1
YMH	11.0	8.0	0.125	56.3	45.2	44.0 ± 3
YHS	15.0	13.4	0.100	54.7	47.8	42.9 ± 5
YHM	15.0	13.4	0.100	54.7	47.8	33.5 ± 3
YHH	15.0	13.3	0.100	54.7	47.8	42.9 ± 4

* First letter indicates yarn, second letter twist of yarn, third letter twist of strand.
† See text for explanation of these values.

the fibers were not throughgoing. Thus, considering only those fibers which are throughgoing, the efficiency of yarn *YSH* would be $\frac{2}{3} \times 51.2 = 34.1\%$. Some strength would be anticipated for the nonthroughgoing fibers in this yarn, but the magnitude would be small and the contribution to efficiency of the order of $36.3 - 34.1 = 2.2\%$. For the *YSM* yarn, where the residual twist is higher, the contribution of the nonthroughgoing fibers to efficiency is probably of the order of $44.0 - \frac{2}{3} \times 53.2 = 8.5\%$, higher than the *YSH* yarn, as would be anticipated. However, as these yarns lie in the strand, additional cohesive forces are created by the strand twist, and thus the low experimental singles strength for yarns *YSM* and *YSH* should not be construed as indicating that the strands which they comprise would be weak.

For the hard-twist yarn series, *YHS*, *YHM*, and *YHH*, the discrepancies are higher than could be accounted for on the basis of experimental strength variation—just slightly higher in the case of *YHS* and *YHH* and considerably higher in the case of *YHM*. A possible explanation for the discrepancies in the cases of yarns *YHS* and *YHH* is that the experimental values of initial twist, N_{yo}, and final twist, N_y, for these yarns were not sufficiently accurate. From previous work it might be concluded that a small variation in twist for moderate helix angle yarns would not affect the strength very much, and this *is* the case where twist effects are mostly angular in nature. However, when excess lengths are considered, the effect of a small change in twist may by no means be small. As an example, the theoretical strength of a yarn removed from a strand with excess lengths present has been calculated on the assumption of initial yarn twist of 13.4, 15, and 17 turns/ft. and final yarn twist of 13.4 turns/ft. The 15-13.4 combination corresponds to the actual, as measured and calculated, hard-twist series. The results are plotted in Figure 13. Over the range covered, it can be seen that the rate of change of efficiency with initial twist is about 5% per turn of twist per foot. The rate with respect to final twist is about the same for this range. Thus, the effects of small twist variations are of the order of the discrepancy.

No similar reasoning can explain all of the very large difference between theoretical and experimental values of efficiency for the *YHM* yarn, nor for the large difference between this yarn and the other two yarns of the hard yarn twist series. On the basis of all parameters considered theoretically, as well as their measured structural geometries, the three yarns are very nearly identical. All that can be said for yarn *YHM* is that some factor, such as fiber tenacity, which was not exhaustively measured for each construction, does not have the value ascribed to it on the basis of previous investigations.

In a subsequent section on strand efficiency it will be shown that the foregoing discussion on excess lengths may be largely of academic interest, since the condition of circular symmetry of the yarn is strongly violated as the yarns lie in strands. Thus, yarns removed from strands do not possess the same characteristics as they do when they lie in the strand, although it is very probable that some residue of large excess lengths is present in yarns as they lie in strands.

The physical reason for excess lengths, which are created by partial untwisting of a yarn, influencing efficiencies so profoundly is that they accentuate the degree of unbalance of elongations amongst fibers in a yarn. The exterior fibers, which by virtue of the helix angles are under a lesser strain than the interior fibers, can be subjected to non-load-bearing extension as a result of the excess lengths. Obviously, this non-load-bearing extensibility would exert less effect for a high-elongation fiber or for a fiber whose stress-strain curve was flat over a wide range of elongations near rupture—*i.e.*, a high a/b. The converse of this effect of excess lengths is also of interest. For example, it is possible from the theoretical data previously published [1] to determine the maximum possible efficiency of a yarn if all of the elongation unbalance between fibers were removed. Such a hypothetical

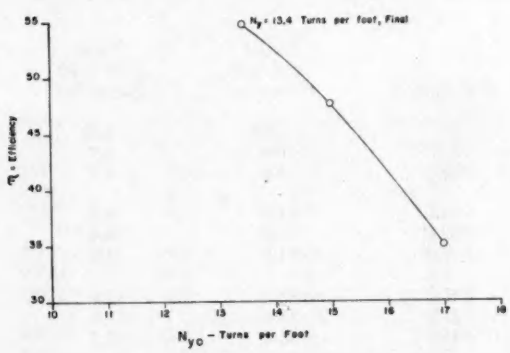

FIG. 13. *Effect of variation in original yarn twist on efficiency of yarn removed from strand.*

structure might be visualized by, say, imagining varying amounts of crimp to be inserted amongst the fibers. The amount of crimp should diminish from the inside to the outside of the yarn. For such a yarn, the efficiency would be determined from

$$\eta_y = \eta_{\text{bundle}} \frac{\ln (\sec^2 \theta_s)}{\tan^2 \theta_s}, \qquad (23)$$

where η_{bundle} is the bundle efficiency for the type of fibers under consideration and θ_s is the surface helix angle of the yarn. In general, efficiencies calculated from equation (23) are higher than those previously published [1], indicating that increases in strength could be achieved by adjusting crimps. However, the extent of such improvements are sizable only for stiff inextensible fibers whose rupture elongation variability is low. A coefficient of variation of fiber elongation to rupture of 10% is sufficiently large to mask the strength increase. It is also clear that the extra yarn weight per unit length resulting from the insertion of crimps as described above would act to diminish the efficiency.

C. Relationship of Initial to Final Twist in Yarns Removed from Strand

In Section I*B* it was shown that in the normal stranding procedure the relationship between final singles twist, N_{yp}, initial singles twist, N_{yo}, strand twist, N_s, and helix angle θ_p, should be

$$N_{yp} = N_{yo} - N_s \cos \theta_p. \qquad (24)$$

Table III gives N_{yp} as determined from the above equation and also as measured directly for the series of yarns whose efficiencies were compared in Table II.

TABLE III. COMPARISON OF CALCULATED AND EXPERIMENTAL YARN TWISTS FOLLOWING STRANDING

Yarn code	N_{yo} (TPF)*	N_s (TPF)	$\cos \theta_p$	l_s/l_y	Final yarn twist, N_{yp} (TPF) Calculated	Final yarn twist, N_{yp} (TPF) Experimental
YSS	6.6Z	4.3S	0.931	0.930	2.6Z	3.5Z
YSM	6.6	5.4	0.897	0.887	1.7	2.9
YSH	6.6	6.9	0.880	0.858	0.5	1.7
YMS	11.0	3.8	0.945	0.944	8.4	9.0
YMM	11.0	4.8	0.917	0.918	6.6	8.4
YMH	11.0	6.0	0.878	0.857	5.7	8.0
YHS	15.0	3.9	0.943	0.934	11.3	13.4
YHM	15.0	3.9	0.942	0.929	11.3	13.4
YHH	15.0	4.3	0.931	0.926	11.0	13.3

* TPF = turns per foot of twist.

The column headed "$\cos \theta_p$" gives the cosine as calculated by the method described in section I*A*. The "l_s/l_y" column gives the ratio of the length of the strand to the length of the yarn contained in that length. Theoretically, $l_s/l_y = \cos \theta_p$, and agreement between these two quantities is very good, the discrepancy always being less than 3%. Unfortunately, the agreement between calculated and theoretical values for N_{yp} is very poor, indicating that equation (24) is not a valid representation of what happens to twist during the stranding operation. There is no obvious reason why singles turns are not removed on a one-to-one basis with strand twist, but clearly they are not. For lack of concrete evidence to support any quantitative explanation, this problem will be left for future exploration, making it necessary to determine final yarn twists experimentally. It should be pointed out that the more rigorous analysis of plied yarn structure developed by Chow [4] does not explicitly refer to final twist, and, even if interpreted as such, does not produce sufficiently different results from equation (24) to account for the differences in Table III.

D. Strand and Plied Yarn Efficiencies

Theoretical formulation of the factors involved in the translation of yarns into higher order structures is somewhat complicated by the inability to characterize accurately the properties of yarns as they lie in such structures. Fortunately, certain approximating assumptions can be made which simplify calculation and yet yield results which check experimental values to within the range of experimental error.

By utilization of the concepts developed earlier in this report, strand or plied yarn efficiency can be calculated from the integration of the following data and assumptions: (*1*) average stress-strain curve of yarns as they exist in the strand or plied yarn; (*2*) variability of elongation to break of yarns as they lie in the higher order structure; (*3*) strand twist and yarn position; (*4*) the assumption that any yarn supports negligible load after attaining maximum load—*i.e.*, that the yarn ruptures completely.

It has been shown that for parallel units the curves of Figure 10 may be expected to give the multiplication factor required to account for the

effects of variability among yarns. To test the accuracy of this assertion, consider the case of bundles containing different numbers of fibers as a special case of a higher order structure. For this special case, the stress-strain curve of the fibers as they lie in the bundle is clearly the same as if they were single. Similarly, the variability of fiber elongation to break is unchanged by the bundle formation. There is no twist, and rupture of the individual fibers is sudden and complete. Thus, only the first two of the above factors apply, and the pertinent data for both are unambiguously defined. Listed in Table IV are the experimental and theoretical results for efficiency of translation of bundles, each of which contains "small" numbers of Manila abaca fibers. Theoretical efficiencies are based on the efficiency curves of Figure 10.

The theoretical values given in Table IV were calculated from the following pertinent fiber data: $b = 42.5$, $e_m = 2.47\%$, and $V = 24\%$; or $m = 25.2$; determinations were from 75 single fiber tests. The units of b are % mean ultimate fiber strength per % elongation. Experimental results are listed in Table IV with a range of ± 2 standard errors, calculated considering only the variance in bundle strength. On the basis of the excellent agreement given in Table IV, there is no reason for not accepting the curves of Figure 10.

A twisted structure with all units lying at the same angle with respect to the structure axis presents no theoretical complexity. Final efficiency for this case would be determined by multiplication of bundle efficiency by the cosine of the angle of inclination for the component of force and again by the cosine of the angle for denier increase due to the twist take-up. The problem, as stated above, is that no yarn parameters are available for the yarn as it lies in the strand or plied yarn. These parameters must be estimated from consideration of single yarn properties outside the strand and the assumed effects of lying in a strand.

TABLE IV. EFFICIENCIES OF TRANSLATION OF MANILA ABACA FIBER STRENGTH INTO BUNDLES CONTAINING A SMALL NUMBER OF UNITS

No. of fibers in bundle	Efficiencies (%) Theoretical	Experimental
2	90	88.3 ± 7
3	81	81.0 ± 5
7	73	76.0 ± 8
15	68	69.8 ± 7.5

Probably the two most important effects of stranding on the singles other than the change of turns of twist, which change can be measured, are: (*1*) increase of cohesive force between fibers, and (*2*) distortion of the circular cross section.

The increase in cohesive force is of importance principally in low-twist singles whose twist, if the yarn were removed from the strand, would be below optimum. Distortion of the circular cross section of the yarn can have a very great effect on cancelling some of the adverse effects of both excess fiber lengths and stress concentrations which would exist in a strand whose yarns were circular. This latter point—*i.e.*, stress concentration—is discussed later. It was stated earlier herein that a careful analysis of the strength of a yarn with excess lengths was largely of academic interest, since such a configuration does not exist within a stranded structure. Thus, while the analysis of yarns removed from strands, calculated considering the existence of excess fiber lengths, is probably valid, it is of little use in the calculation of strand strengths and efficiencies. Before presenting the results of calculations on strand and plied yarn strengths, an analysis of some of the effects of cross-section distortion on removal of excess lengths will be made. This analysis will help to clarify the reasonableness of certain of the assumptions which are made, and thus justify them.

Consider the case of a yarn of circular cross section containing no excess fiber lengths. The yarn will exhibit a moderately firm hand. Now visualize a partial untwisting of the yarn. From the preceding analysis of section I*C*, it is known that excess fiber lengths will exist within the yarn and, clearly, the yarn will feel less firm. If several of these yarns are twisted together there would obviously be a tendency for the circular yarn cross section to distort, and it is well known that such sections are in general not circular in plied and stranded structures. The question now arises as to what effect this distortion will have on the tensile properties of the yarn as it lies in the strand. Two possible effects on yarn structure are: (*1*) changes in the required path length of the fibers and, thus, in the excess fiber lengths; (*2*) changes in inclination of the fibers.

To see how little yarn cross-sectional shape distortion may change fiber helix angles while having a significant effect on excess fiber lengths, consider the case of a yarn of circular section and helix angle

of θ_c. Now distort the section to a square. Under the assumption of equal packing factors, the analysis is as follows:

Let: A = the cross-sectional area of the yarn (same for both round or square yarn); N = turns of twist per unit length; r = radius of yarn; S = length of side of square. Then:

$$A = \pi r^2 = S^2,$$
$$S = r\sqrt{\pi}.$$

Since the fiber progresses an axial distance of $1/N$ for every complete turn, on one side of the square cylinder it will progress $1/4N$ (see Figure 14). The length of fiber in one turn about the circular helix is

$$l_c = \frac{1}{N}\sqrt{1 + 4\pi^2 N^2 r^2} = \frac{1}{N}\sqrt{1 + \tan^2\theta_c},$$

while about the square cylinder it is

$$l_S = 4\sqrt{S^2 + \left(\frac{1}{4N}\right)^2},$$

and, since $S = r\sqrt{\pi}$, this becomes

$$l_S = \frac{1}{N}\sqrt{1 + 16\pi N^2 r^2} = \frac{1}{N}\sqrt{1 + \frac{4}{\pi}\tan^2\theta_c}.$$

The % change in required path length is

$$100\,\frac{l_S - l_c}{l_c} = 100\,\frac{\left(\frac{1}{N}\sqrt{1 + \frac{4}{\pi}\tan^2\theta_c} - \frac{1}{N}\sqrt{1 + \tan^2\theta_c}\right)}{\left(\frac{1}{N}\sqrt{1 + \tan^2\theta_c}\right)}$$
$$= 100\left(\frac{\sqrt{1 + 1.277\tan^2\theta_c}}{\sqrt{1 + \tan^2\theta_c}} - 1\right).$$

The fiber helix angle on the surface of the square cylinder is given by

$$\tan\theta_S = \frac{S}{1/4N} = 4Nr\sqrt{\pi} = 7.092Nr.$$

Since the fiber helix angle on the surface of the circular cylinder is given by

$$\tan\theta_c = 2\pi Nr = 6.283Nr,$$

then

$$\tan\theta_S = 1.129\tan\theta_c.$$

Figure 15 shows the relationship between original helix angle, final angle, and decrease in length according to the analysis given above.

Even for a helix angle of 30°, which is higher than would normally exist in a yarn, the change in angle is only about 3°. Reference to the curves of translational efficiency given previously [1] will show that this in itself will not occasion any very great change in efficiency. However, corresponding to this angular change there is a length take-up

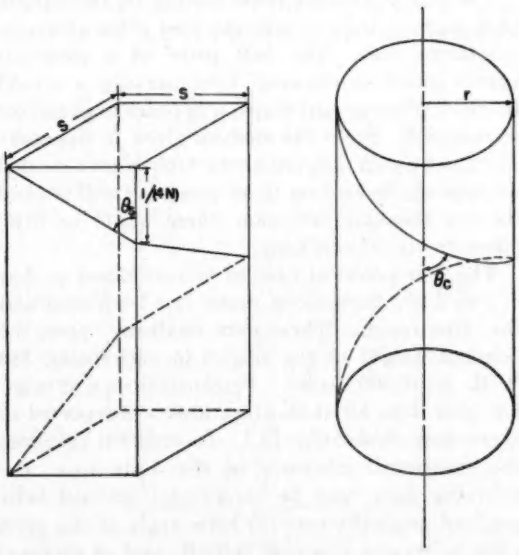

FIG. 14. Left—*Square helix.* Right—*Circular helix.*

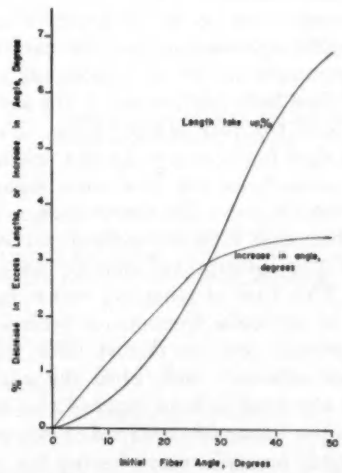

FIG. 15. *Effect of distortion to square section on excess lengths and helix angle.*

of about 3.4%, an amount which is sizable in most considerations of excess lengths. For angles as low as 15°, the length take-up is nearly 1%. This may be quite significant in low elongation-to-break materials.

The square section is, of course, hypothetical. The actual shape of the final section will be determined by a number of things—chiefly, the number of yarns, the strand twist, the yarn twist, and yarn excess lengths. Clearly, the resistance to distortion would be quite large after the excess lengths had been removed from any appreciable number of fibers. Thus, a yarn with low excess lengths would be expected to maintain itself more nearly circular.

While an analysis of the many possible distorted shapes is not practical, it can be said without reservation that any appreciable distortion from a circular shape will, unless accompanied by a large increase in packing factor, cause a take-up of excess fiber length. This distortion will continue to the point where enough excess lengths are fully removed to make further distortion impossible with the forces available from the plying or stranding operation. The distortion is accomplished with little change in angle of inclination. While this information is not very definitive, it does make it reasonable to assume that yarns with small amounts of excess lengths will show virtually no excess length effects when stranded, and those with large amounts of excess lengths will show very much less effect than would be expected on the basis of the circular cross-section analysis.

The general case of an arbitrarily shaped distorted section can be handled for the condition that substantially all excess lengths are removed. Here, the final helix angle is nearly the same as the helix angle of the yarn before plying, since it can be shown that $l_f = l_y/\cos\theta_o$ for the original yarn, and $l_f = l_y/\cos\theta_f$ for the final yarn, regardless of cross-sectional shape. The approximation involved will be discussed in a subsequent section when certain of the assumptions already made are examined. This case of complete excess length removal is of particular importance because a yarn will, in general, tend to distort until the excess lengths are removed, and, while the entire yarn cannot be supposed to have reached this state, the deviations from complete removal of excess lengths will be largely for those fibers having low angles of inclination where excess lengths are small anyway.

Calculation of strand efficiency should then make use of a yarn strength approximately that of the original yarns, or somewhat less for large amounts of untwisting in the plying process. Thus, one cannot in general compute the translation of experimental yarn strength into strands or plied yarns using data on yarn removed from plied or stranded structures, but must instead rely on the theoretical formulation.

The differences between rupture strength of a yarn as it lies in a strand and of a yarn removed from a strand have now been partially accounted for, but any differences in the shape of the stress-strain curves and the variation of elongation to break have not. Thus, the factor $m = b\sigma$, upon which the effects of variability are based, has not been determined. Unfortunately, there is no unequivocal means of obtaining a value which can be considered accurate. It is probable that b, the stiffness, increases slightly from the value obtained for yarns removed from strands, but what happens to σ cannot be predicted. However, the value of $b\sigma$ for a given set of similar yarns, initially the same but with different amounts of twist removed by stranding or plying, does not vary very much, so it is reasonable to assume that the value of m for yarns in strands is close to the value for yarns removed from strands. Also, reference to Figure 10 will show that for the cordage structures studied even a fairly large error in m will introduce only a few % error in the final efficiency.

The final point to be considered is the assumption that yarns support negligible load after attaining maximum load. The best proof of a clean-cut yarn rupture is obtained by observing a strand break. When a yarn snaps, it appears to go almost completely. From the analysis given in Appendix *I*, it can be seen that unless the broken yarn carried an appreciable load up to an extension well beyond its own breaking extension, there would be little effect on strand efficiency.

The first practical case to be considered is that of two 3-ply Sansevieria ropes, one burnished and the other rough. These were small-size ropes, the nominal weight of the singles in each being 380 ft./lb. or 36,000 denier. Pertinent fiber and original yarn data for these structures was reported in a previous publication [1]. In order to calculate the theoretical efficiency of the 3-ply rope, the following data must be known: (*1*) external helix angle of original yarn; (*2*) helix angle of the plied yarn, or rope in this case, initially and at rupture; (*3*) fiber properties—e_m, mean fiber rupture elongation (%); a/b, the ratio of load intercept to slope

of the linear approximation to the average fiber stress-strain curve; V, the coefficient of variation of fiber elongation to rupture; (4) b and σ for the yarn, theoretically as it lies in the final rope.

Using the yarn helix angle and the fiber properties, the singles yarn efficiency can be found from the curves given previously [1]. The twist take-up of the yarn is found from the initial helix angle, as also given in a previous work [1]. The translational factor, μ, due to yarn variability is found from the curves of Figure 10 using a value of m equal to $b\sigma$ for the yarn. The twist take-up factor for the 3-ply rope is given by the cosine of the initial ply angle, and the axial component of force by the cosine of the ply angle at rupture. Usually the initial and rupture ply helix angles will be sufficiently close so that there need be no differentiation between them, but in this case the rope diameter decreased and length increased considerably as the specimen approached rupture, so that a slightly better value is obtained by taking the change in angle into account.

In Figure 16 is given the average stress-strain curve for yarns removed from the rough rope. The slope, b, is determined by the best straight line through the region of the curve near the average rupture point.

Table V gives all parameters and the theoretical results for the 3-ply rough rope compared with experimental results. In Table V, μ is yarn variability factor as given by the curves of Figure 10,

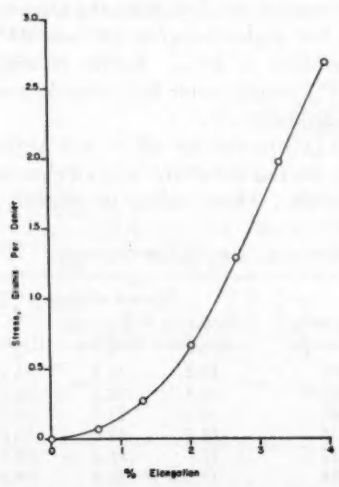

FIG. 16. *Average stress-strain curve for Sansevieria yarns, rough.*

and cos θ_{po} is the rope twist take-up factor. As can readily be seen, the agreement between theoretical and experimental efficiencies is excellent, the difference being approximately 2%. It is to be noted that the combined effects of yarn variability and rope helix angles have accounted for an equivalent loss of yarn tenacity of the order of 25%—*i.e.*, the translation of yarn strength to rope strength is about 75%. Thus, it is apparent that the major cause of the loss of nearly 60% of the fiber strength in this rope is the poor efficiency of translation of the fiber strength into the yarns. This latter is, as already described, the result of both nonuniformity of rupture extensibility among the natural Sansevieria fibers and also their low average extensibility.

No extensive tests were performed on the burnished rope, since it was indicated by gross screening that burnishing did not significantly affect the 3-ply rope efficiencies. Thus, the burnished rope had an experimental efficiency of 42.9 ± 3% *versus* 40.8 ± 3% for the rough rope, the difference not being statistically significant. Experimental efficiencies of yarns removed from the 3-ply ropes were 54.5% for the burnished and 53.5% for the rough ropes. Without consideration of excess fiber lengths, each of these yarns would have given experimental efficiencies of 58.5%. While no formal analysis of excess lengths effects were made, it was apparent from the method of rope formation that the effects would be small, since in roping a partial compensation was made for twist removal, and hence the magnitude of excess lengths was small. In addition, the inherent variability of the

TABLE V. PARAMETERS AND EFFICIENCIES FOR 3-PLY SANSEVIERIA ROPE, ROUGH

Yarn properties	
Single yarn efficiency (%)	55.5
b = slope of yarn stress-strain curve (% of ultimate load/% elongation)	41.6
σ = standard deviation of rupture elongation (%)	0.30
$m = b\sigma$	12.5
μ = yarn variability factor	0.90
Rope helix angles	
$\cos \theta_{po}$ = cosine of original helix angle	0.898
$\cos \theta_{pf}$ = cosine of helix angle at rupture	0.929
Efficiencies of 3-ply rope	
Theoretical efficiency (%)	41.6
Experimental efficiency (%)	40.8 ± 3

Sansevieria fiber in these yarns was greater than that of the Manila abaca fiber [1] for which excess length effects were calculated in Table II. Thus, the higher variability of the Sansevieria fiber would mask the effect of excess lengths to below that of the abaca fiber, and an excess length effect for the former fiber of approximately the 10% experimentally observed is reasonable.

The next case to be considered is that of the series of Manila abaca strands made up of the yarns whose twist structure and strengths were considered in Tables I and II. The approach is the same as that for the Sansevieria ropes with one exception. It will be noted in the derivation of 7-ply yarn strength as given in Appendix *III* that the statistical effects cannot be separated completely from the geometric effects, and thus the exact analysis of the problem is rather complex. Strictly speaking, an analysis similar to that of the 7-ply structure applies to any case in which the constituent elements of the structure do not undergo equal strains as a result of a structure strain. Nonetheless, it can be shown that negligible error is introduced in the case of the 14- or 15-yarn strands if all 14 or 15 units are considered to be equally strained instead of having a more highly strained core yarn, as is actually the case.

This may be demonstrated by considering the case of the 7-ply yarn in two ways: (*a*) efficiencies, η_1, calculated according to the previous rigorous analysis whose results are plotted in Figure 11; (*b*) efficiencies, η_2, calculated under the assumption of all seven units being at the same angle and thus supporting equal strains.

Table VI gives the results for several cases. It can be seen that for any appreciable yarn variability, the values of η_1 and η_2 for a 7-ply yarn are sufficiently close so that the less extreme case of 14 or 15 units with a core would produce negligible differences whether considered as a parallel bundle or as a core and sheath configuration. The discrepancy is obviously less at small ply helix angles. In no case was a higher ply helix angle than 28° found for the Manila strands, whose average yarn rupture elongation variability was of the order of 10%. Clearly, the assumption of the strand structure containing all units in parallel would involve an error considerably less than the errors shown in Table VI for angles between 20° and 30° and for yarn variability of 10%. Errors in efficiency of less than 1% would result from this approximation of strand geometry.

Table VII summarizes all of the pertinent information on the structure and efficiencies of the abaca strands. Three values of efficiency are in-

TABLE VI. COMPARISON OF THEORETICAL 7-PLY YARN EFFICIENCIES

θ	a/b	c_m	V	η_1	η_2
20°	−1	3	0	80.5	93.9
30°				75.0	86.6
20°	−1	3	5	79.5	84.5
30°				70.0	77.8
20°	−1	3	10	76.5	74.9
30°				66.0	69.0
20°	0	any value	0	85.4	93.9
30°				75.0	86.6
20°	0	any value	5	86.0	87.6
30°				71.3	80.7
20°	0	any value	10	81.0	81.3
30°				70.6	74.9
20°	1	3	0	87.6	93.9
30°				75.0	86.6
20°	1	3	5	89.5	89.2
30°				75.0	82.2
20°	1	3	10	83.1	84.4
30°				71.3	77.8

TABLE VII. COMPARISON OF THEORETICAL AND EXPERIMENTAL STRAND EFFICIENCIES

Strand code	Single yarn efficiency (%) No excess lengths	Single yarn efficiency (%) Full excess lengths	Yarn variability parameters m	Yarn variability parameters μ	Cosine strand helix angle	Strand efficiency (%) No excess lengths	Strand efficiency (%) Full excess lengths	Strand efficiency (%) Experimental
SSS	58.8	54.0	11.6	0.80	.931	40.7	37.4	41.4 ± 2
SSM	58.8	53.2	15.0	0.75	.897	35.5	32.1	37.1 ± 3
SSH	58.8	51.2	15.1	0.75	.880	34.3	29.8	31.0 ± 2
SMS	56.3	49.5	14.3	0.76	.945	38.3	33.6	40.6 ± 3
SMM	56.3	47.0	12.0	0.79	.917	37.7	31.2	43.5 ± 2
SMH	56.3	45.2	14.1	0.76	.878	33.1	26.6	29.6 ± 2.5
SHS	52.5	47.8	15.3	0.74	.943	34.6	31.4	31.8 ± 2
SHM	52.5	47.8	15.3	0.74	.942	34.5	31.4	33.2 ± 5.5
SHH	52.5	47.8	15.3	0.74	.931	33.7	30.7	33.4 ± 6

cluded for each strand: (*a*) theoretical efficiency without considering excess lengths; (*b*) theoretical efficiency considering full excess lengths; (*c*) experimental efficiencies. Singles yarn efficiencies neglecing all excess lengths are taken from previous work [1], and for the case of full excess lengths from Table II. It would be supposed that the experimental results would always fall somewhere between the theoretical predictions based on full excess lengths and those based on no excess lengths. For small twist differentials—*i.e.*, small amounts of singles untwisting—there should be a tendency for experimental values to approach the values for no excess lengths since there are only small excess lengths to be absorbed. For large twist differentials, better agreement should occur with the values for full excess lengths. The values for full excess lengths should be most closely approached where the final yarn twist is very small, so that a great distortion would be necessary to restore the original angle and thus remove all excess lengths.

With the exception of one value, Table VII demonstrates these observations quite closely. In most cases, theoretical efficiency calculated without excess lengths are well within experimental efficiency ranges. The only value outside of the experimental range is that for *SMM*, and even here the error is small, being only 9%, or 3.8 units of efficiency from the lower of the experimental limits. No explanation is apparent for the high experimental efficiency of *SMM*, but, in view of the good agreement between experimental and theoretical

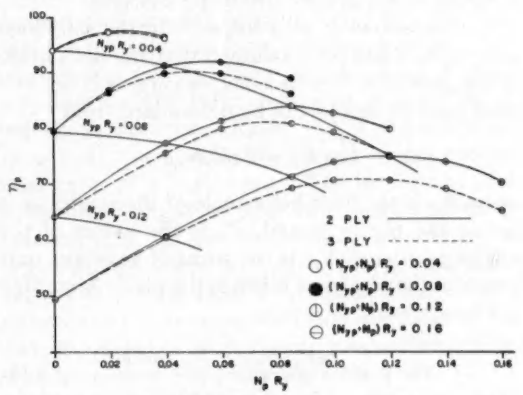

FIG. 17. *Theoretical plied yarn efficiency. Yarn rupture elongation variability = 0. Fiber properties:* V = *0*, a/b = *0.*

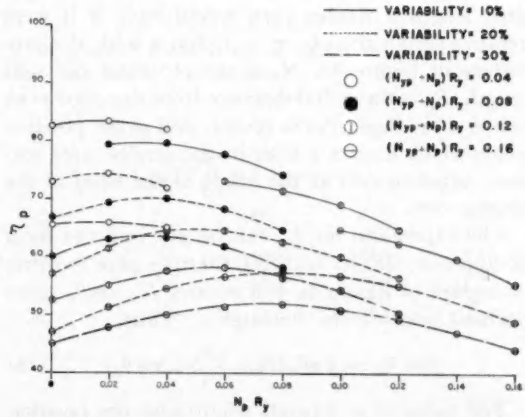

FIG. 18. *Theoretical 3-ply yarn efficiency. Yarn rupture elongation variability = 0. Fiber properties:* a/*b* = *5*, e_m = *10%.*

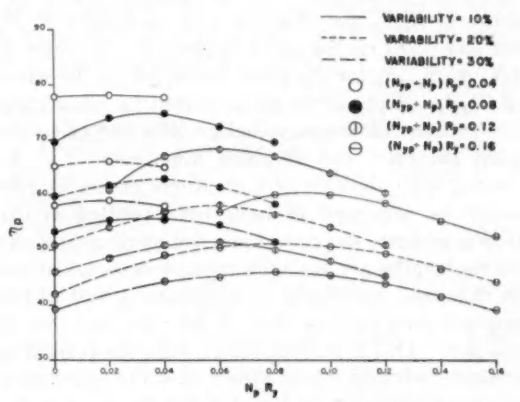

FIG. 19. *Theoretical 3-ply yarn efficiency. Yarn rupture elongation variability = 0. Fiber properties:* a/b = *0*, e_m = *10%.*

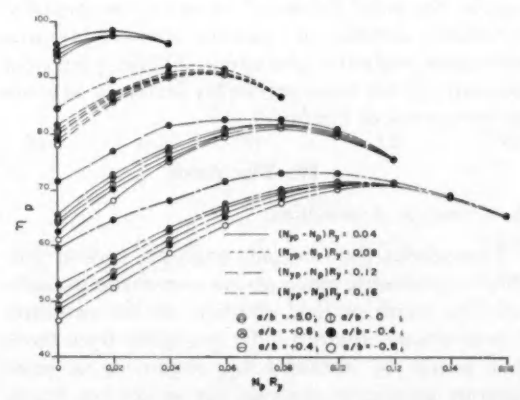

FIG. 20. *Theoretical 3-ply yarn efficiency. Yarn rupture elongation variability = 0. Fiber properties:* V = *0*, e_m = *5%.*

values of efficiency for the other cases, it seems probable that some uncontrolled factor, such as a yarn or fiber not representative of the variables considered, is responsible.

Figures 17–20 illustrate the combined effects of fiber characteristics, singles twist, and ply twist in a form which may sometimes be useful. Each curve is for a given set of fiber parameters, and shows the effect on efficiency of varying combinations of yarn and ply twist under the assumption of no excess lengths and no variation amongst yarns. The convention employed is that all points on a given curve correspond to a constant sum $(N_p + N_{yp})R_y$, where N_p is the ply twist in turns per unit length, N_{yp} is the number of turns per unit length of the yarn as it lies in the ply, and R_y is the singles yarn radius. The abscissa is given in terms of N_pR_y, and thus the yarn parameter $N_{yp}R_y$ for any point on the curve is given by the value of $(N_p + N_{yp})R_y$ for the given curve minus the value of N_pR_y. The curves were plotted by converting the various NR values to helix angles and using the yarn efficiency curves given previously [1]. In dealing with the case of yarn where excess lengths might be supposed to have been created in the plying process, the curves are still applicable if the excess lengths are assumed to have been taken up. In this case, the $N_{yp}R_y$ to be chosen is that of the original yarn and not that of the yarn as it lies in the ply. This is in conformity with the preceding analysis, wherein it was shown that the helix angle of a fiber whose excess length has been taken up by distortion must be very nearly equal to the angle of the fiber before any excess lengths were introduced—that is, before plying. In utilizing these curves, the only additional factors to be employed for plied yarn efficiency calculations are: (*a*) twist take-up of original singles yarns; (*b*) plied yarn twist take-up; (*c*) the yarn variability factor, μ, as given by the curves of Figure 10.

IV. Discussion

A. Geometric Assumptions

Throughout the foregoing analyses, several simplifying geometric assumptions were made to facilitate the mathematical solution of the problem. The results so obtained differ negligibly from those that would be obtained by employing a more rigorous geometric analysis, for structures which are of commercial interest. Portions of the geometrical problem involved here were analyzed quite rigorously by Chow [4]. The geometric results of Chow's work are theoretically valid over a range of helix angles greater than that required for the present problem. In the comparison which follows, it will be shown that: (*a*) The two approaches yield negligibly different results over the practical range of singles, strand, and rope twists; and (*b*) where the results do diverge appreciably, the assumptions involved in either analysis with respect to cross-sectional circularity are strongly violated. Thus, it is not expected that the more involved approach would produce more useful or realistic results, and the comparison is made only to show the order of magnitude of possible errors due to the simplification, and thus justify the exclusion of tortuous twist, as such, from the analysis.

1. Comparison of helix angles. In the simplified approach, it has been assumed that the helix angle of the path of a fiber in a singles yarn as it lies in a plied yarn or strand can be determined from

$$\tan \theta_{yp} = 2\pi R_y N_{yp},$$

where θ_{yp} is the fiber helix angle of the singles as it lies in the ply or strand, R_y is the radius of the singles yarn, and N_{yp} is the turns of twist per unit length of the singles as it lies in the ply. According to Chow's work,

$$\tan \psi = \frac{2\pi R_y (N_{yo} - N_p \cos^2 \theta_p)}{1 - \dfrac{R_y}{R_p} \sin^2 \theta_p \cos \phi}, \qquad (25)$$

where ψ is the angle between the fiber and the singles yarn axes, N_{yo} is defined as the twist per unit length a singles yarn would have if it were removed from the ply in accordance with the procedure of Figure 4a, N_p is the ply twist per unit length, R_p is the radial distance from the plied yarn center to a singles yarn center, and ϕ the position angle which locates a fiber in the singles cross section, equal to zero at the inside of the bend of the singles yarn.

The expression for θ_{yp} can be put into the form of equation (25) by realizing that the pure twisting procedure of Figure 4a will remove $N_p \cos \theta_p$ turns per unit length from the singles. Thus,

$$\tan \theta_{yp} = 2\pi R_y (N_{yo} - N_p \cos \theta_p). \qquad (26)$$

The value of ψ depends slightly on the position angle, ϕ, but the denominator of equation (25) has

an average value very nearly equal to unity, so that the average value of $\tan \psi$ can be taken to be

$$\overline{(\tan \psi)} \doteq 2\pi R_y(N_{yo} - N_p \cos^2 \theta_p). \quad (27)$$

The two angles $\bar{\psi}$ and θ_{yp} can also conveniently be expressed as

$$\tan \theta_{yp} = \tan \theta_0 - \frac{R_y}{R_p} \tan \theta_p \cos \theta_p,$$

$$\tan (\bar{\psi}) \doteq \overline{(\tan \psi)} \doteq \tan \theta_o - \frac{R_y}{R_p} \tan \theta_p \cos^2 \theta_p. \quad (28)$$

To show the magnitude of the differences between θ_{yp} and $\bar{\psi}$, some values for a few different sets of conditions have been compiled in Table VIII.

Clearly, the differences between the results of the two methods are nowhere large, and, in addition, the maximum angular differences occur at the low values of $\bar{\psi}$ or θ_{yp}, where differences are of small importance. The differences also decrease as θ_p and R_y/R_p decrease. $R_y/R_p = 1$ is the condition for a 2-ply yarn, while $R_y/R_p = \frac{1}{2}$ represents the outer layer of a 7-ply yarn. The local value of ψ is slightly changed by the denominator given in equation (25). However, the effect on strength of such a change would be slight unless θ_p were quite large—*i.e.*, greater than 30°. This is most easily understood if it is recognized that for most of the fibers in the entire singles yarn cross section, differences between ψ and $\bar{\psi}$ are negligible.

2. Comparison of excess lengths.—When the helix angle of a yarn is lowered by virtue of partial untwisting, the required helical path length is decreased, but the actual fiber length remains unchanged, giving rise to excess fiber lengths. In this report the required path length of a fiber in a plied yarn per unit length of the plied yarn has been taken to be

$$l_f = \frac{1}{\cos \theta_p} \sqrt{1 + \tan^2 \theta_{yp}}, \quad (29)$$

while Chow's work yields, for a ϕ interval of $2\pi N$, where N is any integer—*i.e.*, for an integral number of fiber cycles—

$$l'_f = \frac{1}{\cos \theta_p} \sqrt{1 + \tan^2 \bar{\psi}}. \quad (30)$$

In either case, the *original* fiber path length is the same, being simply that length corresponding to the original singles helix angle. In Table IX a comparison is made of excess lengths for a wide range of singles and plied yarn twists, as determined from both equations (29) and (30).

TABLE VIII. COMPARISON OF HELIX ANGLES $\bar{\psi}$ AND θ_{yp}

θ_p	Values of $\bar{\psi}$ for: $\theta_{yp} = 5°$	$\theta_{yp} = 10°$	$\theta_{yp} = 20°$	$\theta_{yp} = 30°$
	(a) $\frac{R_y}{R_p} = 1$ (2-ply yarn)			
5°	5°	10°	20°	30°
10	5.1	10	20.2	30
15	5.5	10.5	20.4	30.4
20	6.2	11.1	21.0	30.8
25	7.2	12.2	22.0	31.7
30	8.8	13.6	23.3	32.7
	(b) $\frac{R_y}{R_p} = \frac{1}{2}$ (7-ply yarn)			
20	5.5	—	—	30.4
30	6.8	—	—	31.4

TABLE IX. COMPARISON OF EXCESS LENGTHS l_e AND l'_e

Original singles helix angle, θ_o	θ_{yp}	$\bar{\psi}$	l_e	l_e'
	(a) $\frac{R_y}{R_p} = 1, \theta_p = 30°$			
45.3°	27.2°	30°	21.0%	19.0%
30.5	5.0	8.8	13.4	12.8
26.5	0.0	3.8	10.7	10.5
	(b) $\frac{R_y}{R_p} = 1, \theta_p = 20°$			
42.6°	30°	30.8°	14.0%	13.2%
27.4	10	11.1	10.1	9.7
23.2	5	6.2	7.9	7.7
18.9	0	1.2	4.8	4.7
	(c) $\frac{R_y}{R_p} = 1, \theta_p = 15°$			
24°	10.5°	11°	7.1%	7.0%
	(d) $\frac{R_y}{R_p} = 1, \theta_p = 10°$			
30°	21.9°	22.1°	6.5%	6.3%
20	10.8	10.9	4.5	4.5
15	5.0	5.0	2.9	2.9
10	0.0	0.1	1.5	1.5
	(e) $\frac{R_y}{R_p} = \frac{1}{2}, \theta_p = 15°$			
24°	17.6°	17.8°	5.1%	5.1%

Over the range of ply and singles helix angles covered, which it is believed encompasses the practical range, it is clear that differences in calculated excess lengths are small, with Chow's formula always yielding the slightly smaller value.

It should be noted that calculations of fiber length and strains involve an integration over ϕ from 0 to 2π. This is an impossible procedure if $\theta_o = 0$, for here a given fiber remains at the same angle ϕ throughout its length, and thus this situation represents a point of discontinuity in the equations relating to length. However, the matter is of no practical importance since $\theta_o = 0$ is equivalent to plying zero-twist bundles. It is doubtful whether such a procedure could be made to yield a structure whose original elements remained separate and distinct, much less circular.

3. Comparison of fiber strains.—Fiber strains may be compared on both an average and a local basis, just as angles. In the work of this report, only the average fiber strain has been used and it has been taken to be

$$e_f = e_p \cos^2 \theta_p \cos^2 \theta_{yp}, \qquad (31)$$

where e_p is the strain along the plied yarn axis. Here again, the secondary effects of tortuosity have been neglected, and the singles yarn is considered to have essentially the same geometric properties as if it were removed from the plied yarn and retained its twist as it lay in the ply.

Based upon Chow's analysis, the following expression for the average strain in one complete loop of fiber as it lies in a plied yarn can be derived:

$$e_f' = \sqrt{\frac{(1+e_p)^2+\tan^2\theta_p}{1+\tan^2\theta_p}} \times \frac{\sqrt{1+\left[\dfrac{\tan\theta_o}{1+e_p\cos^2\theta_p}-\dfrac{R_y}{R_p}\dfrac{(1+e_p)\tan\theta_p}{(1+e_p)^2+\tan^2\theta_p}\right]^2}}{\sqrt{1+\left[\tan\theta-\dfrac{R_y}{R_p}\dfrac{\tan\theta_p}{1+\tan^2\theta_p}\right]^2}} - 1. \qquad (32)$$

In Table X the results of equations (31) and (32) are compared. An additional comparison is made in some cases where the simplified formula, equation (31), used in this report is employed, but $\bar{\psi}$ is substituted for θ_{yp}. This value of strain is labelled e_f''.

The differences between e_f and e_f' are small anywhere within the range tabulated. It can be seen that the differences tend to become larger as θ_p or R_y/R_p increase, but R_y/R_p cannot exceed unity. A large part of the difference between e_f and e_f' can be ascribed to the difference between θ_{yp} and $\bar{\psi}$, as is evidenced by the relative closeness of e_f' and e_f''.

From Chow's work, it is also possible to determine the magnitude of the local fiber strain, still, of course, under the assumption of circularity of yarn cross sections. The results, for an extreme case, are given in Table XI.

Table XI would seem to show that very great stress differentials exist among the various portions of a given fiber, depending upon its position angle ϕ. However, a number of factors tend to mitigate the severity of local conditions as shown by this analysis: (*1*) If local differences in strain are admitted, then local differences in excess lengths must also be considered, and the high excess length regions occur just when high strain would be predicted—*i.e.*, at $\phi = 0$; (*2*) Any freedom of motion of fibers whatsoever would tend to equalize strains, and some freedom of motion must exist; (*3*) It has been demonstrated earlier in the report that any distortion of the yarn from circularity will tend to remove excess lengths, and by a direct extension of this reasoning it is easy to see that unequal strains

TABLE X. COMPARISON OF STRAINS COMPUTED FROM EQUATIONS (31) AND (32)

θ_p	θ_o	e_p	$\frac{R_y}{R_p}$	Eq. (31) e_f	Eq. (32) e_f'	Eq. (31) with $\theta_{yp} = \bar{\psi}$ e_f''
25°	30°	0.02	1	0.0160	0.0156	—
25	42	0.02	1	0.0134	0.0125	0.129
25	42	0.10	1	0.067	0.064	0.064
15	23	0.02	1	0.0182	0.0181	—
15	36	0.02	1	0.0153	0.0151	—
25	42	0.10	½	0.056	0.052	0.054
25	34	0.02	½	0.0135	0.0131	0.0133
25	34	0.10	½	0.068	0.067	0.067

TABLE XI. LOCAL FIBER STRAINS FOR A PLIED YARN STRUCTURE
($R_y/R_p = 1$, $\theta_p = 30°$, $\theta_o = 30°$, $e_p = 0.10$)

ϕ	Local strain, e_f (%)
0	11.5
$\pi/2$	7.0
π	4.7
Average	7.5
$e_p \cos^2\theta_p \cos^2\theta_{yp}$	7.5

along the length of a given fiber will cause an equalizing distortion. These distortions can occur either before or during the loading of the structure, or at both times. As stated previously, distortions before loading can occur as the result of the presence of excess lengths. Such distortions tend to alter the local fiber radii of curvature considerably from that for circular yarns. The local strains given in Table XI are critically dependent upon local radii of curvature, whereas the average strains are not so dependent. Examples of distortion under loading, for a circular cross-section yarn with no excess lengths, would be: (*a*) local flattening in the region of high fiber strain; (*b*) higher freedom of fiber relative motion in the region of low fiber strain, with the attendant opportunity of fiber length travel to the region of high fiber strain. Both mechanisms will equalize fiber strain. Thus, differences in local strain may safely be considered negligible, and the average values used. It is also clear from the experimental strength and rupture elongation results that large differences in strains do not exist, since large differences would produce much lower strand and rope efficiencies and elongations than those observed.

It is apparent from the foregoing that for circular yarn cross sections, the simplified geometric relations assumed and used in the body of this report differ inappreciably in most cases from the *average* geometric relationships obtained by Chow. The difficulty of comparing *local* geometric and strain discrepancies has already been discussed, and it has been indicated that local strains and stresses must approach the average when plied yarns are stressed. Nevertheless, it is also evident that with increases in ply or strand helix angles very greatly in excess of 30°, increasing discrepancies arise between the average rigorously derived geometry and the simplified geometry used herein. These discrepancies are in the direction of lowering the plied yarn strength—*i.e.*, lower plied yarn or strand efficiencies would be given using Chow's geometry than those given by the simplified geometry.* While great cross-sectional distortion will usually take place for such high ply or strand helix angles, it is conceivable that some extreme structures may be encountered which will be weaker than the calculations in the body of this report indicate. For such structures, calculations based upon Chow's geometric analysis would determine one limit of efficiency, while the other limit would be determined by the formulas given herein. Cross-sectional distortion would then produce a final result somewhere between the two extreme limits. Clearly, the structures studied in this report are performing under tension in a manner consistent with either Chow's *average* or the simplified geometry. Since these structures cover as broad a range of commercial cordage twists as is feasible, it is clear that they encompass substantially all cordage structures of interest.

* Assuming no excess lengths.

B. Application to Higher Order Structures

Previous work [1] and the present work have covered what appear to be the most significant factors affecting the translation of strength of fibers into practical singles yarns, plied yarns, and strands, with emphasis on cordage materials. It is possible to apply this work directly to higher order structures, such as ropes, simply by interchanging the roles of rope and strand, and strand and yarn. Thus, the rope is treated as a strand composed of yarns which are in reality strands, and whose properties are known. The only additional assumption involved is that strand rupture is complete after maximum strand load is attained. Observations of rope breaks tend to indicate this to be reasonable. Unfortunately, complete sets of data on rope, covering fiber, yarn, and strand properties and rope breaking strength, are not available, but from the scanty data which are at hand, it appears that the above projection yields good results.

Appendix I

Analysis of Parallel Bundle Strength

A parallel bundle, in this work, refers to a group of units all units of which are supporting equal strains as a result of straining the entire group. Thus, a 3-ply yarn contains three units (singles yarns) in parallel. The equal strains would, in the case of a 3-ply yarn, be less than the strain applied to the 3-ply because of the ply helix angle. However, this latter geometrical effect is separable, and merely requires geometric factors to be applied following the analysis of the statistical effect on three yarns in parallel with zero ply helix angle. The statistical analysis follows.

Consider a population of units with a normal distribution of elongations to break and a given average load-elongation diagram (Figure 21). The abscissas are normalized to the statistical t, or number of standard deviations from the mean elongation.

If there are n of the above units in a bundle, there exist the possibilities that maximum load is reached when the first unit breaks, or when the second unit breaks, and so on, to the nth unit. Clearly, if $n = 2$, there is a very low probability for ever attaining a higher load than that reached when the first unit broke (except in cases of very high variability). Conversely, if n is very large, say 100, the maximum bundle load will almost certainly not be reached until several units have ruptured. The factors defining attainment of maximum load will now be formulated analytically.

Assume the first of the n units to break at an elongation corresponding to t_1, and specify that the maximum load shall be attained at this point. The load supported by the bundle here is $ng(t_1)$. In order that this be the maximum bundle load, it follows that the load on the bundle when the second unit breaks, where there are only $(n - 1)$ units intact, shall be less than $ng(t_1)$. In the limiting case of equal loads at both first- and second-unit failure, $(n - 1)g(t_2) = ng(t_1)$. Similarly, for the third-unit rupture, when $n - 2$ units are intact, the limiting equality is $(n - 2)g(t_3) = ng(t_1)$. Thus, the second unit must rupture before the average load per unit is $g(t_2)$, where

$$g(t_2) = [n/(n - 1)]g(t_1);$$

the third before the average load per unit is $g(t_3)$, etc. The values of t_i can be found from the load-elongation diagram since $g(t_1)$ is known from the arbitrarily chosen first break point and the above equalities.

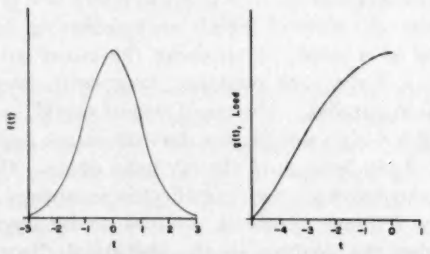

FIG. 21. left—*Normal distribution of rupture elongations.* right—*Average load-elongation curve.*

The above limiting equalities also hold when maximum strength is reached at other than the first break. It is necessary only to determine the strengths corresponding to the arbitrarily chosen value of t_i. Thus, there are several distinct cases to solve: distributions of bundle loads which are maxima first-unit breaks; maxima second breaks, etc. All cases must be calculated which contribute any considerable portion to the total number of bundle breaks.

The formulation of both the separate probabilities for the case of a maximum bundle load being reached when the first unit breaks, the second, etc., and also the efficiency in terms of the various influencing parameters follows.

The following definitions apply to the analysis: p_i = probability of any unit breaking at an elongation within the interval t_{i-1}, and t_i where $t_o = -\infty$

$$p_i = \int_{t_{i-1}}^{t_i} f(t)dt = \frac{1}{\sqrt{2\pi}} \int_{t_{i-1}}^{t_i} e^{-\frac{t^2}{2}} dt$$

(this equation gives the probability integral in terms of t; values of this definite integral can be found in tables of areas under the normal curve). q_i = expohent of p_i factor in any term of the expansion given below. $h(t)_l$ = relative frequency of occurrence of a maximum bundle load at t when the lth unit breaks at t. C = a normalizing constant such that the total probability will equal unity.

It is first desired to plot a curve of relative frequency of maximum bundle load *versus* t for the case of a maximum occurring where the first unit breaks, $h(t)_1$, when the second unit breaks, $h(t)_2$, etc. Consider, for example, the determination of $h(t)_1$.

It is known from probability theory that if the probability of a given event occurring is p_1, another event p_2, etc., that in a total of n events, the probabilities of various combinations can be represented by the expansion of

$$(p_1 + p_2 + \cdots p_n)^n. \qquad (I1)$$

The terms of this expansion will all be of the form

$$Ap_1^{q_1}p_2^{q_2} \cdots p_n^{q_n},$$

where A will have a value depending on the term, and

$$\sum_{i=1}^{n} q_i = n. \qquad (I2)$$

In each term of the expansion the exponents q_i represent the number of occurrences of the event whose probability is p_i, while the whole term, including the coefficient, represents the probability of the *combination* of events designated by the p_i's and q_i's. It is now necessary to formulate some method for rejecting all combinations which do not satisfy the prescribed conditions—in this case, that a maximum is always reached when the first unit breaks. It has already been established that the second unit must break before reaching an elongation corresponding to t_2, the third before t_3, the fourth before t_4, etc. These conditions are satisfied, of course, if the second, third, and fourth units all break before t_2, or if the second and third break before t_2 and the fourth before t_3, etc. The expression to be expanded is

$$(p_2 + p_3 + \cdots p_n)^{n-1}. \qquad (I3)$$

It is obvious that the relative frequency of first-unit breaks which produce maximum bundle loads at an elongation t_1 is the product of the relative frequency of any unit breaking at t_1 and the probability of the existence of a breaking array among the remaining units such that the first-unit break at t_1 is a maximum. Thus,

$$h(t)_1 = Cf(t_1)(p_2 + p_3 + \cdots p_n)^{n-1}, \quad \sum_{i=2}^{k} q_i \geq k - 1, \quad k = 2, 3, \cdots n. \qquad (I4)$$

The exponent is $n - 1$ rather than n since the breaking elongation of the first unit is arbitrarily specified, and the relative frequency of occurrence of this breaking elongation (t_1) is $f(t_1)$. The second of equations (*I4*) specifies the necessary and sufficient conditions such that each of the terms of the expansion (*I3*) satisfies the assumption of maximum bundle load being attained at first-unit break. It is not obvious before beginning calculations how many terms of equation (*I3*) must be considered for numerical accuracy, but, clearly, any very small value for p_i may be omitted from the calculations. Thus, the procedure used in determining the $h(t)_1$ curve involves: (*a*) the selection of a series of arbitrary values of t_1 and the corresponding values of $f(t_1)$; (*b*) for each value of t_1 so chosen, the determination of the corresponding limiting values of t_2, t_3, etc., from the $g(t)$ equalities previously described; (*c*) the determination of p_2, p_3, etc., from the probability integral for each value of t_1 and its corresponding t_2, t_3, etc.; (*d*) the evaluation of the first of equations (*I4*), retaining only those terms which satisfy the second of equations (*I4*).

The curve $h(t)_1$ can be replotted as a curve of strength *versus* t_1, where strength is equal to the product of n, the total number of units in the bundle, and the load per unit, $g(t_1)$. Thus, the average bundle load of those first-unit ruptures which produce maximum bundle loads is $n\overline{g(t_1)}$.

In an entirely analogous manner, all the values of $h(t)_i$ can be formulated, with the following results:

$$h(t)_2 = Cf(t_2)(p_1 + p_3 + p_4 \cdots p_n)^{n-1}; \quad q_1 = 1; \quad \sum_{i=3}^{k} q_i \geq k - 2, \quad k = 3, 4, \cdots n; \qquad (I5)$$

$$h(t)_3 = Cf(t_3)(p_1 + p_2 + p_4 + p_5 \cdots p_n)^{n-1}; \quad q_1 \neq 0, \quad q_1 + q_2 = 2; \quad \sum_{i=4}^{k} q_i \geq k - 3, \quad k = 4, 5 \cdots n. \qquad (I6)$$

The results of the above can be replotted as curves of frequency *versus* bundle strength, the strength being given by the product of $g(t)$ and the number of units intact when maximum bundle load is attained. For the case where a maximum is reached where the first unit breaks, the number of units intact is n; for a maximum when the second unit breaks, it is $n - 1$; for the third, $n - 2$, etc. Average maximum bundle loads are then given as $n\overline{g(t_1)}$; $(n - 1)\overline{g(t_2)}$; $(n - 2)\overline{g(t_3)}$, etc.

In previous work [1] a linear approximation to the stress-strain curve proved very useful for computational purposes. Here again, if a linear curve is used, a great simplification results. Thus, using the terminology of the previous work [1], the load supported by a unit can be expressed as $a + be$, or, in terms of V, t, and e_m, as $a + be_m(1 + Vt/100)$, which is $g(t)$. The assumption of a linear curve permits simplified analytical calculations rather than graphical, but all of the foregoing analysis still applies.

Once the several curves of frequency *versus* strength have been obtained for the various conditions for a maximum, it is necessary only to find the mean value of the abscissas of the curves weighted according to the number of units intact when

maximum load is attained, or

$$\frac{\int_{-\infty}^{\infty}\sum_{l=1}^{n} h(t)_l[n-(l-1)]\left[a+be_m\left(1+\frac{Vt}{100}\right)\right]dt}{n\int_{-\infty}^{\infty}\sum_{l=1}^{n} h(t)_l\,dt}. \quad (I7)$$

Let: $\bar{t}_i$ = mean value of elongation (in terms of t) of all those parallel bundle breaks which attain maximum load when the first unjt ruptures; $\bar{t}_2$ = mean value of elongation of all those parallel bundle breaks which attain maximum load when the second unit ruptures; $\bar{t}_3$ and $\bar{t}_4$ are similarly defined.

For a linear load-elongation curve, the mean value of the loads corresponding to each of the above elongations is $g(\bar{t}_1)$, $g(\bar{t}_2)$, etc. Thus, the corresponding total bundle loads are obviously $ng(\bar{t}_1)$, $(n-1)g(\bar{t}_2)$, $(n-2)g(\bar{t}_3)$, etc. The areas bounded by each of the curves, $h(t)_l$, represent the relative number of all bundle breaks which produce maximum load at first-unit break, second-unit break, etc. Thus, the total number of bundle breaks is proportional to the sum of the areas,

$$(A_1 + A_2 + A_3 + \cdots A_n) = \sum_{n=1}^{n} A_n,$$

and the relative frequency of breaks which exhibit maximum load at first-unit rupture is $A_1/\sum_{n=1}^{n} A_n$, second-unit rupture $A_2/\sum_{n=1}^{n} A_n$, etc. Thus, the average value of maximum bundle loads for all bundle breaks is

$$\bar{P}_B = \frac{A_1}{\sum_{n=1}^{n}(A_n)} ng(\bar{t}_1) + \frac{A_2}{\sum_{n=1}^{n}(A_n)}(n-1)g(\bar{t}_2) + \cdots + \frac{A_n}{\sum_{n=1}^{n}(A_n)}(1)g(\bar{t}_n)$$

$$= \frac{1}{\sum_{n=1}^{n} A_n}[A_1 ng(\bar{t}_1) + A_2(n-1)g(\bar{t}_2) + \cdots A_n g(\bar{t}_n)]. \quad (I8)$$

The average bundle efficiency is then determined as the ratio of average maximum bundle load at rupture divided by the product of the number of units in the bundle, n, and the average breaking load of the units, $a + be_m$. Thus, bundle efficiency is determined as

$$\eta_B = \frac{A_1 ng(\bar{t}_1) + A_2(n-1)g(\bar{t}_2) + \cdots A_n g(\bar{t}_n)}{n(a+be_m)\sum_{n=1}^{n} A_n}.$$

The values of $\bar{t}_1$, $\bar{t}_2$, etc., are determined by inspection of the individual distribution curves, $h(t)_l$, which are substantially symmetrical.

While the foregoing relationships are general, the determination of specific values for $\bar{t}_n$, A_n, and, thus, efficiency, depends upon the particular bundle size, n, and the properties of the units which comprise the bundle—a/b, V, e_m. The curves given in Figure 10 are the results of calculations of a sufficient number of specific cases to permit simple determinations of bundle efficiency for a broad range of the variables. As indicated previously, the parameter $m = be_mV/100$ is used to characterize the properties of the units which comprise the bundle, where, in terms of previously defined parameters, $m = V/[(a/be_m) + 1]$.

A simple example will make the method clear. Consider the case of a bundle of four units whose population parameters are $a/b = 0$ and $V = 20\%$. From the above analysis:

$$h(t)_1 = Cf(t_1)(p_2 + p_3 + p_4)^3;$$

$$\sum_{i=2}^{k} q_i \geq k-1; \quad k = 2, 3, 4. \quad (I9)$$

Assume that the first unit breaks at $t_1 = -2.0$. Then, in order that the second break shall not occur at a higher total bundle load,

$$ng(t_1) \geq (n-1)g(t_2) \quad \text{or} \quad 4g(t_1) \geq 3g(t_2).$$

The curves $4g(t)$, $3g(t)$, $2g(t)$, and $g(t)$ are shown in Figure 22. Since $a/b = 0$, the plots are straight lines passing through the origin, and the load per unit can be expressed as a fraction of mean load as

$$g(t) = \frac{Vt}{100} + 1 = \frac{t}{5} + 1.$$

Thus, for $t_1 = -2.0$, $g(t_1) = -\frac{2}{5} + 1 = 0.6$; $ng(t_1) = 4(0.6) = 2.40$. This condition is shown at point A in Figure 22. When the first unit breaks, the load drops to B on the $3g(t)$ curve and builds up along it until the second unit breaks. To satisfy the condition that a maximum be reached when the first unit breaks, it follows that the point C must be no higher than the point A, or, since $4g(t_1) = 3g(t_2)$ in the limit,

$g(t_2) = \frac{4}{3}g(t_1) = \frac{4}{3}(0.6) = 0.8$. But $g(t) = \frac{t}{5} + 1$, so that $t_2 = 5g(t_2) - 5 = 5(0.8) - 5 = -1$. Similarly, when the second unit breaks, the load drops to the point D and rises along the $2g(t)$ curve. Here, $4g(t_1) = 2g(t_3)$, or $g(t_3) = \frac{4}{2}(0.6) = 1.2$ and thus $t_3 = 5(1.2) - 5 = 1.0$. For t_4 (not illustrated),

$$g(t_4) = \frac{4}{1}(0.6) = 2.4,$$

$$t_4 = 5(2.4) - 5 = 7.$$

In Figure 23 is shown a normal frequency distribution corresponding to the values just calculated. By definition, p_2 is the probability that any unit from the population has a breaking elongation lying between t_1 and t_2. Since $t_1 = -2.0$ and $t_2 = -1.0$, this is represented by the shaded area between these two points under the distribution curve. Similarly, the shaded area from $t = -1.0$ to $t = +1.0$ represents p_3, and that from 1.0 to 7.0, p_4.

These p's must now be substituted into the expression for $h(t)_1$ [equations (*I*4)]. The expansion of equations (*I*4) yields

$$h(t)_1 = Cf(t_1)(p_2^3 + p_3^3 + p_4^3 + 3p_2^2p_3 + 3p_2^2p_4 + 3p_3^2p_2 + 3p_3^2p_4 + 3p_4^2p_2 + 3p_4^2p_3 + 6p_2p_3p_4); \quad (I10)$$

$$\sum_{i=2}^{k} q_i \geq k - 1; \quad k = 2, 3, 4.$$

Each term of the expression must be examined, and if it does not fulfill the conditions specified in the second of equations (*I*10), it must be rejected. This process eliminates all terms which are representative of cases where a maximum value of load is not reached when the first unit breaks. The following table illustrates the method:

				Values of Σq_i for:				
Terms	q_2	q_3	q_4	$k = 2$	$k = 3$	$k = 4$	Accept	Reject
p_2^3	3	0	0	3	3	3	√	
p_3^3	0	3	0	0*	3	3		√
p_4^3	0	0	3	0*	0*	3		√
$3p_2^2p_3$	2	1	0	2	3	3	√	
$3p_2^2p_4$	2	0	1	2	2	3	√	
$3p_3^2p_2$	1	2	0	1	3	3	√	
$3p_3^2p_4$	0	2	1	0*	2	3		√
$3p_4^2p_2$	1	0	2	1	1*	3		√
$3p_4^2p_3$	0	1	2	0*	1*	3		√
$6p_2p_3p_4$	1	1	1	1	2	3	√	
Σq_i for acceptance:				≥ 1	≥ 2	≥ 3		

A single value followed by an asterisk in any row is sufficient for rejection. Thus, the first term, p_2^3, is acceptable. It represents the case where all three remaining units break in the region between t_1 and t_2. The second term, p_3^3, is not acceptable. It represents the case where no breaks occur between t_1 and t_2 with three breaks between t_2 and t_3. This violates the condition that at least one must rupture between t_1 and t_2 in order that the load at t_1 be a maximum. The other terms can be handled in a similar manner. In each case the value of $\sum q_i$ in the k column must satisfy the value given at the bottom of the column in order to conform to the restrictions imposed by the requirement of a maximum bundle load at first-unit break.

In the $k = 4$ column, the restriction imposed is that $\sum_{i=2}^{4} q_i \geq 3$. Clearly, $\sum_{i=2}^{4} q_i$ is always exactly 3 in this example, but the form of the table has been

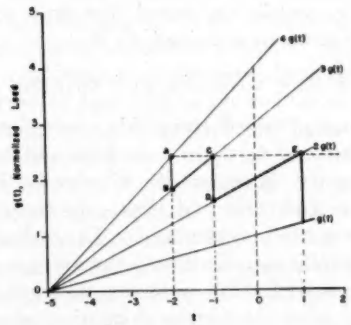

FIG. 22. *Successive ruptures for limiting conditions for maximum bundle loads.*

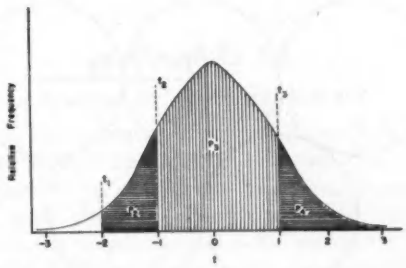

FIG. 23. *Illustration of* p_i *for* $n = 4$, $V = 20\%$, $a/b = 0$.

kept general in order to facilitate immediate extension to larger size groups.

The terms in the $n = 4$ case which satisfy the conditions of maximum bundle load occurring at first-unit break are

$$p_2^3 + 3p_2^2p_3 + 3p_2^2p_4 + 3p_2p_3^2 + 6p_2p_3p_4.$$

For computational purposes, this is most conveniently written as

$$(p_2 + p_3 + p_4)^3 - (p_3 + p_4)^3 - 3p_2p_4^2.$$

All necessary numbers can now be found from a table listing areas under the normal distribution curve, and ordinates to the curve. For this example, where $t_1 = -2.0$, $t_2 = -1.0$, $t_3 = 1.0$, and $t_4 = 7$, the tables yield

$$f(-2.0) = 0.05399$$

$$p_2 = \frac{1}{\sqrt{2\pi}} \int_{-2.0}^{-1.0} e^{-\frac{t^2}{2}} dt = 0.1359$$

$$p_3 = \frac{1}{\sqrt{2\pi}} \int_{-1.0}^{1.0} e^{-\frac{t^2}{2}} dt = 0.6827$$

$$p_4 = \frac{1}{\sqrt{2\pi}} \int_{1.0}^{7.0} e^{-\frac{t^2}{2}} dt = 0.1587$$

and thus

$$h(-2.0)_1 = C(0.05399) \times [(0.1359 + 0.6827 + 0.1587)^3 - (0.6827 + 0.1587)^3 - 3(0.1359)(0.1587)^2] = 1.769(10^{-2})C.$$

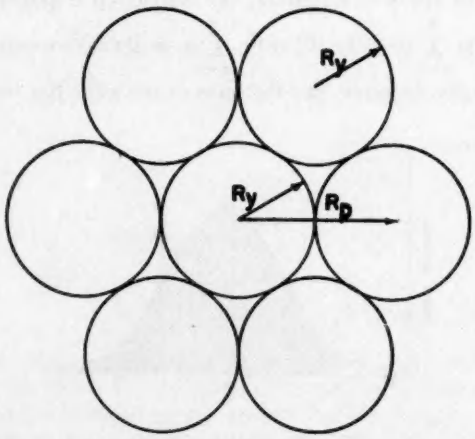

FIG. 24. *Idealized 7-ply yarn.*

In a like manner, values of t_1 of -2.5, -1.5, -1.0, -0.5, 0.00, 0.5, and 1.0 were employed. The resulting curve is plotted in Figure 9.

Next the case of a maximum at second-unit break must be treated. Here

$$h(t)_2 = Cf(t_2)(p_1 + p_2 + p_4)^3;$$

$$\sum_{i=3}^{k} q_i \geq k - 2, k = 3, 4; \quad q_1 = 1. \qquad (I11)$$

A chart similar to the one used for the previous case appears below.

				Values of Σq_i for:				
Terms	q_1	q_2	q_4	q_1	$k = 3$	$k = 4$	Accept	Reject
p_1^3	3	0	0	3*	0*	0*		√
p_2^3	0	3	0	0*	3	3		√
p_4^3	0	0	3	0*	0*	3		√
$3p_1^2p_2$	2	1	0	2*	1	1*		√
$3p_1^2p_4$	2	0	1	2*	0*	1*		√
$3p_1p_2^2$	1	2	0	1	2	2	√	
$3p_1p_4^2$	1	0	2	1	0*	2		√
$3p_2^2p_4$	0	2	1	0*	2	3		√
$3p_2p_4^2$	0	1	2	0*	1	3		√
$6p_1p_2p_4$	1	1	1	1	1	2	√	
Σq_i for acceptance:				$q_1 = 1$	≥ 1	≥ 2		

A single value followed by an asterisk in any row is sufficient for rejection.

Clearly, the requirements are more stringent here than in the case of first-unit rupture, and only the terms $3p_1p_2^2$ and $6p_1p_2p_4$ are acceptable. Then

$$h(t)_2 = Cf(t_2)(3p_1p_2^2 + 6p_1p_2p_4).$$

This curve, $h(t)_2$, is plotted in Figure 9 together with $h(t)_1$. For the case of a maximum being reached where the third unit breaks, a similar table was made, and it was found that only the $3p_1^2p_4$ and $6p_1p_2p_4$ terms remained, so that

$$h(t)_3 = Cf(t_3)(3p_1^2p_4 + 6p_1p_2p_4).$$

The values obtained from this expression are so small compared to those from $h(t)_1$ and $h(t)_2$ that the $h(t)_3$ curve is neglected. Obviously, $h(t)_4$ will also be insignificant, and thus only the $h(t)_1$ and $h(t)_2$ curves need be averaged. The ordinate scale is of no significance since only the average abscissa value is required. The process is now very simple. The $h(t)_1$ curve has a mean elongation occurring at $t = -0.84$, as determined by inspection, and an enclosed area of 24.52 units, as determined by a

planimeter. For the $h(t)_2$ curve, the corresponding figures are -0.13 and 5.93, respectively. In the example, the elongation variability (coefficient of variation of unit elongation to break) is 20%, and a/b is zero, so that the abscissa can be expressed as % mean unit rupture load per unit as follows: for the $h(t)_1$ curve,

$$g(i_1) = 100 - 0.84(20) = 83.2;$$

and for the $h(t)_2$ curve,

$$g(i_2) = 100 - 0.13(20) = 97.4.$$

In the first case all four units are intact when the maximum bundle load occurs, but in the second case only three units are intact. Then the efficiency of translation, which is the average bundle load expressed as % mean unit rupture load, is

$$\frac{4(83.2)(24.52) + 3(97.4)(5.93)}{4(24.52 + 5.93)} = 81.2\%.$$

Appendix II

Analysis of Strength of Bundle When First Unit Breaks

In Appendix *I* the case of maximum bundle strength was analyzed. For many purposes a structure may be considered to have failed when the first element has ruptured. If there are a small number of units in the group, and the mechanical interaction between units is large, then it is possible that the elastic recovery of those portions of the broken unit to either side of the break can stress the remaining unbroken units, and in some cases break them. This "snap-back" effect can be of significance when the total number of units is small and the coefficient of variation of elongation to break of the units is small. In a practical sense, there is no difficulty in predictability since under the conditions of maximum effect of "snap-back" there is only a very small difference between average bundle load at first-unit break and average maximum bundle load. This does not, however, deny the very practical fact that in many cases the mechanical utility of the structure is destroyed as soon as the first unit breaks, and thus it is of significance to consider the analysis of the problem. The method for finding the average load supported by a bundle of parallel units when the first unit breaks follows.

Consider a population of units with a mean breaking elongation e_m and a normal distribution of elongations to break with a coefficient of variation of elongation to break V. Now define the following quantities: p, probability of any unit breaking at an elongation in excess of t, $= \frac{1}{\sqrt{2\pi}} \int_t^\infty f(t)\,dt$; $f(t)$ = relative frequency of break at t (ordinate to normal curve); h = relative frequency of first-unit break at elongation t.

If a bundle of n parallel units is stressed to a given elongation t, then the probability of having $(n-1)$ units intact at this point will be the probability of having any given individual unit intact taken to the $(n-1)$ power, or $(p)^{n-1}$. The additional restriction, that the first unit shall have just ruptured, is satisfied by multiplying this quantity by f, the relative frequency of break at t. A normalizing constant, described in Appendix *I*, has been omitted here since it was shown to have no effect on the mean. A curve can now be plotted of h, the relative frequency of a first-unit break, *versus* t, where

$$h = f(t)p^{n-1}. \qquad (II1)$$

By assigning various values to t and determining for each such value the corresponding value of p, it is possible to evaluate equation (*II*1) for all bundle sizes—*i.e.*, all values of n.

The results for values of n from 1 to 15 are plotted in Figure 7. The mean value of t for each of these curves is plotted versus n in Figure 8. This mean value can be interpreted as an efficiency using a linear approximation to the stress-strain curve. That is, one need only find the load on the linear curve corresponding to the t value found and divide this by the mean breaking load. Using the parameter m as previously described, curves of efficiency *versus* bundle size for m = 10, 20, and 30 have been plotted with the calculated points indicated by crosses. These curves appear in Figure 10 of the text.

Appendix III

Analysis of 7-Ply Yarn Strength

From the definition of a parallel bundle given at the beginning of Appendix *I*, it is clear that a 7-ply yarn cannot be considered as such a group. In 2- or 3-ply yarns of uniform geometry, the yarn strain is the same in all yarns, by symmetry. The idealized 7-ply yarn, although rotationally symmetric, is not radially symmetric, and thus all of the singles yarns are not equally strained. The

presence of the core in a 7-ply yarn creates the difference between this structure and a parallel bundle.

The analysis of 7-ply yarn strength, however, is similar to that of the parallel bundle strength, the only differences arising as a result of the variation in strain between the core and the external units.

The idealized geometry for the 7-ply yarn consists of a circular core of radius R_y surrounded by six circular units with the same radius as illustrated in Figure 24.

If the external units are inclined to the core at an angle θ_p, then their strain in terms of the plied yarn strain, e_p, will be $e_p \cos^2 \theta_p$ [2] and the load on the external yarns will be that corresponding to this strain as given by the stress-strain curve of the singles yarns. Thus, if a linear approximation to the shape of the singles yarn stress-strain curve is used here as before, the tension in the core will be $(a + be_p)$, and in each of the outside yarns, $(a + be_p \cos^2 \theta_p)$. For purposes of statistical calculation, all quantities must, as previously, be expressed in terms of t.

Let primed letters refer to the external singles yarns and unprimed letters to the core yarn. Then

$$e = e_p; \quad e' = e_p \cos^2 \theta_p. \tag{III1}$$

By definition,

$$t = \frac{e - e_m}{\sigma}, \tag{III2}$$

and thus

$$t' = \frac{e' - e_m}{\sigma} = t - \frac{e(1 - \cos^2 \theta_p)}{\sigma} = t - \frac{e}{\sigma} \sin^2 \theta_p. \tag{III3}$$

But since

$$\sigma = \frac{e_m V}{100},$$

$$t' = t - \frac{100e}{e_m V} \sin^2 \theta_p. \tag{III4}$$

Since

$$t = \frac{e - e_m}{\sigma} = \frac{e - e_m}{e_m V} 100,$$

$$e = \frac{te_m}{100} V + e_m = \frac{e_m}{100} (tV + 100). \tag{III5}$$

Therefore,

$$t' = t - \frac{e_m}{100} \frac{(tV + 100)}{e_m V} \sin^2 \theta_p \times 100, \tag{III6}$$

or

$$t' = t - \left(t + \frac{100}{V}\right) \sin^2 \theta_p.$$

The plied yarn load contributed by each of the external yarns is equal to the tension in each external yarn multiplied by the cosine of the ply helix angle. Thus, if the load-elongation diagram of the singles yarns is expressed as a function of t, $g(t)$, the tension on the plied yarn when all units are intact is

$$p = g(t) + 6g(t') \cos \theta_p. \tag{III7}$$

Following an analysis very similar to that of Appendix *I*, a number of different breaking configurations are assumed, and the strength of each configuration together with the probability of such a configuration not attaining a higher strength is calculated.

For example, let the core yarn break at an elongation t_1, with all external yarns intact. The strength of the configuration at this point will be

$$g(t_1) + 6g(t_1') \cos \theta_p.$$

In order that no subsequent load shall be greater than this, it follows, in the limit, that

$$g(t_1) + 6g(t_1') \cos \theta_p = 6g(t_2') \cos \theta_p = 5g(t_3') \cos \theta_p = 4g(t_4') \cos \theta_p, \text{ etc.,} \tag{III8}$$

where t_2' is the point at which the first external yarn ruptures, t_3' when the second ruptures, etc. The probability of such a configuration, using the nomenclature of Appendix *I*, is

$$Cf(t_1)(p_2' + p_3' + \cdots p_7')^6;$$

$$\sum_{i=2}^{k} q_i \geq k - 1, k = 2, 3 \cdots 7. \tag{III9}$$

By using different values of t and assuming different breaking configurations, sets of curves similar to those given in Appendix *I* can be plotted and averaged. For example, another configuration to be assumed is that for which maximum load takes place when the first unit breaks, and the first unit is not the core but instead one of the external yarns, with the second unit which ruptures being either the core yarn or one of the five remaining external yarns. Thus, this case is not a single configuration. In the computations, a sufficient number of configurations were analyzed to yield results of engineering accuracy. The plotting and averaging procedure is very similar to that described in Appendix *I*, and will not be repeated here. The

only difference is that in weighting the contributions to maximum bundle strength of each configuration, the weighting factor is dependent not only upon how many units are intact, but also upon whether these remaining yarns are core or external units—*i.e.*, the $\cos \theta_p$ of the external yarns must be included. The results, for several cases, are plotted in Figure 11 of the text.

Acknowledgment

The authors wish to acknowledge the assistance of Mr. David Himmelfarb of the Boston Naval Shipyard both for supplying the various strands and ropes studied in this work and also for his very valuable suggestions and discussions on strand and rope performance. The labors of Mrs. M. Teixeira and Miss J. Rea in making the numerous tests and calculations are gratefully noted. The work has benefited from numerous discussions with Professor S. Backer of the Massachusetts. Institute of Technology. Acknowledgment is also made to Professor E. R. Schwarz of the Textile Division, Massachusetts Institute of Technology, for permission to use the thesis of T. Chow for geometric analysis comparisons.

Literature Cited

1. Platt, M. M., Klein, W. G., and Hamburger, W. J., Mechanics of Elastic Performance of Textile Materials, Part IX, Textile Research Journal **22**, 641–67 (Oct. 1952).
2. Platt, M. M., Mechanics of Elastic Performance of Textile Materials, Part III, Textile Research Journal **20**, 1–15 (Jan. 1950).
3. Schwarz, E. R., Twist Structure of Plied Yarns, Textile Research Journal **20**, 175–9 (Mar. 1950).
4. Chow, T., unpublished Master's thesis, Massachusetts Institute of Technology, Textile Division, June 1948.
5. Platt, M. M., Klein, W. G., and Hamburger, W. J., Mechanics of Elastic Performance of Textile Materials, Supplement to Part IX, Textile Research Journal **22**, 827–9 (Dec. 1952).

(*Manuscript received June 14, 1954.*)

Fundamental Fiber-Fabric Relationships
A Symposium

Six Saturday textile conferences are scheduled to be held at the Polytechnic Institute of Brooklyn, Institute of Polymer Research.

The first conference will be held Saturday, November 13, 1954; the subject, Intrinsic Fiber Properties. Succeeding conferences will be concerned with Fiber Form Factors, Fiber Interactions, Blend Engineering, Fiber-Yarn-Fabric Relationships, and A Challenge to Industry.

For details concerning the conferences write to Polytechnic Institute of Brooklyn, 99 Livingston Street, Brooklyn 1, N. Y.

Book Review

The Collected Papers of Peter J. W. Debye. New York, Interscience Publishers, Inc., 1954. xxii + 700 pages. Price, $9.50.

(Reviewed by Joseph H. Dusenbury, Textile Research Institute, Princeton, New Jersey.)

"This selection of the classical papers of Professor Debye is being presented to him by his pupils, friends, and the publishers on the occasion of his seventieth birthday on March 24, 1954." With this sentence the preliminary survey of the collection is started and its purpose explained. The papers included were selected by Debye himself and are grouped, according to general topic, into five sections: X-Ray Scattering, Dipole Moments, Electrolytes, Light Scattering, and Miscellaneous. After a brief biographical sketch by Professor R. M. Fuoss at the beginning of the volume, short comments on the papers in the first four sections are made by Professors R. M. Fuoss, H. Mark, and C. P. Smyth.

The sections on x-ray and light scattering are likely to be of particular interest to researchers in the polymer and textile fields, dealing as they do with methods used to elucidate the structure of large molecules. The papers on x-ray scattering include the famous ones by Debye and Scherrer describing the experiments and theory for the scattering of x-rays by small randomly distributed crystalline particles. Since its inception, the "Debye-Scherrer method" has been used with great success in studies of crystals with high symmetry. The papers on light scattering are concerned with more recent studies of Debye and his associates at Cornell and show how this method is used as a tool to determine the molecular weight and shape of large molecules. Also included in the section on light scattering are papers on the thermal diffusion of polymer solutions and on the viscosity and diffusion of polymers in solution. For no apparent reason this section also includes a paper concerned with reaction rates in ionic solutions.

The section on dipole moments includes a paper on van der Waals forces published in 1921 and, of more recent vintage, a paper with F. Bueche in 1951 on electric moments of polar polymers. The two classic papers in 1923 by Debye and Hückel ("Zur Theorie der Elektrolyte," I and II) start the group of papers concerned with electrolytic solutions. The first of these papers, with its historical introduction, is a splendid illustration of the Debye approach and of his capacity for bringing order into a previously chaotic field. The Miscellaneous section includes the famous 1912 paper on the theory of specific heats, and the 1926 paper where Debye, independently of Giauque, proposed adiabatic demagnetization as a means of obtaining additional refrigeration at extremely low temperatures. It is surprising to find under "Miscellaneous" a paper with Pauling on the interionic attraction theory of ionized solutes and a paper concerned with the scattering of light by sound waves. These are surely more appropriate in earlier sections.

The volume is attractively put together and is a good example of high quality work in photo-offset. The papers originally in English have been reproduced directly from the original journals. Papers originally in German and Dutch have been translated into English. Unfortunately, some of the reproduced graphs are almost illegible. The reviewer has no knowledge of the Dutch language, but he feels that the translation of the papers in German leaves something to be desired. The problem in many cases is caused by a too literal translation. As a consequence, a large number of apparently misarranged sentences are to be found. This surely does not do justice to their eminent author. The usual trivial number of misspellings and word omissions are also to be found in the translated papers.

The reader of these papers will be continually impressed with the originality of thought of their author. Originally trained as a mathematician, later a professor of theoretical and of experimental physics, and still later a professor of chemistry, Debye has been able to utilize this broad background of knowledge to attack with great success some of the most difficult problems in physical chemistry. This success has been recognized with many awards, including that of the 1936 Nobel Prize in Chemistry. The description of Debye as a creative artist of science is aptly given by Professor Fuoss at the end of his short biography, when he says, "Debye is the Leonardo of today's science."

Today's fabrics must be different, too!

LOOKING at the past is often amusing. Living in it can be sheer folly. For the world has changed—more people travel, more wives are working, and families are larger. That means people are busy! And busy people haven't time for tedious clothes care. That's why today's customers are looking to you for textiles that combine beauty and practicality.

Du Pont's modern-living fibers give *your* fabrics many care-free extras like wrinkle resistance, pleat and shape retention, easy washing, speedy drying and a minimum of ironing—advantages keyed to the needs of modern living.

Look to Du Pont's know-how in fiber research and fabric development to help you profit from the demands of today's market. Depend on it to help you keep pace with the changing needs of tomorrow.

DU PONT

"BETTER THINGS FOR BETTER LIVING ... THROUGH CHEMISTRY"

DU PONT'S MODERN-LIVING FIBERS

NYLON) RAYON) ACETATE) ORLON® ACRYLIC FIBER) DACRON® POLYESTER FIBER)

TRITON GR-5

THIS NEW WETTING AGENT ALSO GIVES YOU HIGHLY EFFECTIVE REWETTING EVEN AFTER PROLONGED FABRIC STORAGE

TRITON GR-5 is not only soluble in water in all proportions but is stable—particularly to lime and magnesium salts—and electrolytes. And TRITON GR-5 is economical, too. But that's only half the story.

TRITON GR-5 is an excellent *rewetting* agent. It wets back after it has dried into the fabric, permitting high absorption under normally difficult conditions, and maintaining fabric absorbency through prolonged storage.

What's more, TRITON GR-5 puts a real sales feature into towelings. They are extra absorbent *when new*—don't need usual pre-use washings housewives complain about.

CONSIDER THE SPECIAL FEATURES OF THIS ECONOMICAL NEW WETTING-REWETTING AGENT; THEN CALL YOUR NEAREST ROHM & HAAS OFFICE.

CHEMICALS FOR INDUSTRY

ROHM & HAAS COMPANY

WASHINGTON SQUARE, PHILADELPHIA 5, PA.

Representatives in principal foreign countries

TRITON is a trade-mark, Reg. U.S. Pat. Off. and in principal foreign countries.